THESIS

FIELD DELINEATION OF GEOMORPHIC PROCESS DOMAINS ALONG RIVER NETWORKS IN THE COLORADO FRONT RANGE

Submitted by

Bridget Livers

Department of Geosciences

In partial fulfillment of the requirements

For the Degree of Master of Science

Colorado State University

Fort Collins, Colorado

Fall 2013

Master's Committee:

Advisor: Ellen Wohl

Sara Rathburn
Brian Bledsoe

Copyright by Bridget Livers 2013

All Rights Reserved

ABSTRACT

FIELD DELINEATION OF GEOMORPHIC PROCESS DOMAINS ALONG RIVER NETWORKS IN THE COLORADO FRONT RANGE

Many of the conceptual models developed for river networks emphasize progressive downstream trends in morphology and processes. Such models are well-suited for larger, low-gradient rivers, but fall short in describing the extreme variability associated with headwater streams, which occupy the majority of length of stream networks, provide unique biological productivity and habitat, and can be sites of great sediment production. A more thorough understanding of the influence of local variability of process and form in headwater stream channels is required to remotely and accurately predict channel geometry characteristics for management purposes. Local variability of valley types and sediment production, or local process domains defined as glacial versus non-glacial valleys and levels of valley confinement, was evaluated for the Colorado Front Range by systematically following stream channels, categorizing them into stream type and process domain, and evaluating a number of channel geometry characteristics. The 111 reaches were then evaluated for significant differences in channel geometry among stream types and process domains, location and clustering of stream types on a slope-drainage area (*S*-*A*) plot, and downstream hydraulic geometry relationships. Statistical analyses revealed significant correlations between channel type and channel gradient, and channel type and substrate size. Although downstream hydraulic geometry relationships are well-defined using all reaches in the study area, reaches in glacial valleys display much more variability in channel geometry characteristics than reaches in fluvial valleys, as evidenced in larger ranges of channel geometry characteristics, greater difficulty in efficiently classifying stream types, less pronounced downstream hydraulic geometry relationships, and greater scatter of reaches on an *S*-*A* plot. Streams flowing through inherited terrain in glacial valleys continue to adjust to sediment and water dynamics, and level of confinement influences locations of certain stream

types. Thus, local spatial variability associated with process domains at the reach scale (10^1-10^2 m) overrides progressive downstream relationships in mountain headwaters, and field calibration of relations between reach-scale channel gradient and channel characteristics is necessary to predict process and form of headwater streams in the Colorado Front Range.

ACKNOWLEDGMENTS

I extend many thanks to the people who supported me throughout my thesis project. First, I would like to thank the U.S. Forest Service for funding of this project, as well as the Colorado State University Warner College of Natural Resources and Department of Geosciences for funding and the opportunity to teach as a graduate teaching assistant, all of which was imperative to my success and experience as a graduate student. None of this could have been achieved without the dedicated help of my field assistant, Kyle Grimsley, whose positive attitude and educated insight made long days of data collection a pleasure. Special thanks also go out to my fluvial family of graduate students who provided constant support, feedback, help with statistics, and differing perspectives all along the way, particularly JoJo Mangano for help with GIS and Natalie Anderson for help with statistics. Thank you to my committee members, Dr. Sara Rathburn and Dr. Brian Bledsoe, who provided me with thoughtful and valuable perspectives and feedback on my thesis, and who challenged me in a positive way to think outside my intellectual box. Endless gratitude goes out to my family, particularly my grandmothers, whose support and love was felt throughout this learning process and who were always there when I needed encouragement. And to my friends, my amazing friends, both near and far, thank you so much for understanding, listening, encouraging me, making me laugh, keeping me grounded, and constantly reminding me of who I am and why science is my passion. But most of all I want to thank my advisor, Dr. Ellen Wohl, whose mentorship, friendship, expertise, humor, insight, generosity, and belief in me made this thesis happen. I am continually and incredibly grateful for the opportunity to work with such an accomplished scientist.

DEDICATION

I dedicate this thesis to my late grandfather, Leonard Dattilo, whose belief in education, knowledge, and following your dreams made me into the person I am today. You inspire me in more ways than you could have ever known. This hard work is for you, Papa.

TABLE OF CONTENTS

1 Introduction 1
1.1 Previous work 1
1.2 Objectives 5
1.2.1 Objective 1 5
1.2.2 Objective 2 8
1.2.3 Objective 3 11
1.2.4 Objective 4 12
1.3 Rationale 13
2 Field area and methods 15
2.1 Field area 15
2.2 Field Methods 19
2.3 Data Analysis 22
2.3.1 Objective 1 22
2.3.2 Objective 2 24
2.3.3 Objective 3 25
2.3.4 Objective 4 26
2.4 Limitations to this analysis 27
3 Results 28
3.1 Objective 1 28
3.2 Objective 2 41
3.3 Objective 3 45

3.4 Objective 4 49

4 Discussion 53

5 Conclusions 59

5.1 Future Work 60

6 References 61

7 Appendices 64

7.1 Appendix A: Valley geometry comparisons 64

7.2 Appendix B: Raw data 67

7.3 Appendix C: Boxplots of raw data 74

7.4 Appendix D: Reach location maps 83

7.5 Appendix E: Field photographs 85

7.6 Appendix F: Classification trees by confinement 104

7.7 Appendix G: Downstream hydraulic geometry plots 107

LIST OF TABLES

Table 1: Summary of all field sites subdivided by number of reaches with respect to stream type, valley history and confinement, and predominant substrate. 28

Table 2: Summary of the range of variables by stream type and valley history; summary of the range of variables by confinement and valley history.. 29

Table 3: Summary of the mean of variables by stream type and valley history and by confinement and valley history. 31

Table 4: Summary of significant differences in variables between stream types......................... 34

Table 5: Summary of significant differences in variables between stream types in glacial valleys. 42

Table 6: Summary of significant differences in variables between stream types in fluvial valleys. 43

Table 7: Summary of significant differences in variables between valley types (glacial versus fluvial) by stream type. 44

Table 8: Summary of significant differences in variables between confinement types. 45

Table 9: Coefficients, exponents, and R^2 values for downstream hydraulic geometry power relationships of width versus discharge for different groups of reaches. 49

Table 10: Coefficients, exponents, and R^2 values for downstream hydraulic geometry power relationships of depth versus discharge for different groups of reaches. 51

LIST OF FIGURES

Figure 1: Re-creation of the Sklar and Dietrich (1998) log-log *S-A* diagram according to predominant substrate with hypothetical bedrock-alluvial transition represented by the equation S = $A^{-0.5}$. 3

Figure 2: Summary of objectives, hypotheses, and associated statistical tests for this study....... 13

Figure 3: Study area location map. 17

Figure 4: Locations of reach endpoints by stream type 33

Figure 5: Plot of slope from DEM versus slope in field. 36

Figure 6: Classification tree for all data.. 37

Figure 7: Classification tree for all glacial reaches versus all fluvial reaches. 38

Figure 8: Biplot of PC1 versus PC2 with locations of explanatory variables. 39

Figure 9: Stream types plotted in the PC1 versus PC2 space. 40

Figure 10: *S-A* diagram with all reaches. 46

Figure 11: *S-A* diagram with all reaches plotted by confinement. 47

Figure 12: *S-A* diagram with all reaches plotted by Montgomery and Buffington (1997) stream type. 48

Figure 13: Comparison of Montgomery and Buffington (MB) (1997) stream type slope ranges versus slope ranges found in this study for the Colorado Front Range (CFR) and slope ranges by valley type. 54

1 INTRODUCTION

1.1 Previous work

Many conceptual models have been developed for river networks which emphasize progressive downstream trends in channel morphology and processes (e.g., the River Continuum Concept (Vannote et al., 1980), downstream hydraulic geometry (Leopold and Maddock, 1953; Wohl, 2004), and slope-drainage area (*S*-*A*) relationships (Sklar and Dietrich, 1998)). Although these models are useful for large or lowland rivers, they are not as applicable for headwater rivers in mountainous areas because mountain rivers are located across a multitude of landscapes, landscape histories, and climates, making them more difficult to study universally. Further complicating downstream trends is the spatial variability in morphology found over short distances (10^1-10^2 meters) of channel in mountain streams due to external controls and limited ability to adjust channel morphology. Because of this variation, mountain rivers are typically studied within a regional context and compared among other regions.

Mountain rivers, which are typically the headwaters for larger river systems, have been less extensively studied than their low-gradient plains counterparts. Headwater streams typically compose over two-thirds of total stream length of a drainage basin (Freeman et al., 2007), and their abundance and influence on the river system as a whole can be underestimated and inadequately acknowledged from a management perspective (Gomi et al., 2002). The location and spatial abundance of mountain streams make them important sources of sediment, water, nutrients, and organic matter for their downstream counterparts (Milliman and Syvitski, 1992). In addition, the small drainage areas and variation in roughness elements associated with mountain streams lead to storage of organic matter and particles, which in turn provide essential food sources and habitats for the base of the food chain (Gomi et al., 2002). The variety of food and habitat in turn support specific niches for species unique to such streams or surrounding riparian areas or species that may use such streams during specific seasons or periods of their life cycle (Meyer et al., 2007). All of these features of headwater streams collectively indicate disproportionately high physical and ecological significance of mountain streams in the context of an entire watershed.

The widely used channel classification system developed by Montgomery and Buffington (1997) for mountain rivers, for example, focuses on reach-scale channel geometry. Channel geometry is categorized in terms of dominant bedform (cascade, step-pool, plane-bed, pool-riffle, dune-ripple). This classification is widely used in part because much resource management focuses at the reach-scale: typically 10^1-10^3 m lengths of channel (Wohl et al., 2007). Montgomery and Buffington (1997) proposed that channel geometry correlates with reach-scale gradient and subsequent studies have supported this (e.g., Wohl and Merritt, 2005, 2008; Wohl et al., 2007). Strong correlations between gradient and channel geometry are particularly useful to managing rivers because reach-scale gradient can be readily extracted and mapped from remote data such as digital elevation models (DEMs), which facilitates mapping the spatial distribution and abundance of channel geometry (e.g., Buffington et al., 2004). Individual categories of channel geometry differ in their response to changes in water and sediment yield, as well as types and abundance of aquatic and riparian habitat (Wohl et al., 2007). Therefore, being able to map the distribution of channel geometries across a river network or a landscape provides a great deal of insight for resource managers. While studies cited above include only limited channel reaches from the Colorado Front Range, Flores et al. (2006) demonstrated that slope combined with an index of specific stream power that uses drainage area effectively differentiated among diverse channel geometries when using data from various regions in the United States. In addition, Ferguson (2012) suggested that dimensionless stream power, which uses a measurement of grain size, influences bed sorting and in turn channel geometry.

In addition to studies that display the relationship between reach-scale gradient and channel geometry, a few papers published over the last decade have explored the idea that consistent correlations exist between stream channel geometry/substrate type and channel slope-drainage area (*S*-*A)* such that similar channel geometry/substrate reaches will plot distinctly in *S*-*A* space (Sklar and Dietrich, 1998, Figure 1; Montgomery and Buffington, 1997).

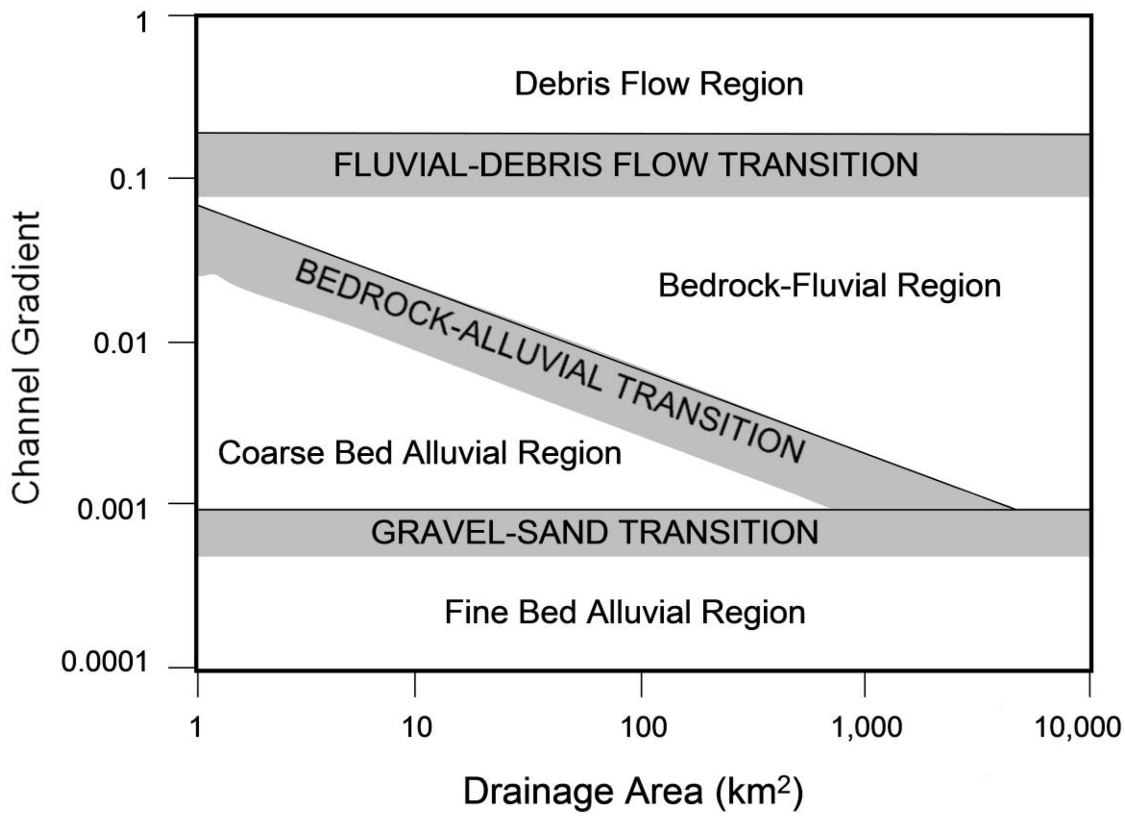

Figure 1: Re-creation of the Sklar and Dietrich (1998) log-log *S*-*A* diagram according to predominant substrate with hypothetical bedrock-alluvial transition represented by the equation $S = A^{-0.5}$.

What makes mountain rivers so different from their lowland counterparts from a geological perspective are their typically steeper gradients, the influence of local and regional tectonics, the presence or absence of glaciation, hydrologic regime (snowmelt-dominated versus precipitation-dominated hydrograph), and the strong influence exerted directly on rivers by hillslope sediment dynamics, disturbance regimes, and differences in rock resistance. From an ecological perspective, mountain rivers possess wide ranges of gradient, light, temperature, water chemistry, substrate, food sources, and species composition, which combine to form a wide variety of habitats (Meyer et al., 2007). Low-gradient rivers or lower gradient reaches of mountain rivers tend to be transport limited with respect to fine sediments and are ‘response’ reaches in which changes in sediment supply are likely to cause changes in channel morphology. In contrast, high-gradient reaches of mountain streams tend to have high transport capacity relative to sediment supply because of their steeper slopes, meaning they are supply limited with respect to pebble-sized sediments and finer (Montgomery and Buffington, 1997). The nature of sediment dynamics in mountainous headwaters, and how sediment is stored or transported, is directly related to the diverse morphology seen in mountain streams. The persistence of a specific stream morphology is maintained by roughness and energy dissipation influenced by sediment dynamics and by larger clasts that are only moved in extreme events (Montgomery and Buffington, 1997; Thompson et al., 2008; Flores et al., 2006).

Mountain rivers typically have segmented longitudinal profiles that correspond to abrupt changes in gradient and valley and channel geometry (Wohl, 2010b). Individual segments reflect longitudinal variation in geomorphic history (e.g., glaciation; Brardinoni and Hassan, 2007), tectonic activity, lithology (e.g., Thompson et al., 2008), and supply of hillslope colluvium. The widespread occurrence of such segmentation is what has brought into question whether the conceptual models mentioned above apply to mountain rivers. The absence or weak development of progressive downstream trends in mountain river networks indicates the need to focus on reach-scale patterns, with a reach defined as a length of channel at least several times channel width that has consistent gradient and channel geometry.

One way to examine how local variations affect morphology in mountain streams is through process domains (Montgomery, 1999). A process domain is a spatially discrete area that is characterized by a distinct geomorphic history and assemblage of geomorphic processes, which together create distinctive forms and disturbance regimes. This refers to disturbances with similar size, frequency, and duration within a process domain (Montgomery, 1999). In relation to river systems, process domains can be used to understand and predict sediment input, transport, and storage, as well as ecological structure along and within stream segments (Wohl and Merritt, 2005, Wohl 2010a; Polvi et al., 2011). For example, at high elevations, rockfalls may be the dominant disturbance regime, whereas flooding may be the dominant disturbance regime in low-gradient rivers downstream. Disturbance regimes can thus physically modify expected or progressive downstream trends by influencing sediment and water dynamics, which in turn dictate channel morphology. Although process domains can be defined in a number of ways, the main process domains identified for the Colorado Front Range specifically address valley history (glacially-formed versus fluvially-formed valleys) and lateral valley-bottom confinement (confined, partly confined, and unconfined valleys) (Wohl et al., 2012).

Much of the previous research regarding predictability of mountain streams either (i) comes from climate regimes outside the semiarid Colorado Front Range, e.g. the Pacific Northwest region (Montgomery and Buffington, 1997; Montgomery, 1999; Buffington and Tonina, 2009; Buffington et al., 2004; Brardinoni and Hassan, 2007) and southeast Australia (Thompson et al., 2008), (ii) was not designed to include the entire range of channel types in Figure 1 (e.g. Wohl and Merritt, 2005; Wohl and Merritt, 2008), or (iii) does not explicitly evaluate how correlations between channel type and potential control variables differ between process domains. A more thorough study of a semiarid region such as the Colorado Front Range is required to understand whether and how these correlations vary with respect to climate, lithology, or tectonic regime. Therefore, I systematically evaluated relations among *S-A*, channel geometry and channel type in the semiarid Colorado Front Range in order to supplement previous studies of how these relations vary with climate and lithology. Relations developed for the Front Range are compared between glacial and fluvial process domains, as well as varying confinement types, within the Front Range.

1.2 Objectives

1.2.1 Objective 1

Objective 1: The primary objective of my thesis research was to develop a dataset that includes channel geometry and gradient for numerous channel reaches in the Colorado Front Range in order to systematically examine correlations between channel morphology, geometry, and gradient.

Channel morphology in this study refers to Montgomery and Buffington (1997) stream type (cascade, step-pool, plane-bed, pool-riffle). Channel geometry characteristics assessed include water-surface gradient S (which is here assumed to be approximately equal to channel-bed gradient), bankfull width W, average bankfull depth D, width/depth (W/D) ratio, predominant substrate (bedrock, boulder, cobble, pebble), and grain size (D_{50}, D_{84}). D_x refers to the grain size diameter where x percent of grains are finer. Once these characteristics were quantified, I compared field-measured reach-scale channel gradients to reach gradients delineated from 10-meter digital elevation models (DEMs). Determination of these differences helped to guide how accurate remote characterization of streams could be for future work. Although some of the reach-scale slopes from 10-meter DEMs were not significantly different from field-delineated slopes and may be a reliable source for reach-scale slope prediction, many DEM-derived gradients did not match those measured in the field in this study, indicating the need to determine the conditions under which the greatest differences occur (e.g., at very small drainage areas), and use these to recommend guidelines for determining reach-scale gradient.

Once channel characteristics were quantified and assessed, I determined whether individual populations of stream types (e.g., pool-riffle vs. plane-bed) have statistically different means for channel geometry characteristics of S, W, D, W/D, D_{50}, D_{84}, and predominant substrate type. This research examines which channel characteristics correlate more strongly with channel type, and therefore provide more accurate prediction of channel type. There may be an ideal combination of variables (e.g., S, D_{50}, D_{84}, W/D, A) or single variable that provides the most accurate differentiation between specific channel types. By comparing the significance of each variable within each channel type, I determined whether one can use an ideal set of variables to distinguish *a priori* among the different channel types.

Hypothesis 1_{null}: Categories of stream type populations do not exhibit significantly different mean channel geometry characteristics.

Hypothesis $1_{alternative}$: Categories of stream type populations exhibit significantly different mean channel geometry characteristics.

For hypothesis 1, I tested whether there was a difference in channel geometry characteristics (*S*, *W*, *D*, *W/D*, D_{50}, and D_{84}) between channel types at the statistical significance level of alpha = 0.05 using all data.

Another conceptual model relevant to my thesis research is that of geomorphic process domains, as mentioned earlier (Montgomery, 1999). Process domains provide another aspect of the question of whether progressive downstream trends or local features predominantly influence mountain river process and form. If the relations between gradient or channel geometry and channel type differ significantly between process domains, this implies that local-scale controls are more useful in understanding mountain rivers.

In the context of this study, geomorphic history primarily refers to whether a portion of the river network experienced Pleistocene valley glaciation (glacial process domain) or was below the elevation limit of glaciation (fluvial process domain). The elevation of lowest glacial extent, ~2400m, also corresponds to the two different hydroclimate regimes associated with this study, above which peak flows are the result of spring snowmelt, and below which larger but less frequent peak flows also occur in response to summer convective storms (Wohl, 2011a). Valley history is the primary process domain considered for this study due to the substantial influence glacial-interglacial cycles had on the topography of the upper portion of the study area in contrast to the fluvially-formed valleys downstream. Glaciation removed massive amounts of sediment from the region, widened and deepened valleys, created steep valley walls and headwalls, and flattened the lower portions of glacial valleys (Anderson et al., 2006; Amerson et al., 2008). These effects on previously glaciated valleys have decoupled hillslope processes from inner stream valleys; stream channels flow through valleys that are not simply adjusted to current fluvial sediment, water, and disturbance regimes, but to inherited glacial terrain and characteristics. Thus, streams in glaciated valleys continue to adjust their channels to the sediment, water, and disturbance dynamics through inherited terrain. In contrast, streams in unglaciated valleys have maintained their coupling with hillslopes and have created and maintained their own channels according to historical and current sediment, water, and disturbance regimes.

1.2.2 Objective 2

Objective 2: The second objective of my research was to examine whether relations between gradient or channel geometry and channel type vary significantly between glacial and fluvial process domains in the Colorado Front Range.

Three valley types (unconfined, partly confined, and confined) can be found both above and below the limit of Pleistocene glaciation (glacial and fluvial process domains, respectively). Confinement in the Colorado Front Range is mostly a function of joint spacing. Joint spacing can directly affect confinement by influencing the rate of bedrock weathering, which can in turn influence valley and channel width, coarse sediment supply from valley walls, and lateral channel mobility (Ehlen and Wohl, 2002). Because of this influence, local variations in jointing or confinement can strongly influence stream geometry and prediction of channel morphology.

The six process domain types described earlier reflect the magnitude, frequency, and type of disturbances to water and sediment entering channels, and the valley geometry in which channels adjust to water and sediment supply. Disturbances include, but are not limited to, floods, wildfire, and hillslope mass movements. Disturbances and valley geometry in turn influence water and sediment dynamics of channels, creating different process domains. For instance, the response of a confined channel reach to a large discharge (flash flood) may result in deepening of the stream and initiation of movement of large clasts downstream, whereas the response of an unconfined stream to a large discharge results in overbank flow and deposition of fine sediments on the floodplain. Mass movements on a glaciated valley wall may deposit at the bottom of the valley wall, having no effect on a stream, whereas mass movements on a fluvial valley wall may be delivered directly into a stream, altering flow paths. (This is not to imply that glaciation always results in unconfined, decoupled conditions for stream reaches.) By evaluating channel types by process domain, I examine whether local controls and disturbances, in this case represented by valley history and confinement, outweigh consistent trends in channel type from mountainous headwaters toward plains rivers.

Hypothesis 2_{null}: Categories of stream type populations do not exhibit significantly different mean channel geometry characteristics within a process domain.

Hypothesis $2_{alternative}$: Categories of stream type populations exhibit significantly different mean channel geometry characteristics within a process domain.

For hypothesis 2, I tested whether there was a difference in channel geometry (S, W, D, W/D, D_{50}, and D_{84}) between channel types at the statistical significance level of alpha = 0.05. This involved comparing all sites by stream type against one another within the fluvial process domain and comparing all sites by stream type against one another within the glacial process domain.

Hypothesis 3_{null}: Individual stream type populations do not exhibit significantly different mean channel geometry characteristics between process domains.

Hypothesis $3_{alternative}$: Individual stream type populations exhibit significantly different mean channel geometry characteristics between process domains.

For hypothesis 3, I tested whether there was a difference in channel geometry (S, W, D, W/D, D_{50}, and D_{84}) within a stream type at the statistical significance level of alpha = 0.05. This involved comparing all sites of an individual stream type between those located in the fluvial process domain and those found in the glacial process domain.

Hypothesis 4_{null}: Streams do not exhibit significantly different mean channel geometry characteristics between different levels of confinement.

Hypothesis $4_{alternative}$: Streams exhibit significantly different mean channel geometry characteristics between different levels of confinement.

For hypothesis 4, I tested whether there was a difference in channel geometry (*S, W, D, W/D*, D_{50}, and D_{84}) between confinement levels at the statistical significance level of alpha = 0.05. This involved comparing all sites within a level of confinement (confined, partly confined, and unconfined) to those sites located in other levels of confinement. This is another version of assessing the influence of process domains on channel geometry.

The Montgomery-Buffington channel classification emphasizes local-scale variation based on the idea that the slope, among other variables, of a stream channel is uniquely adjusted to sediment supply and transport capacity and that slope consequently dictates morphology. In contrast, Sklar and Dietrich (1998) emphasize local-scale variation based on how stream power, which incorporates both slope and discharge, which is related to drainage area, results in transport or storage of certain substrate sizes. Sklar and Dietrich proposed that diverse channel types designated by predominant substrate (fine- and coarse-bed alluvial, bedrock) consistently occur within specific ranges of channel gradient (*S*) and drainage area (*A*) (Figure 1). Drainage area is used in lieu of discharge due to the ease with which drainage area can be obtained from elevation maps, while discharge records are more scarce and discharge must be extrapolated using regional equations. Sklar and Dietrich's hypothetical *S*-*A* diagram, which is based on stream power, is intuitively appealing and would provide great predictive power in understanding the spatial distribution of river form and process, but the diagram has remained largely unquantified and untested against field data. However, variability in *A* for channel types occurs across different hydroclimatic regions (Flores et al., 2006) and thus may require local calibration in order to effectively predict regional channel types using Figure 1.

1.2.3 Objective 3

Objective 3: The third objective of my thesis research was to develop a field data set for the Colorado Front Range against which to test patterns between *S-A* and channel type.

By collecting data on channel type over a range of *S-A* values for a specific geographic region, I was able to systematically evaluate whether the patterns illustrated in Figure 1 actually exist, or whether local- or reach-scale variation creates so much scatter in the data that this 'noise' overwhelms the progressive downstream trends implied by the *S-A* threshold for the transition between bedrock and coarse-bed alluvial channels, for example.

In order to meet objective 3, I categorized channel reaches according to the channel types in Figure 1 (debris flow, bedrock, coarse bed alluvial, and fine bed alluvial) to determine whether observed relationships for the Front Range are consistent with Sklar and Dietrich's diagram. The Front Range represents a semi-arid environment with low tectonic activity, and the aim was to determine whether the Sklar and Dietrich diagram has global applicability or whether the diagram must be interpreted within a regional context. Integrated in this comparison was the determination of whether consistent correlations exist between channel types and gradient and whether gradient can be an efficient predictor of stream type.

Hypothesis 5_{null}: Field-delineated stream types do not differ from stream types predicted from Sklar and Dietrich's diagram using slope and drainage area.

Hypothesis $5_{alternative}$: Field-delineated stream types differ from stream types predicted from Sklar and Dietrich's diagram using slope and drainage area.

In order to evaluate hypothesis 5, I plotted sites on a log-log slope versus discharge plot by predominant substrate and added the line for the transition between coarse-bed alluvial and bedrock-bedded channels, $S=0.07A^{-0.5}$, originally from Montgomery et al. (1996), where S is slope as m/m and A is drainage area in km^2. Because of the conceptual nature of the Sklar and Dietrich plot, I did not conduct statistical analyses to evaluate how sites in the Colorado Front Range compare to the diagram, but instead did a visual analysis of where the sites plotted in relation to the transitional line mentioned above. This involved making multiple plots: all sites; all glacial sites versus all fluvial sites; and sites plotted by all six process domains.

Hypothesis 6_{null}: Categories of stream type populations will cluster together in discrete areas when plotted on an *S*-*A* diagram.

Hypothesis $6_{alternative}$: Categories of stream type populations will not cluster together in discrete areas when plotted on an *S*-*A* diagram.

Hypothesis 6 provides an additional component to evaluating *S*-*A* relations for stream types in the Colorado Front Range. The visual assessment used the plots made for hypothesis 5 plus identical plots that are categorized as Montgomery and Buffington (1997) types in lieu of predominant substrates. In other words, I wanted to evaluate whether stream types clustered together more definitively in an *S*-*A* diagram by morphology or predominant substrate.

1.2.4 Objective 4

Objective 4: The fourth objective of this research was to assess downstream hydraulic geometry relationships in streams in the Colorado Front Range using the morphological characteristics (*W* or *D* versus discharge *Q*) collected in the field.

The goal of plotting downstream hydraulic geometry relationships with these data was to explore another avenue with which to determine the influence of specific stream morphology (here, Montgomery and Buffington (1997) stream type) or local variations (here, valley history and confinement) on progressive downstream relationships in mountain streams. Assessment of downstream hydraulic geometry relationships involved: plotting all data; plotting all glacial sites versus all fluvial sites; plotting by stream types; and by both valley history and confinement. Once the values of coefficients and exponents found in power functions and correlation values for downstream hydraulic geometry relationships for the Colorado Front Range were determined, I compared the values to values previously published both in the Colorado Front Range and other regions.

Figure 2 summarizes all of the research objectives and associated hypotheses, as well as the statistical analyses used to test the hypotheses, which are described in the methods section.

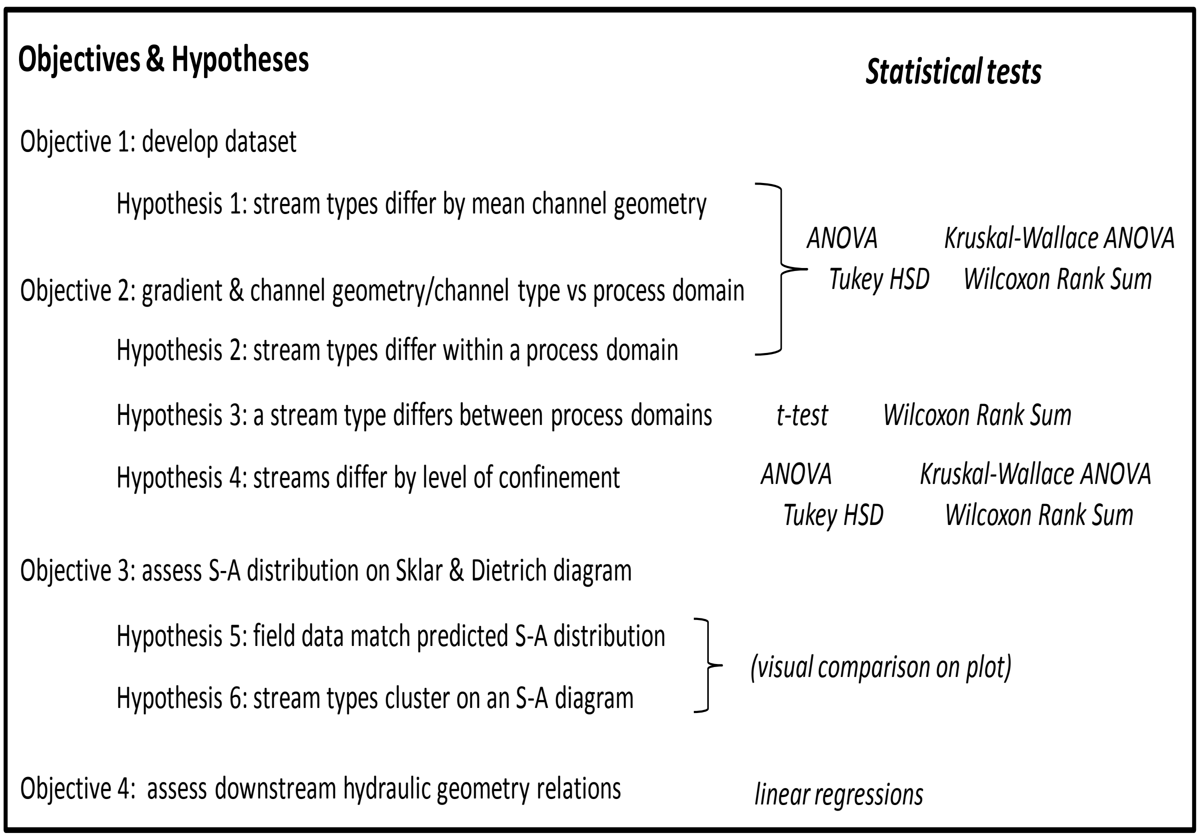

Figure 2: Summary of objectives, hypotheses, and associated statistical tests for this study.

1.3 Rationale

This research (i) expands on existing work by focusing on a semiarid region with potentially different relations among *S*, *A* and channel characteristics than delineated in previous studies in the Pacific Northwest, (ii) evaluates whether relations among *S*, *A* and channel characteristics differ across process domains within an otherwise homogeneous geographic region, and (iii) creates a large dataset against which to evaluate the patterns among *S*, *A*, and channel type predicted by Sklar and Dietrich. If reach-scale gradient and other channel characteristics are known, relative variations in many other characteristics such as channel planform, riparian extent, or hydraulic roughness can be inferred (Wohl, 2010b). Because this research shows that there is a significant and consistent correlation among gradient, grain size and channel morphology, I have the means to develop a system in which to predict channel morphology throughout a catchment by knowing only slope and limited additional parameters. Because the results demonstrate that reach-scale slopes extracted from DEMs are accurate (objective 1) for streams in glacial valleys but less accurate in fluvial valleys, this research provides a mechanism for remotely determining channel morphology throughout a glacial catchment and as a first step in remotely determining channel morphology throughout a fluvial catchment. This approach could substantially enhance existing understanding of form and process in mountainous river networks with relatively little field work required.

2 FIELD AREA AND METHODS

2.1 Field area

The Colorado Front Range, which is the headwaters for the South Platte River basin, is located in north-central Colorado, with the Continental Divide at ~4050 m in elevation representing the western border and the base of the mountains at ~1500 m in elevation representing the eastern border (Anderson et al., 2006). Following uplift during the Laramide Orogeny in the Mesozoic and early Cenozoic, most overlying Paleozoic and Mesozoic sedimentary rocks in the Front Range eroded, leaving Precambrian crystalline rocks as the dominant core (Braddock and Cole, 1990). The crystalline rocks that underlie the study area are known as the Precambrian Silver Plume Granite, which is composed of granite with some biotite schist and granodiorite (Braddock and Cole, 1990). Since the end of the Tertiary, relatively little tectonic activity has occurred in the Front Range (Anderson et al., 2006).

The upper portions of the catchments studied were glaciated during the Pleistocene epoch. Pinedale glaciation extended to approximately 2430 m elevation in the study area, where the terminal moraine is located (Polvi et al., 2011; Wohl et al., 2004). This elevation divides the study area between the glaciated and fluvial (unglaciated) process domain types. Pleistocene glaciation specifically impacted the eastern side below the narrow, summit spine of the Continental Divide due to climatic patterns that move east and headward glacial incision that removed bedrock and sediments in pulses resulting from glacial-interglacial cycles. Below the summit spine, from ~3000-2300 m elevation, lies a low-relief and widespread surface called the subsummit surface; this portion of the Front Range contains deeply incised fluvial bedrock canyons, which become more deeply incised downstream due to continued exhumation of the Denver Basin below the mountain front (Anderson et al., 2006).

Glaciation substantially changed the topography of the upper portion of the study area from the fluvial valleys that likely existed before glaciation and fluvial valleys located downstream. Glacial-interglacial cycles removed sediment from the region, widening and deepening valleys and creating steep valley walls and headwalls, in addition to flattening the lower portions of glacial valleys. Ice also created steps in the longitudinal profile (e.g., hanging valleys) at tributary junctions due to differences in ice volume between valleys (Anderson et al., 2006). An assessment of valley width, valley height, and valley cross-sectional area for glacial versus fluvial valley segments in the study area indicates significant differences in valley width and valley cross-sectional area, with glacial valleys both wider and larger than fluvial valleys. When the data are plotted as normalized valley width and cross-sectional area (i.e., valley width/drainage area and cross-sectional area/drainage area), even larger differences between glacial and fluvial valley segments emerge, with glacial sites having larger values and a much greater range in values (Appendix A, Wohl, unpublished data). Streams located in the glaciated portions of the study area thus have inherited valley characteristics to which modern channels continue to adjust. Conversely, streams located in unglaciated portions of the study area have adjusted their channel and valley geometries specifically to historical and current water and sediment regimes that have shaped their channels, including past glacial outwash and meltwater.

Bedrock jointing patterns in the study area have a strong influence on valley width and canyon evolution. Although the resistance of bedrock may also be due in part to changes in lithology or bedding, joints that are more closely spaced within the bedrock typically correspond to more rapid weathering of bedrock, whereas more widely-spaced joints correspond to slower weathering. Areas with a history of shearing tend to have more closely spaced joints in the Colorado Front Range. Dense jointing patterns may increase weathering, plucking, abrasion, and rock fall, producing small blocks that are readily removed by stream activity, which can create a positive feedback for continued bedrock removal. Such differential weathering throughout the Colorado Front Range has created canyons that have substantial variability in valley width that alternates throughout the longitudinal stream profile, regardless of glacial or non-glacial history. Wider valley segments tend to have lower gradients and minimal stream-hillslope coupling, while narrow, bedrock confined segments tend to have steeper gradients and maximum stream-hillslope coupling (Ehlen and Wohl, 2002).

Mean annual precipitation for North St. Vrain Creek and its tributaries is 70-80 cm in the upper portion of the catchment, with a snowmelt-dominated hydrograph that peaks during May-June. Mean annual precipitation in the lower portion of the catchment is approximately 36 cm. In this lower portion of the catchment below approximately 2300 m, summer convective storms create the largest peak flows, which recur much less frequently than the annual snowmelt peak flows (Wohl et al., 2004; Wohl, 2011a). The peak flows created from thunderstorms at lower elevations are disturbances that maintain depositional and erosional features of streams located in the fluvial domain (Wohl, 2011b). A gaging station in the middle portion of the catchment, which has been maintained since 1926, gives a mean annual peak discharge of 20 m^3/s and peak unit discharge of 0.24 $m^3/s/km^2$ (Wohl and Beckman, 2013). A USGS gaging station, 402114105350101, located on the Big Thompson River below Moraine Park, which was maintained from 1995 to 1997, and maintained since 2001, gives a mean annual peak discharge of 15 m^3/s and peak unit discharge of 0.15 $m^3/s/km^2$ (USGS NWIS, 2013).

The headwaters of the four catchments (North St. Vrain Creek, Glacier Creek, Big Thompson River, and Cache la Poudre River) surveyed in this study begin at the eastern side of the Continental Divide in Rocky Mountain National Park, Colorado (Figure 3). The main stem of the primary catchment used in the study, North St. Vrain Creek, and its tributaries (Cony Creek, Ouzel Creek, Hunter's Creek, and Sandbeach Creek) flow eastward through the park into Roosevelt National Forest and beyond the Colorado Front Range, where North St. Vrain Creek flows into the South Platte River, draining approximately 250 km^2 of the Colorado Front Range (Wohl and Beckman, 2013). All four catchments surveyed in this study drain eastward into the South Platte River. Study sites for this project were collected from near the headwaters to approximately 1945 m in elevation, where North St. Vrain Creek enters Buttonrock Reservoir. Field sites above Buttonrock Reservoir on North St. Vrain Creek and within Rocky Mountain National Park in the other three catchments were chosen because of the lack of flow diversion or regulation structures, land development or recent land-use impacts. Access to the various

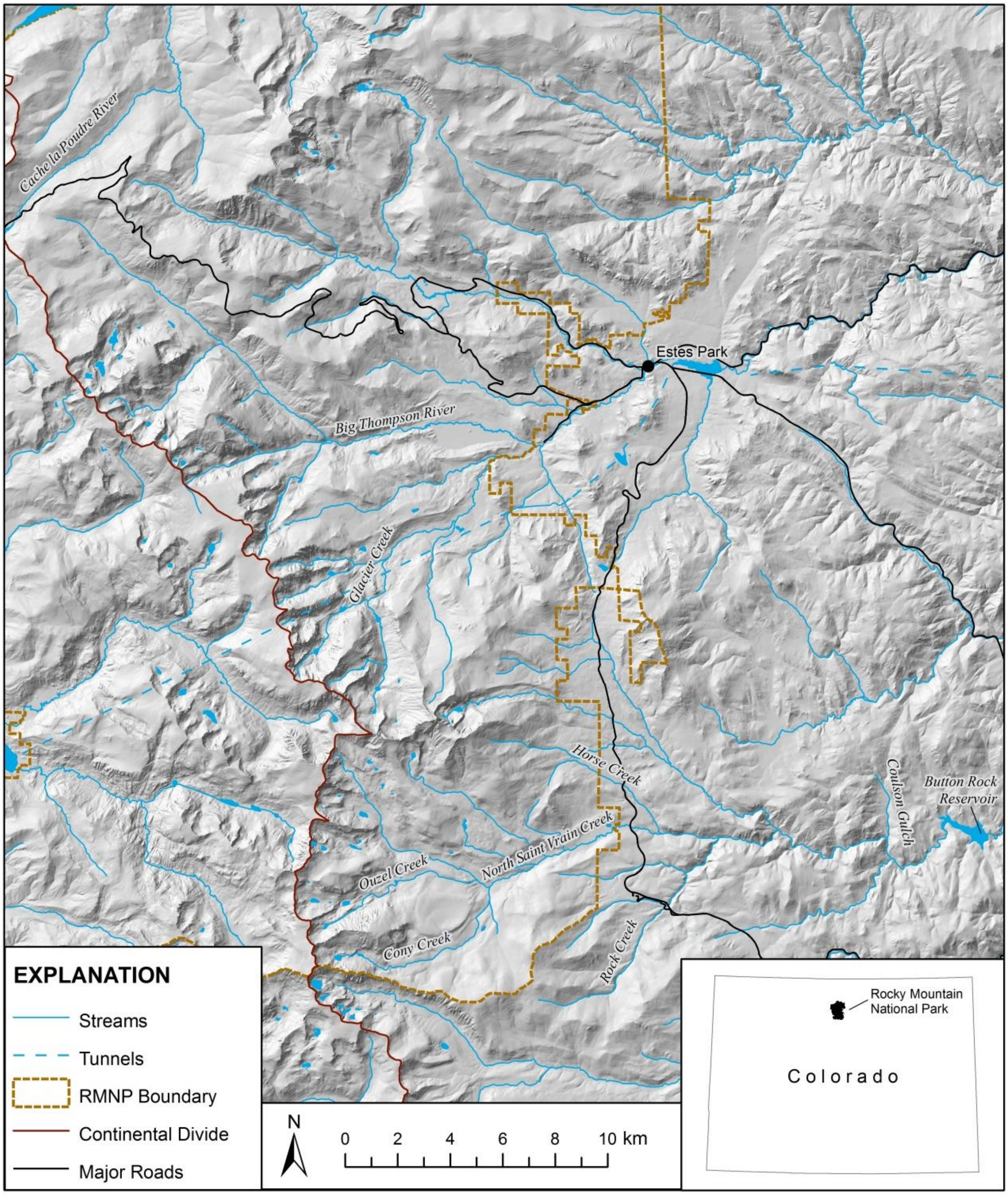

Base map: modified from U.S. Geological Survey 10-meter resolution DEM
Hydrology: U.S. Geological Survey National Hydrography Dataset
Projection: UTM, Zone 13N, NAD 1983

Figure **3**: Study area location map.

portions of the catchments is very limited, with few paved or unpaved roads, and primarily foot trails. In other words, the portions of the catchments surveyed have been largely unaltered by human activity. In addition, no sites within the study area have undergone major disturbances in approximately 30 years or more, and it is assumed that sites have recovered since last disturbance.

2.2 Field Methods

Field collection of data took place between early June and mid-August 2012. Surveyed channel segments were primarily located within the North St. Vrain Creek catchment. Additional sites in other catchments were surveyed in order to increase the number of reaches for specific Montgomery and Buffington (1997) channel types. These additional surveyed reaches were located on Glacier Creek, the Big Thompson River catchment, and the uppermost portions of the Cache la Poudre River, all within Rocky Mountain National Park within previously glaciated valleys.

Site selection began by accessing an arbitrary uppermost portion of a stream that represented the upper boundary of the first reach on that stream. I followed the stream continuously and divided it into reaches. Reaches were field-selected as a continuous length of channel at least ten times bankfull width having consistent and uniform gradient, substrate, and Montgomery and Buffington (1997) classification (cascade, step-pool, plane-bed, pool-riffle). I used Montgomery and Buffington's (1997) descriptions of morphologies to qualitatively classify reaches. Cascades had large clasts and jet-and-wake flow around clasts. Step-pools had channel-spanning steps formed from clasts or wood with corresponding pools below that contained finer material. Plane-beds had no discernible pattern of bedforms. Pool-riffle reaches required the presence of pools, riffles, and bars. I created an additional channel type, riffle-run, for low-gradient reaches with interspersed riffle and run sections displaying characteristics that did not appear to fit within the designated Montgomery and Buffington (1997) channel types. For each reach, endpoints were mapped using a handheld GPS device. For each reach, the first criterion noted was the Montgomery and Buffington (1997) classification. I determined the process domain for each reach by valley history (glacial or fluvial) based on elevation and confinement (confined, partly confined, or unconfined). Confinement categorization used the following guidelines: confined – valley bottom width less than two times bankfull width; partly confined – valley bottom width approximately two to eight times bankfull width; unconfined – valley bottom width greater than eight times bankfull width. I visually approximated confinement first and measured with field tape or a laser rangefinder if there was uncertainty; I only recorded the width of the valley in partly confined valleys. I noted whether the reach was dominated by fluvial or debris flows. Instead of categorizing predominant substrate into coarse bed alluvial and fine bed alluvial, I further visually categorized substrate as sand, pebble, cobble, boulder, or bedrock. Using the distribution results of the pebble count, I verified or updated predominant substrate after data collection.

I chose a substrate sampling location that appeared to represent the average characteristics of the entire reach. I conducted a Wolman (1954) pebble count by crossing the channel perpendicular to flow and, with each step, randomly extracting the first clast touched and measuring the intermediate axis in millimeters with measuring tape; measurements were recorded to the nearest five millimeters. For each reach, I measured 100 clasts, except in 11 cases where high stream flow prevented measurement of 100 clasts, in which case 50 clasts were measured. If the opposite stream bank was reached before I measured 100 clasts, a new transect across the stream, approximately one meter downstream, was used for the pebble count in the same fashion until I measured the full number of clasts. The distributions of the pebble counts determined D_{50} and D_{84} for each reach, which refer to the grain size diameter where 50 and 84 percent of grains are finer, respectively.

To estimate the location of bankfull elevation, I used field indicators such as changes in bank geometry, slope, or vegetation; areas of organic debris collection; and/or stains on rocks along channel banks (Wohl and Merritt, 2005). Once bankfull elevation was determined, I estimated bankfull width by stretching a field measuring tape across the channel perpendicular to flow, staking both ends of tape at bankfull elevation, and measuring the distance in meters. The measured bankfull width was divided into four and, using a stadia rod, I recorded the depth from the bottom of the stream channel to the height in meters of the staked measuring tape at the first, second, and third quartiles of the total length of tape. I then averaged the three depth measurements.

Using a laser rangefinder, I measured water-surface gradient (*S*, in m/m) by choosing a straight section of the reach and aiming the laser upstream and downstream to find the vertical and horizontal distance between the two points. Once all field parameters were measured, I took a digital photograph of the sampled section of the reach looking upstream. I added information from two additional pool-riffle reaches collected in a previous study from North Fork Cache la Poudre River in order to increase the number of pool-riffle reaches used for statistical analysis.

For each reach, I estimated drainage area (*A*) and two-year peak discharge (Q_2) using USGS StreamStats, which employs empirical regression equations between drainage area and discharge using values obtained from Colorado stream gage records (Capesius and Stephens, 2009). Using 10-meter digital elevation models (DEMs) in ArcGIS, I estimated overall reach gradient for each reach. I calculated total stream power for each reach from Q_2 and *S*:

$$\mathbf{\Omega = \gamma QS} \qquad \mathbf{(1)}$$

Where Ω is stream power in W/m, γ is the specific weight of water (9800 N/m^3), Q is discharge in m^3/s, and S is slope. Using the values for stream power, I calculated unit stream power for each reach using:

$$\mathbf{\omega = \Omega/W} \qquad \mathbf{(2)}$$

Where ω is unit stream power in W/m^2, Ω is stream power in W/m, and W is bankfull width in meters. Taking this one step further to calculate more unique stream power values for each reach, I calculated dimensionless stream power, which includes grain size, as derived in Ferguson (2012):

$$\mathbf{\omega_* = \omega/(\rho(gRD_{50})^{3/2})} \qquad \mathbf{(3)}$$

Where ω_* is dimensionless stream power (no units), ω is unit stream power in W/m^2, ρ is the density of water (1000 kg/m^3), g is gravity acceleration (9.8 m/s^2), R is specific gravity (1.65, no units), and D_{50} is in meters.

2.3 Data Analysis

I input and organized all field data and data obtained (or calculated from USGS StreamStats) using Microsoft Excel. For the twelve quantitative variables (S from field, S from DEM, bankfull W, D, W/D, D_{50}, D_{84}, Q_2, A, Ω, ω, and ω_*), I calculated mean, range, and standard deviation. In addition to the entire data set, I calculated mean, range, and standard deviation for the quantitative variables for: each of the stream types; each of the stream types by valley history; each of the levels of confinement; each of the levels of confinement by valley history. To visualize these distributions, I made boxplots, organized by stream type, for each of the first ten variables. I made a second set of these boxplots, but divided each stream type by valley history. I made a third set of boxplots, organized by confinement and valley history. For the second and third sets, I only made boxplots for S (from field), W/D, D_{50}, and D_{84} because I was specifically interested in stream morphology.

Using the statistical program R version 2.15.1, I tested the quantitative variables for normality using histograms, qq-plots and the Shapiro-Wilk normality test (Royston, 1982). For most variables, a log transformation or log transformation plus a constant was sufficient to attain normality, but W, D_{84}, Q_2, and A did not have a straightforward transformation to attain normality. For these four variables, I used nonparametric statistical tests for further analyses. For all analyses, I determined significance at an alpha value of 0.05.

2.3.1 Objective 1

Hypothesis $1_{\text{alternative}}$: Categories of stream type populations exhibit significantly different mean channel geometry characteristics.

To address hypothesis 1, I performed an ANOVA test for each of the transformed channel geometry variables (*S*, *S* from DEM, *D*, *W/D*, D_{50}) to determine whether there was a significant difference in means of that variable between any of the five stream types using all data. If the ANOVA resulted in significance, I performed a Tukey HSD (Ott and Longnecker, 2010) test. This test allowed me to perform pairwise comparisons and attain p-values between each of the stream types to determine which stream types were significantly different from one another. For variables that were not normal (*W*, D_{84}), I performed a Kruskal-Wallis (Ott and Longnecker, 2010) nonparametric analysis of variance test to determine whether there was a significant difference in that variable between any of the five stream types. If the test was significant, I performed a Wilcoxon Rank Sum test (nonparametric t-test equivalent) on each of the pairs to determine which stream types were significantly different from one another. In order to use this method, however, I had to use the Bonferroni correction (Ott and Longnecker, 2010) to the p-value in order to determine significance. For example, if I performed ten pairwise comparisons this way, I have to divide my alpha value by ten, meaning the Wilcoxon Rank Sum test had to result in a p-value less than 0.005 in order to be classified as significantly different.

In addition to the above analyses, objective 1 had the goal of determining whether reach-scale slopes gathered from DEMs were reliable. Because neither data set (*S* from field or *S* from DEM) was normal or required the same transformation, I performed a Wilcoxon Rank Sum test between the two slope sets in order to determine whether their means were significantly different. I then performed the same test on all fluvial sites, all glacial sites, and by confinement to see whether certain subsets had DEM slopes that were better predictors of field slope than others. I plotted slope from field versus slope from DEM against one another and fit a linear regression line and an R^2 correlation value. I added a 1:1 line to the plot in order to visualize the range in which slope in field is most similar to slope from DEM.

Another aspect of objective 1 was to determine whether there is an ideal combination of variables or single variable that provides the most accurate delineation of specific channel types. To address this, I developed a classification tree using the ‘tree’ package version 1.0-33 in R to classify all reaches by stream type using the following variables as potential control variables: confinement, *S*, *A*, Ω, ω, ω_*, *W*,

D, W/D, D_{50}, and D_{84}. I chose the best tree and control variables using cross validation, lowest residual mean deviance, lowest misclassification error rate, and lowest number of end nodes that produced the lowest partitioning of channel types. I used bagging and random forest in the 'randomForest' package version 4.6-7 in R to determine the relative importance of the control variables with respect to classifying the reaches by stream type. Once this was completed, I divided the data into fluvial versus glacial and ran the same tests to determine whether fluvial sites and glacial sites had different variables that were the most important in stream type delineation. The same process was performed for the three confinement types.

To further understand the importance of the control variables, I ran principal components analysis on the data to reduce the dimensions of the data. I plotted the first two principal components as a biplot to visualize which variables explained the most variance in the data. The reaches were then plotted by stream type on the first two principal components to determine whether stream types accurately clustered together in the plot.

2.3.2 Objective 2

Hypothesis 2$_{\textbf{alternative}}$: Categories of stream type populations exhibit significantly different mean channel geometry characteristics within a process domain.

To address hypothesis 2, I performed the same analyses used for hypothesis 1, except that analyses were performed on all sites within the glacial process domain and then analyses were performed on all sites within the fluvial process domain.

Hypothesis 3$_{\textbf{alternative}}$: Individual stream type populations exhibit significantly different mean channel geometry characteristics between process domains.

To address hypothesis 3, I performed a t-test for each of the transformed channel geometry variables (S, S from DEM, D, W/D, D_{50}) to determine whether there was a significant difference in means of that variable between the glacial versus fluvial of each category of the five stream types. For variables that were not normal (W, D_{84}), I performed a Wilcoxon Rank Sum (Ott and Longnecker, 2010) test to determine whether there was a significant difference in that variable between the glacial versus fluvial of each category of the five stream types.

Hypothesis $4_{\textbf{alternative}}$: Streams exhibit significantly different mean channel geometry characteristics between different levels of confinement.

To address hypothesis 4, I performed an ANOVA test for each of the transformed channel geometry variables (*S*, *S* from DEM, *D*, *W/D*, D_{50}) to determine whether there was a significant difference in means of that variable between the three types of confinement using all data. I did not use stream types as part of this analysis; I only categorized data with respect to level of confinement. If the ANOVA resulted in significance, I used a Tukey HSD test to perform pairwise comparisons and attain p-values between each of the confinement levels to determine which were significantly different from one another. For variables that were not normal (*W*, D_{84}), I performed a Kruskal-Wallis nonparametric analysis of variance test to determine whether there was a significant difference in that variable between the confinement levels. If the test was significant, I performed a Wilcoxon Rank Sum test (nonparametric t-test equivalent) on each of the pairs to determine which confinement levels were significantly different from one another. I used the Bonferroni correction for this analysis, meaning the Wilcoxon Rank Sum test had to result in a p-value less than 0.017 (three comparisons) in order to be classified as significantly different.

2.3.3 Objective 3

Hypothesis $5_{\textbf{null}}$: Field-delineated stream types do not differ from stream types predicted from Sklar and Dietrich's diagram using slope and drainage area.

I did not perform formal statistical analysis to address hypothesis 5. I made multiple log-log *S-A* plots by predominant substrate for all sites, all glacial sites versus all fluvial sites, and sites plotted by all six process domains. For each grouping, I plotted the hypothetical transition between coarse-bed alluvial and bedrock channels as estimated by Sklar and Dietrich (1998) and Addy et al. (2011) and visually assessed sites for their location relative to this line. I also developed regression power relationships for each of the predominant substrate types to compare among coefficients, exponents, and correlations.

Hypothesis 6$_{\mathbf{alternative}}$: Categories of stream type populations will not cluster together in discrete areas when plotted on an *S*-*A* diagram.

I used the same diagrams created for hypothesis 5 to evaluate hypothesis 6. I did not perform formal statistical analyses for this hypothesis, but once again made a visual assessment of where specific stream types, classified as predominant substrate or Montgomery and Buffington (1997) stream type, plotted in relation to one another. The goal in this evaluation was to determine whether sites cluster more obviously using substrate or morphology.

2.3.4 Objective 4

Objective 4: The fourth objective of this research was to assess downstream hydraulic geometry relationships in streams in the Colorado Front Range using the morphological characteristics (*W* or *D* versus *Q*) collected in the field.

To address objective 4, I plotted all sites by *W* versus *Q* and *D* versus *Q* and fit a power relationship and correlation value (R^2) to the points. The assessment of downstream hydraulic geometry relationships involved plotting power relationships and correlation values for: all sites together, separating sites into valley history, separating sites into full process domain, and separating sites into stream types. The reasoning behind separating the sites into groups was to determine whether sites within specific stream types or process domains had more pronounced downstream hydraulic geometry than present among all data. I compared the values of coefficients and exponents to previously published values of downstream hydraulic geometry relationships to compare mountain streams in the Colorado Front Range to previously studied streams. I also compared the correlation values among the different groupings to determine which grouping of sites resulted in a power function of best fit.

2.4 Limitations to this analysis

There are a number of limitations to the analyses in this research. The first limitation is that all of the data collected in the field and used to make assumptions and conclusions represent only a snapshot in time. The location of reach types, as well as reach geometry, could change with each type of disturbance possible in this region (e.g., floods, debris flows, massive wood inputs from fire or blowdowns, etc.) and with time since disturbance.

In regard to the specifics of the data collected, two-thirds of the data are from glacial valleys and only one-third of the data are from fluvial valleys. Thus, I am comparing many more data from the glacial process domain to many fewer data from the fluvial process domain. Furthermore, despite the large number of complete data sets (reaches), the sample size becomes small when I divide into groups (e.g., stream types or full process domains) for analyses. For example, the data include only nine plane-beds, only one fluvial unconfined reach, and only one reach with sand as predominant substrate. These limitations reflect the relative rarity of plane-bed and sand-bed channels, and the rarity of unconfined fluvial reaches that have not been altered by human activity. Limited sample sizes when subdividing data can create difficulties in achieving statistical significance when comparing among smaller groups.

3 RESULTS

3.1 Objective 1

Tables 1-3 provide a summary overview of the entire dataset. Raw data for all reaches are located in Appendix B. Boxplots of all reaches by potential control variables, as well as boxplots of reaches by control variables divided into fluvial versus glacial, are located in Appendix C. Figure 4 displays the study area with all downstream ends of reaches, displayed by stream type; Appendix D provides magnified versions of the reach location maps; Appendix E provides field photographs of each reach.

Table 1: Summary of all field sites subdivided by number of reaches with respect to stream type, valley history and confinement, and predominant substrate.

		Valley History		Confinement			Predominant Substrate				
Mont-Buff Stream Type	# of Sites	Glac.	Fluv.	Conf.	Part. Conf.	Unconf.	Sand	Peb.	Cob.	Bould.	Bedr.
Cascade	18	14	4	13	3	2			7	6	5
Step-pool	52	30	22	33	16	3	1	14	28		9
Riffle-run	13	7	6	6	6	1		1	9		3
Plane-bed	9	6	3	0	6	3		6	3		
Pool-riffle	19	15	4	6	9	4		11	8		
TOTAL	111	72	39	58	40	13	1	32	55	6	17
		Glacial		37	23	12					
		Fluvial		21	17	1					

Hypothesis $1_{\text{alternative}}$: Categories of stream type populations exhibit significantly different mean channel geometry characteristics.

Table 4 shows that *D, W*, and *W/D* are not typically significantly different between the stream types, with a few exceptions. Slope, D_{50}, and D_{84}, however, are typically significantly different between the stream types, with the exception of some stream types that are closely related by slope (e.g., plane-bed and pool-riffle have overlapping slope ranges). Riffle-run and plane-bed streams have no significant differences between each other for any of the channel geometry characteristics; nor do plane-bed and

Table 2: Summary of the range of variables by stream type and valley history; summary of the range of variables by confinement and valley history. An * indicates only one reach in that category.

	Slope (field)		Slope (DEM)		Width (m)		Depth (m)		W/D		D50 (mm)	
Variable	**MIN**	**MAX**	**MIN**	**MAX**	**MIN**	**MAX**	**MIN**	**MAX**	**MIN**	**MAX**	**MIN**	**MAX**
All	0.002	0.450	0.006	0.368	0.4	25.8	0.11	1.67	2.35	55.97	1	430
CASCADE	0.032	0.400	0.013	0.321	1.7	25.8	0.45	1.67	2.35	26.41	160	430
glacial	0.032	0.400	0.013	0.321	1.7	14.7	0.45	1.23	2.35	26.41	160	430
fluvial	0.053	0.115	0.049	0.106	15.2	25.8	0.67	1.67	14.12	22.80	180	310
STEP POOL	0.027	0.450	0.018	0.368	0.4	17.0	0.11	1.45	2.85	19.67	1	240
glacial	0.031	0.450	0.018	0.368	0.4	12.2	0.11	0.89	2.85	18.25	35	240
fluvial	0.027	0.253	0.035	0.111	1.5	17.0	0.24	1.45	4.21	19.67	1	240
RIFFLE RUN	0.013	0.057	0.010	0.078	4.5	18.3	0.40	0.97	5.40	24.29	50	230
glacial	0.013	0.057	0.015	0.078	4.8	9.4	0.40	0.93	5.40	15.49	50	220
fluvial	0.017	0.037	0.010	0.050	4.5	18.3	0.40	0.97	9.85	24.29	75	230
PLANE BED	0.002	0.035	0.007	0.071	1.6	22.2	0.38	0.94	3.53	55.97	20	115
glacial	0.002	0.022	0.007	0.047	6.5	22.2	0.40	0.38	8.48	55.97	35	115
fluvial	0.020	0.035	0.016	0.071	1.6	4.0	0.94	0.45	3.53	10.62	20	40
POOL RIFFLE	0.003	0.052	0.006	0.090	1.5	22.8	0.23	0.80	3.88	47.83	20	193
glacial	0.003	0.052	0.006	0.090	1.5	22.8	0.26	0.67	3.88	47.83	30	110
fluvial	0.012	0.030	0.012	0.060	1.6	14.4	0.23	0.80	6.64	20.67	20	193
CONFINED	0.011	0.450	0.009	0.368	1.0	25.8	0.19	1.67	2.35	45.38	30	430
glacial	0.011	0.450	0.009	0.368	1.0	14.7	0.19	1.23	2.35	45.38	30	430
fluvial	0.012	0.253	0.012	0.111	1.5	25.8	0.24	1.67	4.29	22.80	45	310
PARTLY CONFINED	0.003	0.192	0.006	0.173	1.5	22.8	0.23	0.94	2.85	55.97	1	270
glacial	0.003	0.192	0.006	0.173	1.5	22.8	0.33	0.94	2.85	55.97	35	270
fluvial	0.017	0.080	0.010	0.078	1.6	18.3	0.23	0.75	3.53	24.29	1	130
UNCONFINED	0.002	0.400	0.011	0.321	0.4	13.1	0.11	0.94	2.80	20.53	35	360
glacial	0.002	0.400	0.011	0.321	0.4	13.1	0.11	0.94	2.80	20.53	35	360
*fluvial	0.022		0.040		6.0		0.42		14.29		55	

Table 2: Continued

Variable	D84 (mm)		QPK2 (cms)		DA (km^2)		Stream power (W/m)		Specific stream power (W/m2)		Dimensionless stream power	
	MIN	**MAX**	**MIN**	**MAX**	**MIN**	**MAX**	**MIN**	**MAX**	**MIN**	**MAX**	**MIN**	**MAX**
All	1	940	0.22	21.36	1.24	986.00	55.70	17038.69	6.95	3924.06	0.008	112.268
CASCADE	390	940	1.18	15.33	3.76	95.57	1160.45	17038.69	172.67	2337.56	0.021	0.169
glacial	390	940	1.18	15.21	3.76	83.92	1160.45	9962.08	172.67	2337.56	0.021	0.169
fluvial	440	580	15.18	15.33	84.43	95.57	7904.88	17038.69	520.06	661.70	0.059	0.105
STEP POOL	1	540	0.22	21.36	1.24	208.49	156.86	11415.02	60.33	3924.06	0.046	112.268
glacial	70	540	0.42	17.20	1.24	85.21	331.87	11415.02	128.87	3924.06	0.054	7.544
fluvial	1	490	0.22	21.36	2.05	208.49	156.86	10396.88	60.33	896.12	0.046	112.268
RIFFLE RUN	90	430	3.14	21.36	8.70	207.98	636.80	5562.69	113.71	483.71	0.044	0.276
glacial	90	400	4.25	17.25	8.70	86.51	636.80	3450.42	113.71	423.98	0.044	0.165
fluvial	100	430	3.14	21.36	25.90	207.98	890.63	5562.69	194.69	483.71	0.048	0.276
PLANE BED	40	200	0.57	15.24	4.74	83.92	111.05	2872.30	18.93	359.04	0.014	0.429
glacial	75	200	3.82	15.24	10.08	83.92	248.01	2872.30	18.93	359.04	0.014	0.186
fluvial	40	120	0.57	1.07	4.74	7.41	111.05	368.26	27.76	223.19	0.053	0.429
POOL RIFFLE	45	367	0.74	19.24	1.84	986.00	55.70	2493.96	6.95	314.64	0.008	1.128
glacial	55	220	0.74	15.27	1.84	83.66	55.70	2493.96	6.95	314.64	0.008	0.605
fluvial	45	367	1.09	19.24	7.80	986.00	321.48	2262.05	105.46	207.41	0.028	1.128
CONFINED	60	940	0.22	21.36	1.24	986.00	82.02	17038.69	6.95	1992.92	0.021	1.863
glacial	60	940	0.49	17.25	1.24	86.51	82.02	11415.02	6.95	1992.92	0.021	1.863
fluvial	150	580	0.22	21.36	2.05	986.00	156.86	17038.69	60.33	896.12	0.028	0.378
PARTLY CONFINED	1	530	0.39	21.30	3.50	198.13	55.70	4940.38	10.45	1568.51	0.008	112.268
glacial	55	530	0.92	15.24	3.50	83.92	55.70	4940.38	10.45	1568.51	0.008	0.415
fluvial	1	270	0.39	21.30	3.63	198.13	111.05	3568.73	27.76	528.87	0.053	112.268
UNCONFINED	60	470	0.42	15.27	1.24	83.92	171.98	4675.13	18.93	3924.06	0.014	7.544
glacial	60	470	0.42	15.27	1.24	83.92	171.98	4675.13	18.93	3924.06	0.014	7.544
*fluvial	90		2.89		20.56		632.79		105.46		0.126	

Table 3: Summary of the mean of variables by stream type and valley history and by confinement and valley history. An * indicates only one reach in that category.

	Slope (field)	Slope (DEM)	Width (m)	Depth (m)	W/D	D50 (mm)	D84 (mm)	QPK2 (cms)	DA (km^2)	Stream power (W/m)	Specific stream power (W/m2)	Dimensionless stream power
Mean all	0.073	0.075	6.9	0.59	11.43	123	247	5.96	48.84	2664.99	491.04	1.306
St. Dev. All	0.085	0.067	5.3	0.25	8.83	88	172	6.32	135.79	2985.04	552.70	10.607
CASCADE	0.126	0.113	9.4	0.82	11.23	267	526	6.92	32.49	5943.14	817.26	0.092
glacial	0.140	0.125	6.7	0.73	9.52	279	529	4.55	16.81	4412.46	878.57	0.092
fluvial	0.076	0.072	18.5	1.13	17.21	225	515	15.22	87.35	11300.54	602.70	0.092
STEP POOL	0.096	0.094	5.0	0.53	8.48	103	221	4.54	27.37	2544.37	625.21	2.632
glacial	0.121	0.115	5.0	0.53	8.40	107	226	4.36	16.50	2855.20	842.25	0.684
fluvial	0.062	0.065	5.1	0.53	8.59	98	213	4.79	42.19	2120.51	329.25	5.289
RIFFLE RUN	0.030	0.039	8.6	0.67	12.83	133	238	9.99	64.92	2681.68	302.76	0.119
glacial	0.033	0.045	6.4	0.64	10.59	136	239	7.08	25.59	2019.58	310.36	0.115
fluvial	0.027	0.033	11.3	0.71	15.44	129	237	13.38	110.81	3454.13	293.88	0.124
PLANE BED	0.018	0.031	8.3	0.58	15.41	58	109	6.64	33.36	827.33	115.90	0.164
glacial	0.015	0.023	11.3	0.66	20.09	70	126	9.59	47.13	1141.00	119.45	0.098
fluvial	0.026	0.046	2.4	0.41	6.06	33	77	0.74	5.83	200.01	108.80	0.298
POOL RIFFLE	0.018	0.030	7.7	0.48	16.86	67	127	5.84	119.42	748.51	121.34	0.179
glacial	0.017	0.030	7.5	0.48	17.38	58	111	4.57	18.24	583.34	110.24	0.137
fluvial	0.019	0.031	8.6	0.51	14.90	103	187	10.60	498.84	1367.93	162.98	0.333
CONFINED	0.091	0.089	7.7	0.66	11.22	155	320	7.29	72.89	3903.21	587.83	0.232
glacial	0.110	0.104	6.0	0.60	10.24	156	314	4.95	19.29	3340.93	694.78	0.294
fluvial	0.059	0.062	10.5	0.76	12.94	152	332	11.42	167.32	4893.90	399.41	0.123
PARTLY CONFINED	0.040	0.048	6.4	0.52	12.46	87	171	4.18	21.77	1255.24	257.94	2.996
glacial	0.039	0.046	8.2	0.59	15.48	104	206	5.15	19.56	1520.20	278.90	0.124
fluvial	0.042	0.050	4.0	0.43	8.36	64	123	2.86	24.76	896.77	229.58	6.881
UNCONFINED	0.095	0.094	4.8	0.49	9.23	96	157	5.48	24.83	1478.27	776.46	0.897

Table 3: Continued

glacial	0.101	0.098	4.7	0.50	8.81	99	163	5.69	25.19	1548.73	832.37	0.961
*fluvial	0.022	0.040	6.0	0.42	14.29	55	90	2.89	20.56	632.79	105.46	0.126

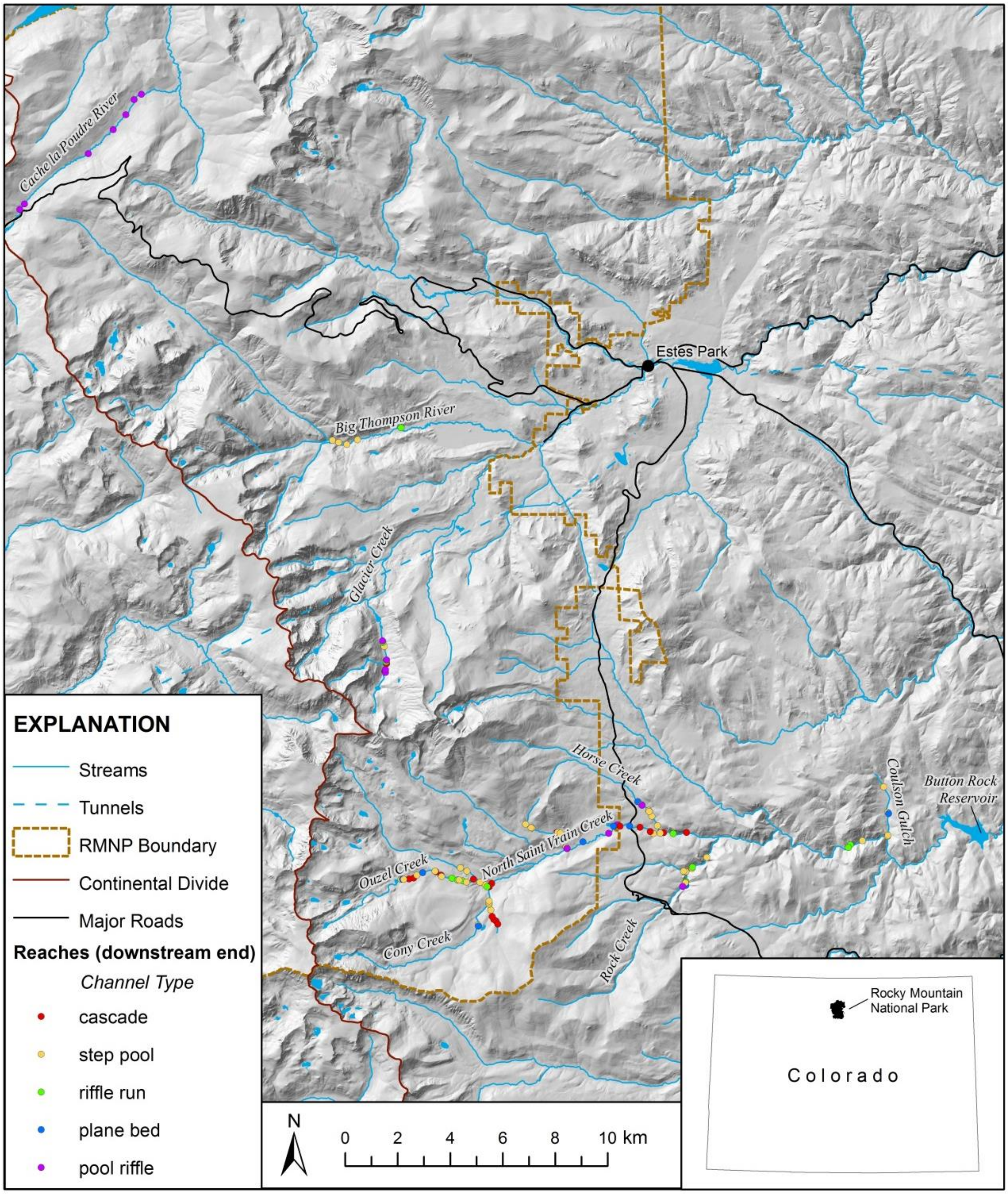

Base map: modified from U.S. Geological Survey 10-meter resolution DEM
Hydrology: U.S. Geological Survey National Hydrography Dataset
Projection: UTM, Zone 13N, NAD 1983

Figure 4: Locations of reach endpoints by stream type. Note four watersheds shown: Cache la Poudre River, Big Thompson River, Glacier Creek, and North Saint Vrain Creek.

pool-riffle streams. In summary, some channel geometry characteristics support the *H1* alternative (*S*, *S* from DEM, D_{50}, and D_{84}), while others do not (*W*, *D*, *W/D*). The *H1* alternative hypothesis is partly supported.

Table 4: Summary of significant differences in variables between stream types. Cas refers to cascade, SP refers to step-pool, RR refers to riffle-run, PB refers to plane-bed, PR refers to pool-riffle. 'Yes' refers to significant difference at alpha = 0.05. An * refers to significant difference at alpha = 0.10.

Slope

	Cas	SP	RR	PB
SP	no			
RR	yes	yes		
PB	yes	yes	no	
PR	yes	yes	yes	no

D_{50}

	Cas	SP	RR	PB
SP	yes			
RR	yes	no		
PB	yes	no*	yes	
PR	yes	yes	yes	no

Slope DEM

	Cas	SP	RR	PB
SP	no			
RR	yes	yes		
PB	yes	yes	no	
PR	yes	yes	no	no

D_{84}

	Cas	SP	RR	PB
SP	yes			
RR	yes	no		
PB	yes	yes	yes	
PR	yes	yes	yes	no

Depth

	Cas	SP	RR	PB
SP	yes			
RR	no	no		
PB	no	no	no	
PR	yes	no	no	no

Width

	Cas	SP	RR	PB
SP	no*			
RR	no	no*		
PB	no	no	no	
PR	no	no	no	no

W/D

	Cas	SP	RR	PB
SP	no			
RR	no	no*		
PB	no	no	no	
PR	no	yes	no	no

Also, the Wilcoxon Rank Sum test (paired) for *S* in field versus *S* from DEM resulted in a p value of 0.096. This means that the two groups are not significantly different at the chosen alpha 0.05, but are significantly different at alpha = 0.10. For this reason, slopes acquired from DEMs are relatively reliable and could be used as a first step in determining stream morphology remotely, but may not be reliable enough to use alone as an indicator of stream morphology. The same test for all glacial sites resulted in a p value of 0.4778, while fluvial sites resulted in a p value of 0.05537. This indicates that DEMs are more accurate for determining reach slopes in glacial valleys than fluvial valleys. The same test on confined, partly confined, and unconfined valleys resulted in p values of 0.642, 0.1542, and 0.2633, respectively, indicating that slopes acquired from DEMs in confined reaches are more similar to slopes measured in the field than slopes in other confinements. Obtaining accurate gradient from DEMs is more difficult for streams with very low slopes due to the lack of contour lines that can be used to accurately measure elevation changes, particularly if a stream type is short in length.

Figure 5 is a plot of slope from DEM versus slope from the field for each reach, with reaches divided into glacial and fluvial sites. The solid black line represents a 1:1 slope that would represent where points would plot if DEM and field slopes were identical. As can be seen in the figure, slopes in lower gradient streams tend to be slightly overestimated by DEMs, while slopes in higher gradient streams tend to be underestimated by DEMs. At lower slopes, the points appear evenly distributed about the 1:1 line up to about a 0.25 slope (with two outliers well below the line). At slopes above 0.25, field slopes are much lower than measured DEM slopes. Slopes from the field and slopes from DEMs are more correlated in glacial sites than fluvial sites, as seen from comparing the regression equations and correlation values between the two data sets.

Figure 6 displays the classification tree designed for all reaches. Variables used in construction of this tree are S, Ω, and D_{50}. The misclassification error rate for this tree is 0.2162. Stream types with lower gradients (pool-riffle, plane-bed, and riffle-run) are easily delineated using S and Ω, whereas stream types with larger gradients (step-pool and cascade) are more complex to delineate and require additional measures of substrate. Riffle-run reaches are located on both sides of the first split. The results of bagging and random forest imply that the most important variables in delineating stream types are, in order of decreasing importance, S, D_{84}, D_{50}, ω, ω*, and Ω. However, ω and ω* were not more efficient delineators of stream type than Ω in the classification tree analysis. The remaining variables have varying influence, but none appear to be important in delineating stream type.

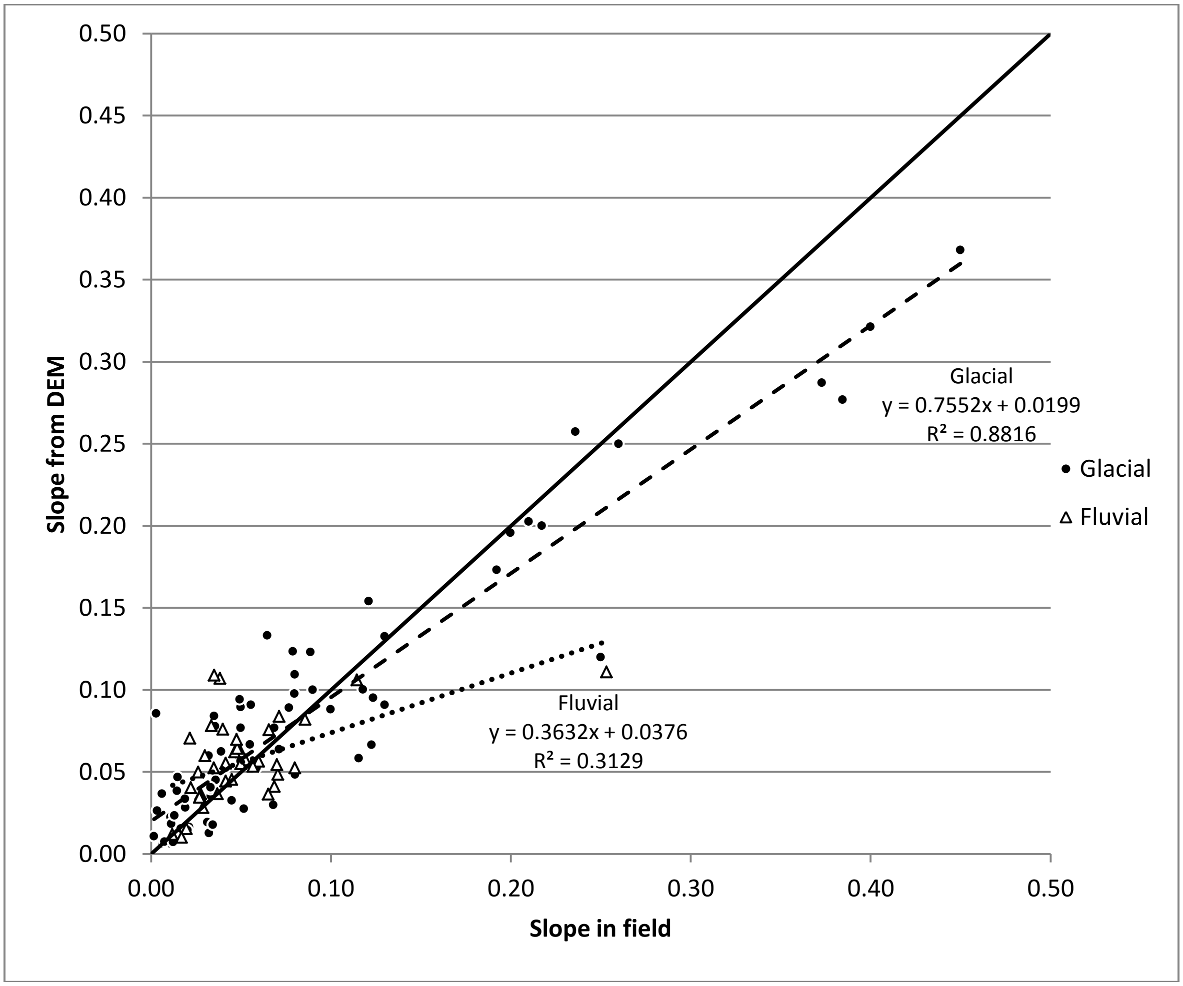

Figure 5: Plot of slope from DEM versus slope in field. Each point represents one reach from this study, divided into glacial and fluvial reaches. Linear regression lines were fit to the two data sets: the dashed line represents glacial sites while the dotted line represents fluvial sites. Regression equations and correlation values are labeled on the plot. The solid black line has a 1:1 slope and represents where points should plot if the two slopes were identical.

Figure 7 displays the two classification trees built for glacial sites and fluvial sites. Variables used in construction of the glacial tree are S, D, ω_*, and D_{50}. Variables used in construction of the fluvial tree are S, A, and W. Misclassification error rates for the glacial and fluvial reaches are 0.2361 and 0.1795, respectively. Stream types in glacial valleys with lower gradients (pool-riffle and plane-bed) are

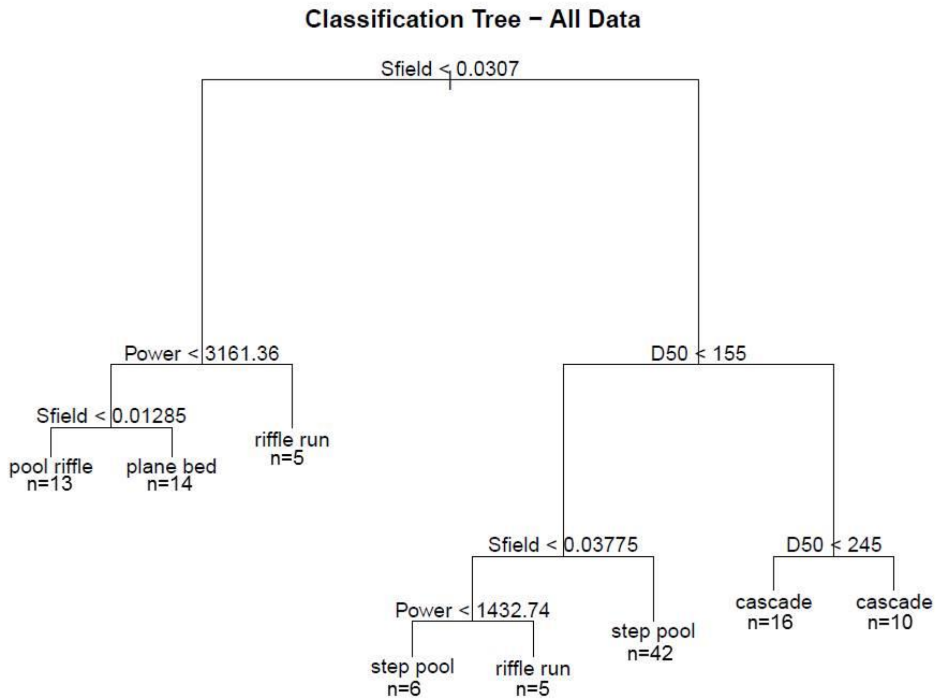

Figure 6: Classification tree for all data. If condition listed at split is positive, continue left from split. Note which variables are present in delineation of stream type and which are not. Misclassification error rate is 0.2162. 'Sfield' refers to slope recorded in the field; n values refer to the number of sites partitioned out in that terminal node.

delineated using S, D, and ω_*, whereas stream types with larger gradients (step-pool and cascade) are delineated with only S and D_{50}; riffle-run reaches are more closely related in the tree to the larger gradient stream types. Stream types in fluvial valleys are very easily classified, with only five terminal nodes corresponding to the five stream types; riffle run reaches are more closely related to lower gradient streams in the fluvial classification tree. The results of bagging and random forest imply that the most important variables in delineating stream types in glacial valleys are, in order of decreasing importance, S, D_{50}, D_{84}, ω_*, ω, and Ω, despite the absence of some of these variables in the classification tree. The most important variables in delineating stream types in fluvial valleys are, in order of decreasing importance, S, W/D, A, Ω, and W. The remaining variables have varying influence, but none appear to be important in delineating stream type.

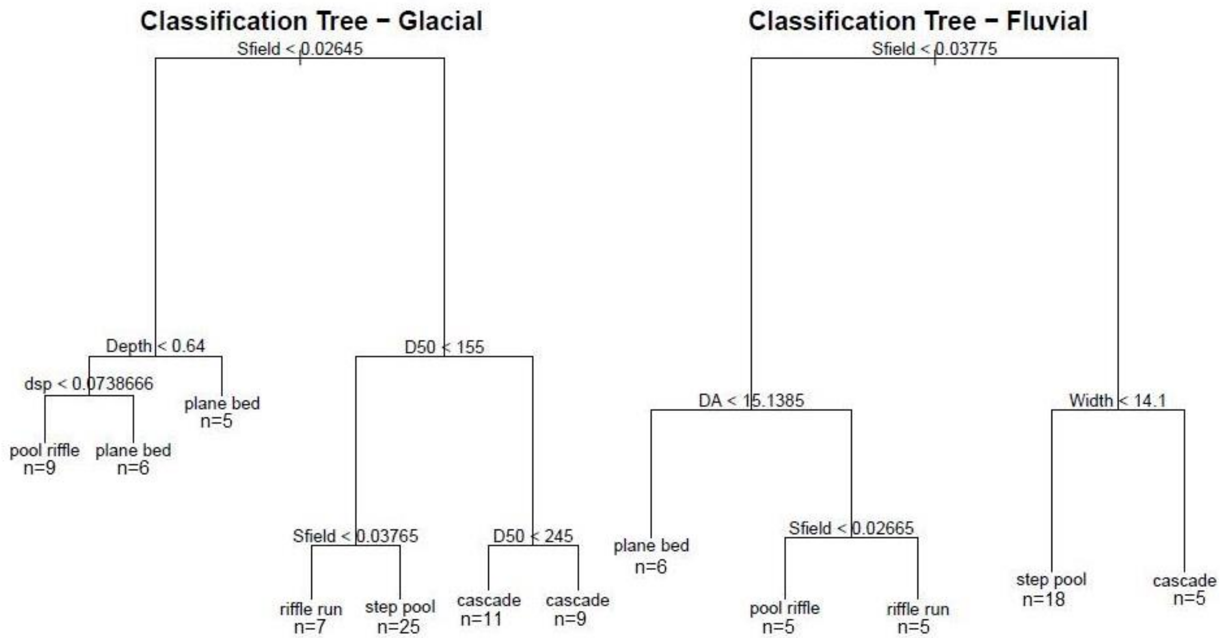

Figure 7: Classification tree for all glacial reaches versus all fluvial reaches. If condition listed at split is positive, continue left from split. Note the different variables used to delineate stream types in the different valleys. Misclassification error rates for the glacial and fluvial reaches are 0.2361 and 0.1795, respectively. 'Sfield' refers to slope recorded in the field; n values refer to the number of sites partitioned out in that terminal node.

Tree results for the three confinements (Appendix F) are less straightforward. Trees for stream types in confined, partly confined, and confined reaches had misclassification error rates of 0.1552, 0.275, and 0.4615, respectively. Bagging and random forest implies that for confined reaches the most important variables are, in order of decreasing importance, S, W/D, Ω, and A; for partly confined reaches: S, ω_*, ω, D_{50}, W/D, D_{84}; and for unconfined reaches: D_{84}, D_{50}, D, W, ω_*, and ω. The remaining variables have varying influence, but none appear to be important in delineating stream type.

Figure 8 shows the results of the biplot of the first two principal components. Principal components analysis lowers the dimensions of the explanatory variables and rotates the data to account for variability in the data. The first principal component describes variability in the data by expressing which explanatory variables describe the most variability in the data itself and plotting where each datum lies in the context of such variability. The second principal component describes the second highest

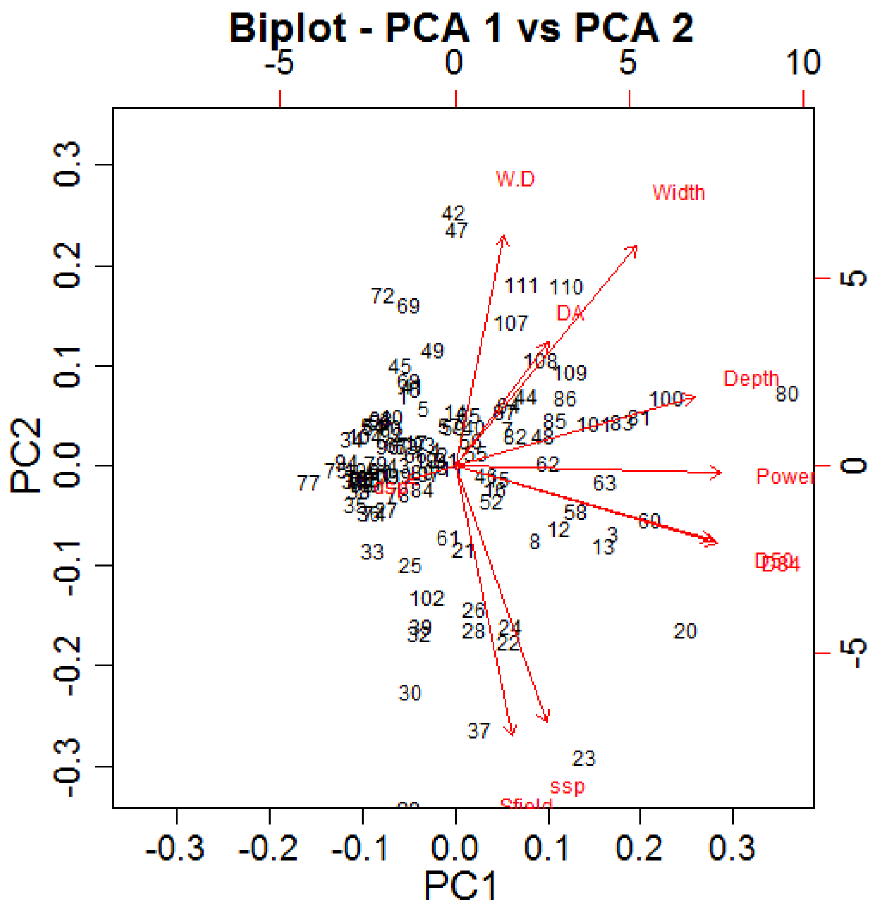

Figure 8: Biplot of PC1 versus PC2 with locations of explanatory variables.

amount of variability in the data, and so on. A principal component can be described by more than one variable, as seen in Figure 8. In the biplot, variables are influential along the axis direction in which the arrow is pointing and the length of the arrow is proportional to the amount of variability that particular variable explains in the data. The numbers in the biplot correspond to the stream reach in the data set (n=111). In other words, *Ω* describes the most variability in the data since *Ω* varies along the first principal component. Slope and *W/D* describe the variability in the explanatory variables along the second principal component, but have opposing influence on stream type because their arrows point in different directions. Width, D_{50}, and D_{84} are equally explained by the first two principal components, as is seen by their 45° orientation with the principal components.

Figure 9 is similar to Figure 8, but with stream types labeled by name and same color in lieu of numbers listed in Figure 8. The plot of variables is not labeled, but the influence of the variables

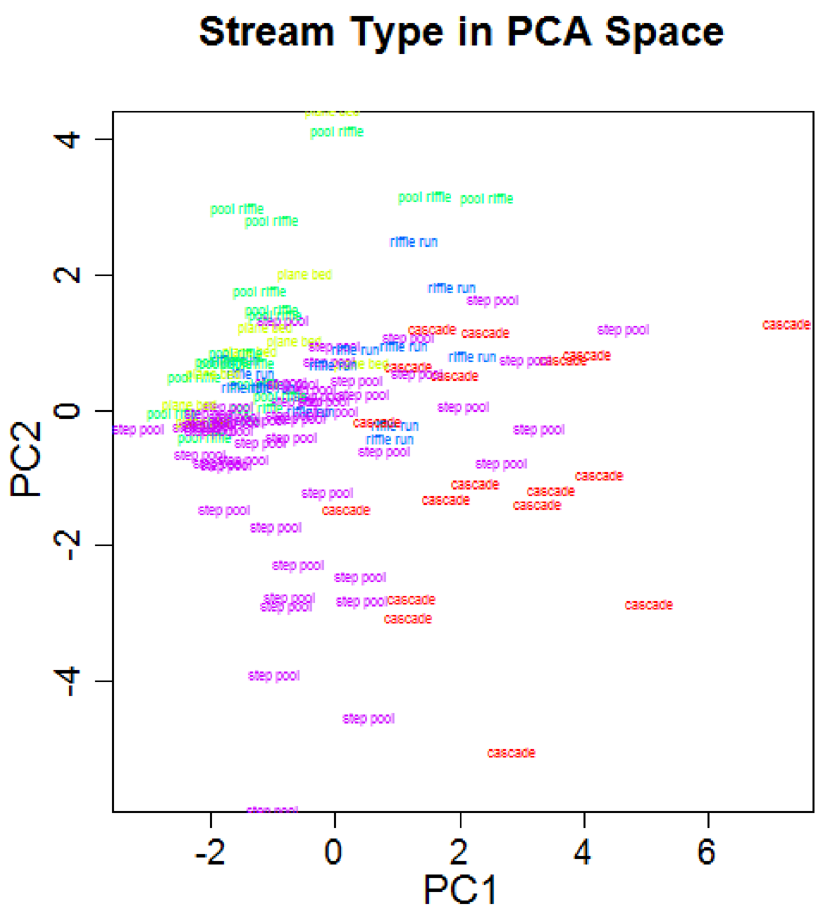

Figure 9: Stream types plotted in the PC1 versus PC2 space. Compare to Figure 8 in regard to variables of influence and their explanation of variance.

according to the principal components can be more easily visualized. For example, *D* increases as the value of PC1 increases, which corresponds to the gradation from pool-riffle to cascade from left to right on Figure 8. Slope increases with decreasing value of PC2, which corresponds to the gradation from pool-riffle to cascade from top to bottom on Figure 9. The stream types appear to cluster well in Figure 9, and Figure 8 provides a guide with which to understand the variables that best describe each stream type.

3.2 Objective 2

Hypothesis $2_{alternative}$: Categories of stream type populations exhibit significantly different mean channel geometry characteristics within a process domain.

Table 5 shows that *D*, *W*, and *W/D* are not typically significantly different between the stream types in glacial valleys, with a few exceptions. Slope is typically significantly different between the stream types, with the exception of some stream types that are closely related by *S* (e.g., plane-bed and pool-riffle have overlapping slope ranges). Substrate (D_{50} and D_{84}) of glacial cascades is significantly different from other glacial stream types and substrate of glacial pool-riffles is significantly different from other glacial stream types except plane-bed. Other glacial stream types are not significantly different in substrate. Riffle-run and plane-bed streams in glacial valleys have no significant differences between each other for any of the channel geometry characteristics; nor do plane-bed and pool-riffle streams in glacial valleys. In summary, some glacial channel geometry characteristics support the *H2* alternative (*S*, *S* from DEM, some D_{50}, and some D_{84}), while others do not (*W, D, W/D*, some D_{50}, and some D_{84}). The *H2* alternative hypothesis is partly supported.

Table 6 shows that D_{50}, D_{84}, *D*, and *W* are not typically significantly different between the stream types in fluvial valleys, with a few exceptions: Fluvial cascades and step-pools are significantly different with respect to these four geometry characteristics. Slope is significantly different between the fluvial cascades and other stream types and between fluvial step-pools and other stream types, except that fluvial cascades and step-pools are not significantly different. The lower gradient fluvial stream types do not have significantly different slopes between one another. Slopes acquired from DEMs have varied results. Width-to-depth ratios for streams with fluvial valleys are, interestingly, significantly different between stream types closely related by slope (Cas-SP, SP-RR, etc.) and between PB-Cas, but not between other stream types. Riffle-run and pool-riffle streams in fluvial valleys have no significant differences between one another for any of the channel geometry characteristics. In summary, some fluvial channel geometry characteristics support the *H2* alternative (some *S*, some *S* from DEM, some *W/D*), while others do not

Table 5: Summary of significant differences in variables between stream types in glacial valleys. Cas refers to cascade, SP refers to step-pool, RR refers to riffle-run, PB refers to plane-bed, PR refers to pool-riffle. 'Yes' refers to significant difference at alpha = 0.05. An * refers to significant difference at alpha = 0.10.

GLACIAL - Slope

	Cas	SP	RR	PB
SP	no			
RR	yes	yes		
PB	yes	yes	no	
PR	yes	yes	no	no

GLACIAL - D_{50}

	Cas	SP	RR	PB
SP	yes			
RR	yes	no		
PB	yes	no	no	
PR	yes	yes	yes	no

GLACIAL - Slope DEM

	Cas	SP	RR	PB
SP	no			
RR	yes	yes		
PB	yes	yes	no	
PR	yes	yes	no	no

GLACIAL - D_{84}

	Cas	SP	RR	PB
SP	yes			
RR	yes	no		
PB	yes	no	no	
PR	yes	yes	no*	no

GLACIAL - Depth

	Cas	SP	RR	PB
SP	yes			
RR	no	no		
PB	no	no	no	
PR	yes	no	no	no

GLACIAL - Width

	Cas	SP	RR	PB
SP	no			
RR	no	no		
PB	no	no	no	
PR	no	no	no	no

GLACIAL - W/D

	Cas	SP	RR	PB
SP	no			
RR	no	no		
PB	no	no*	no	
PR	no	no*	no	no

(some S, some S from DEM, W, D, some W/D, D_{50}, and D_{84}). The *H2* alternative hypothesis is partly supported, but on the whole is not supported.

Hypothesis 3$_{\text{alternative}}$: Individual stream type populations exhibit significantly different mean channel geometry characteristics between process domains.

Table 6: Summary of significant differences in variables between stream types in fluvial valleys. Cas refers to cascade, SP refers to step-pool, RR refers to riffle-run, PB refers to plane-bed, PR refers to pool-riffle. 'Yes' refers to significant difference at alpha = 0.05. An * refers to significant difference at alpha = 0.10.

FLUVIAL - Slope

	Cas	SP	RR	PB
SP	no			
RR	yes	yes		
PB	yes	yes	no	
PR	yes	yes	no	no

FLUVIAL - D_{50}

	Cas	SP	RR	PB
SP	no*			
RR	no	no		
PB	yes	no	no*	
PR	no	no	no	no

FLUVIAL - Slope DEM

	Cas	SP	RR	PB
SP	no			
RR	no*	yes		
PB	no	no	no	
PR	yes	yes	no	no

FLUVIAL - D_{84}

	Cas	SP	RR	PB
SP	yes			
RR	no*	no		
PB	no	no	no	
PR	no	no	no	no

FLUVIAL - Depth

	Cas	SP	RR	PB
SP	yes			
RR	no	no		
PB	yes	no	no	
PR	no*	no	no	no

FLUVIAL - Width

	Cas	SP	RR	PB
SP	yes			
RR	no	no*		
PB	no	no	no	
PR	no	no	no	no

FLUVIAL - W/D

	Cas	SP	RR	PB
SP	yes			
RR	no	yes		
PB	yes	no	yes	
PR	no	no	no	yes

Table 7 shows that D_{50} and D_{84} are not typically significantly different for a stream type between the valley types, with the exception of plane-bed streams. Slope is significantly different between glacial and fluvial step-pools regardless of statistical method and between glacial and fluvial cascades and glacial and fluvial plane-beds, depending on statistical method. Other stream types do not have significant differences in slope between valley types. Significant differences in *D, W,* and *W/D* between glacial and fluvial valleys typically occur with cascade and plane-bed streams, but not between valley types for other stream types. Riffle-run streams display no significant differences between valley types for any of the channel geometry characteristics, nor do pool-riffle streams. In summary, some stream types support the *H3* alternative with respect to differences of channel geometry between valley types, but no stream displays significant differences for every variable and riffle-run and pool-riffle streams do not support the *H3* alternative. The *H3* alternative hypothesis is partly supported, but on the whole is not supported.

Table 7: Summary of significant differences in variables between valley types (glacial versus fluvial) by stream type. The student's t test could only be performed on variables that displayed normality. The Wilcoxon Rank Sum test was required for non-normal variables; normal variables were tested as well. 'Yes' refers to significant difference at alpha = 0.05. An * refers to significant difference at alpha = 0.10.

Student's t test

	Slope	**S DEM**	**Width (m)**	**Depth (m)**	**W/D**	**D_{50} (mm)**	**D_{84} (mm)**
Cascade	no*	no		no	yes	no	
Step-pool	yes	yes		no	no	no	
Riffle-run	no	no		no	no*	no	
Plane-bed	no	no		yes	no*	yes	
Pool-riffle	no	no		no	no	no	

Wilcoxon Rank Sum test

	Slope	**S DEM**	**Width (m)**	**Depth (m)**	**W/D**	**D_{50} (mm)**	**D_{84} (mm)**
Cascade	no*	no	yes	no*	yes	no	no
Step-pool	yes	yes	no	no	no	no	no
Riffle-run	no	no	no	no	no	no	no
Plane-bed	yes	no	yes	no*	yes	no*	no
Pool-riffle	no	no	no	no	no	no	no

Hypothesis $4_{\text{alternative}}$: Streams exhibit significantly different mean channel geometry characteristics between different levels of confinement.

Table 8 shows that *W* and *W/D* are not significantly different for streams between confinement types. D_{50} and D_{84} (and *D* and *S* at alpha=0.10) are significantly different between confined streams and all other streams. Partly confined streams are not significantly different from unconfined streams for any channel geometry characteristics. In summary, some streams support the *H4* alternative with respect to differences of channel geometry between confinement types, but no confinement type displays significant differences for every variable and partly confined streams are not different from unconfined streams. The *H4* alternative hypothesis is partly supported.

Table 8: Summary of significant differences in variables between confinement types. ‘Conf’ refers to confined valleys, ‘P. Conf’ refers to partly confined valleys. ‘Unconf’ refers to unconfined valleys. ‘Yes’ refers to significant difference at alpha = 0.05. An * refers to significant difference at alpha = 0.10.

Slope

	Conf	P. Conf
P. Conf	yes	
Unconf	no*	no

D_{50}

	Conf	P. Conf
P. Conf	yes	
Unconf	yes	no

SDEM

	Conf	P. Conf
P. Conf	yes	
Unconf	no	no

D_{84}

	Conf	P. Conf
P. Conf	yes	
Unconf	yes	no

Depth

	Conf	P. Conf
P. Conf	no*	
Unconf	no*	no

Width

	Conf	P. Conf
P. Conf	no	
Unconf	no	no

W/D

	Conf	P. Conf
P. Conf	no	
Unconf	no	no

3.3 Objective 3

Hypothesis $5_{\text{alternative}}$: Field-delineated stream types differ from stream types predicted from Sklar and Dietrich’s diagram using slope and drainage area.

The hypothetical bedrock-coarse-bed transition proposed by Sklar and Dietrich (1998) takes the form of:

$$\mathbf{S = 0.07A^{-0.5}} \qquad \mathbf{(4)}$$

where *S* is slope in m/m and *A* is drainage area in km^2. This line was plotted on an *S*-*A* diagram with all reaches plotted by predominant substrate. In every combination of plotting reaches, neither of the hypothetical transition lines divided bedrock and coarse-bed reaches. In fact, the hypothetical transition line does not appear to coincide with any transition with the Colorado Front Range dataset in this study. Figure 10 shows the *S-A* diagram with all reaches, with black shapes indicating glacial sites and white shapes indicating fluvial sites. The bedrock-coarse bed transition line associated with my data has an intermediate intercept with a gentler slope than that proposed by previous studies. Bedrock (with alluvium) reaches are surrounded by boulder reaches and cobble reaches, meaning that coarse-bed alluvium reaches are not plotting separately from bedrock reaches, although size of predominant substrate does appear to grade nicely from bedrock to pebble reaches toward the lower left corner on the figure. The one sand reach is anomalous, as it was located in a morphology forced by instream wood.

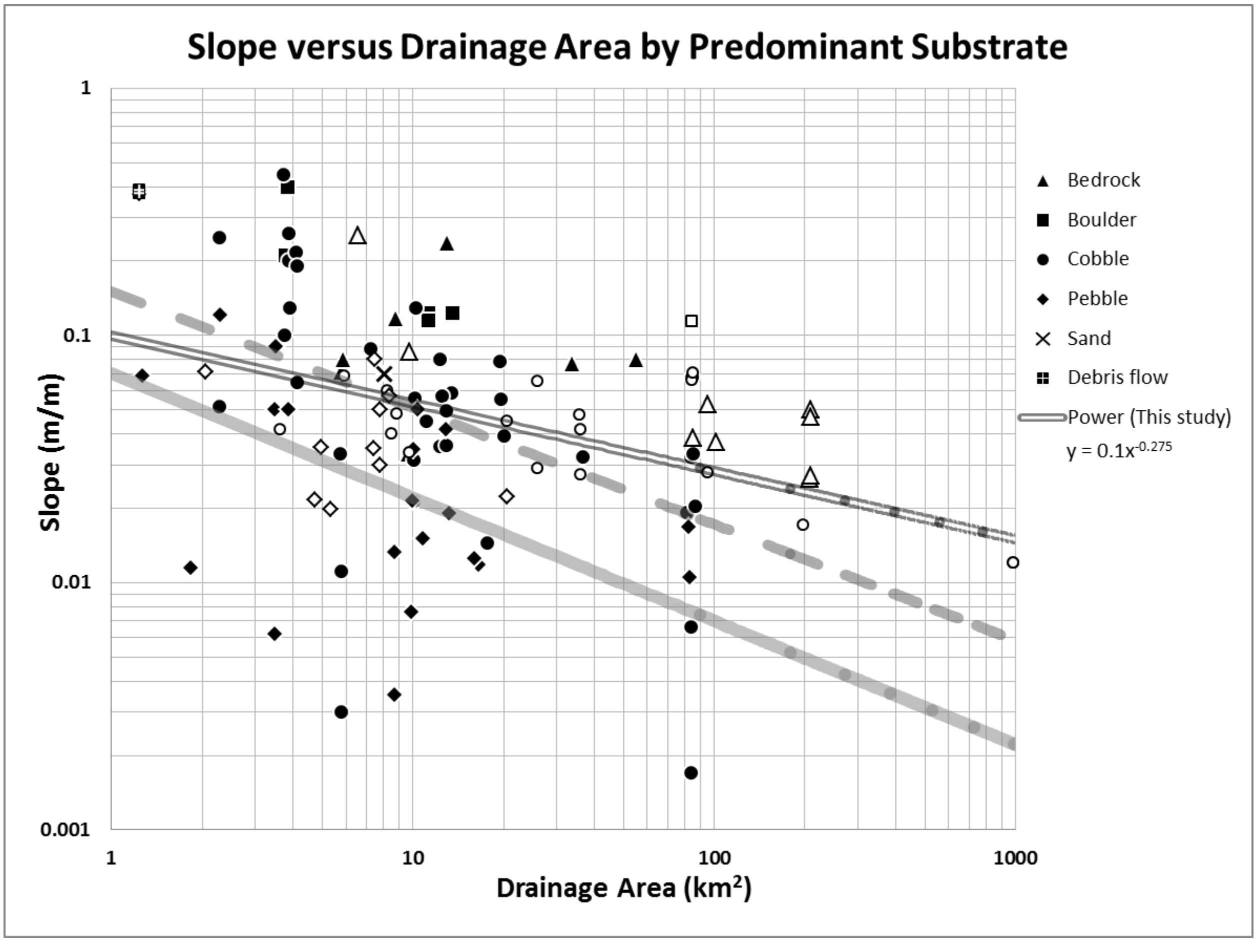

Figure 10: *S-A* diagram with all reaches. Black shapes indicate glacial sites; white shapes indicate fluvial sites. The solid gray line represents the Sklar and Dietrich (1998) hypothetical bedrock-coarse bed transition; the dashed gray line represents the Addy et al. (2011) bedrock-coarse bed transition; the white line with solid gray outline represents the bedrock-coarse bed transition for this study.

When examining reaches plotted by predominant substrate according to valley history, fluvial bedrock reaches are more clearly located above most other fluvial reaches, with the exception of a few boulder and cobble sites. The pattern of grading to finer substrate occurs as it did using all reaches. For glacial reaches, however, bedrock reaches plot within an area that also contains many boulder and cobble reaches. The pattern of grading to finer substrate is less pronounced for the glacial reaches.

When reaches are plotted on the *S-A* diagram by confinement according to valley history (Figure 11), fluvial reaches grade nicely from confined reaches to partly confined reaches to unconfined reaches moving toward the lower left corner of the plot. For glacial reaches, confined reaches typically plot above partly confined reaches, but confined reaches are scattered throughout the plot; there is not a clear

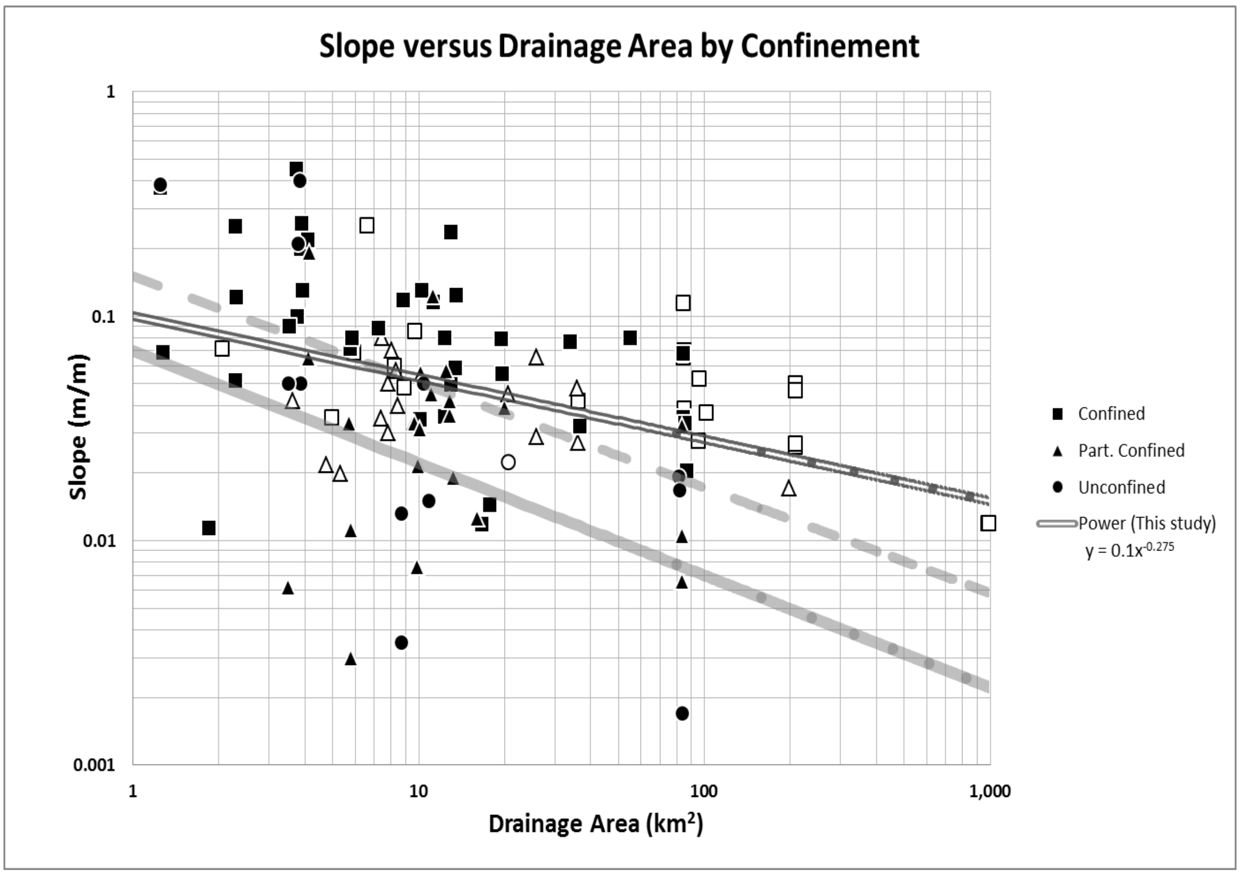

Figure 11: *S-A* diagram with all reaches plotted by confinement. Black shapes indicate glacial sites; white shapes indicate fluvial sites. The solid gray line represents the Sklar and Dietrich (1998) hypothetical bedrock-coarse bed transition; the dashed gray line represents the Addy et al. (2011) bedrock-coarse bed transition; the white line with solid gray outline represents the bedrock-coarse bed transition for this study.

distinction between different confinements in glacial valleys on an *S*-*A* plot. The *H5* alternative hypothesis is supported.

Hypothesis 6$_{\textbf{alternative}}$: Categories of stream type populations will not cluster together in discrete areas when plotted on an *S*-*A* diagram.

Figure 12 shows where stream types plot on the *S*-*A* diagram. While there is some overlap of stream types within the diagram, there is a pattern of stream type from upper left to lower right in order of decreasing slope according to Montgomery and Buffington (1997); i.e., cascade to pool-riffle. For the most part, the stream type populations do cluster by stream type, with the spread varied, but interpretation

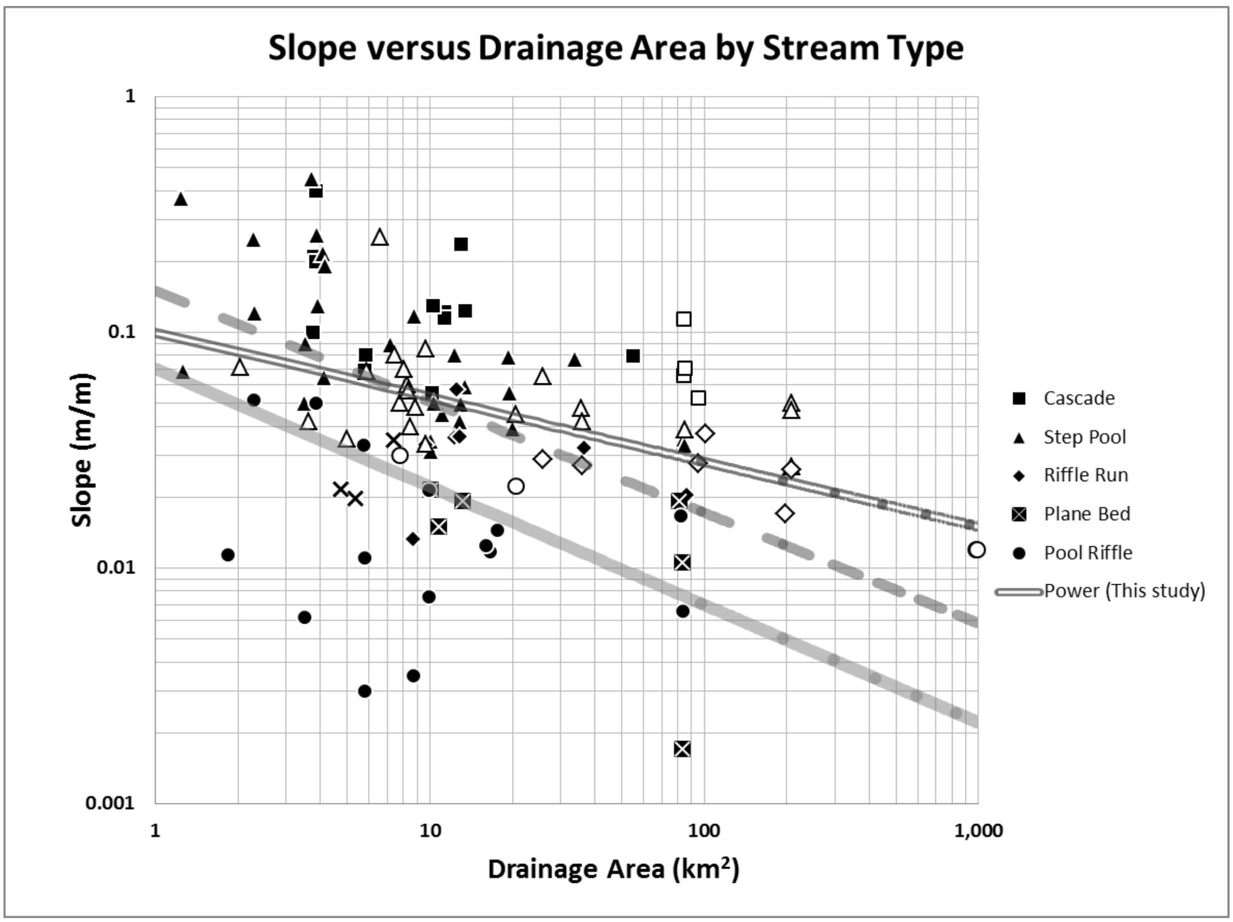

Figure 12: *S*-*A* diagram with all reaches plotted by Montgomery and Buffington (1997) stream type. Black shapes indicate glacial sites; white shapes indicate fluvial sites. The solid gray line represents the Sklar and Dietrich (1998) hypothetical bedrock-coarse bed transition; the dashed gray line represents the Addy et al. (2011) bedrock-coarse bed transition; the white line with solid gray outline represents the bedrock-coarse bed transition for this study.

of how reach types plot is limited due to the different number of reaches per type. The *H6* alternative hypothesis is not supported.

3.4 Objective 4

Objective 4: The fourth objective of this research was to assess downstream hydraulic geometry relationships in streams in the Colorado Front Range using the morphological characteristics (*W* or *D* versus *Q*) collected in the field.

Appendix G provides the plots made for each of the relationships studied for objective 4. Table 9 lists the summary of the results of downstream hydraulic geometry power relationships for *W* versus *Q* as fit for the different groups of data. The basic equation that corresponds to this relationship is:

$$\mathbf{W = aQ^b} \qquad \mathbf{(5)}$$

where *W* is bankfull width of the channel in meters, *Q* is 2-year peak discharge in m^3/s, and *a* and *b* vary according to the best fit of the data. All the power relationships have good correlation (R^2) values,

Table 9: Coefficients, exponents, and R^2 values for downstream hydraulic geometry power relationships of width versus discharge for different groups of reaches.

Width versus Discharge			
	Coefficient (a)	Exponent (b)	R^2
All data	2.3789	0.6282	0.7365
Glacial (G)	2.1504	0.6864	0.6672
Fluvial (F)	2.6683	0.5778	0.8694
Confined	2.6223	0.5760	0.7473
Part. Confined	2.4180	0.6908	0.7309
Unconfined	1.3587	0.7970	0.8867
G Confined	2.3962	0.6024	0.6361
G Part. Confined	2.4383	0.7237	0.5941
G Unconfined	1.2846	0.7995	0.9208
F Confined	3.1825	0.5260	0.8880
F Part. Confined	2.3584	0.5871	0.7525
Cascade	2.1232	0.7813	0.7969
Step-pool	2.1660	0.6325	0.7809
Riffle-run	2.0292	0.6465	0.9354
Plane-bed	3.0216	0.5686	0.7468
Pool-riffle	3.3545	0.4598	0.4064

meaning there is a well-defined, positive relationship between *W* and *Q*. While the relationship with all data is very good ($R^2 = 0.7365$), a pattern emerges when the reaches are divided into subgroups and fit to a power relationship.

When reaches are divided into glacial sites versus fluvial sites, the corresponding correlation value for fluvial sites is higher than the correlation value for all sites, while the corresponding correlation value for glacial sites is lower. When reaches are divided into confinement types, correlation values are equal to or greater than correlation values associated with all data, with unconfined reaches displaying the greatest correlation between *W* and *Q*. When reaches are divided into full process domain, excluding fluvial unconfined because there is only one reach, fluvial sites still have typically higher correlation values than glacial sites except for glacial unconfined sites, which are very well correlated. When reaches are divided into stream type, correlation between *W* and *Q* is greater than for all data in every case except pool-riffle reaches.

Table 10 lists the summary of the results of downstream hydraulic geometry power relationships for *D* versus *Q* as fit for the different groups of data. The basic equation that corresponds to this relationship is:

$$\mathbf{D = cQ^f} \qquad \mathbf{(6)}$$

where *D* is bankfull depth of the channel in meters, *Q* is 2-year peak discharge in m^3/s, and *c* and *f* vary according to the best fit of the data. The relationship between *D* and *Q* is well-defined ($R^2 = 0.572$), but not as well as the relationship between *W* and *Q*.

Much like *W* versus *Q*, *D* versus *Q* becomes more correlated in all fluvial sites and less correlated in all glacial sites in comparison to the relationship using all data. When reaches are divided into confinement types, confined reaches display the best relationship between *D* and *Q*. When reaches are divided into full process domain, excluding fluvial unconfined because there is only one reach, all reach groups except fluvial partly confined and glacial partly confined display better correlation than using all data at once. When reaches are divided into stream type, step-pools display the greatest *D*-*Q* relationship, while all other stream types have lower correlation values than when using all data at once.

Table 10: Coefficients, exponents, and R^2 values for downstream hydraulic geometry power relationships of depth versus discharge for different groups of reaches.

Depth versus Discharge			
	Coefficient (c)	Exponent (f)	R^2
All data	0.3861	0.2827	0.572
Glacial (G)	0.3862	0.2786	0.4579
Fluvial (F)	0.3876	0.2865	0.7237
Confined	0.4055	0.2929	0.6858
Part. Confined	0.3975	0.2195	0.3963
Unconfined	0.3176	0.2996	0.4553
G Confined	0.3941	0.3151	0.6602
G Part. Confined	0.4726	0.1265	0.0945
G Unconfined	0.3186	0.2994	0.4552
F Confined	0.4227	0.2729	0.6936
F Part. Confined	0.3733	0.2277	0.5656
Cascade	0.5267	0.2466	0.4850
Step-pool	0.3677	0.3320	0.7139
Riffle-run	0.3947	0.2372	0.3135
Plane-bed	0.4579	0.1490	0.3665
Pool-riffle	0.3593	0.2043	0.4649

Summary of Results of Hypotheses:

$H1_a$: Categories of stream type populations exhibit significantly different mean channel geometry characteristics.

Partly supported: S, D_{50} and D_{84} effectively distinguish most stream types, but the specific variables that most effectively distinguish stream types vary slightly between process domains and between degrees of valley confinement.

$H2_a$: Categories of stream type populations exhibit significantly different mean channel geometry characteristics within a process domain.

Partly supported: although S, D_{50} and D_{84} distinguish most stream types within the glacial process domain, and S and W/D distinguish most stream types within the fluvial process domain, none of the variables are able to consistently distinguish between all stream types within a process domain.

$H3_a$: Individual stream type populations exhibit significantly different mean channel geometry characteristics between process domains.

Not supported: although a few variables differ between process domains for one or two stream types, no variable differs consistently between process domains for all stream types.

$H4_a$: Streams exhibit significantly different mean channel geometry characteristics between different levels of confinement.

Not supported: no channel geometry characteristic varies consistently among different levels of confinement.

$H5_a$: Field-delineated stream types differ from stream types predicted from Sklar and Dietrich's diagram using slope and drainage area.

Supported: Sklar and Dietrich's *S*-*A* transition line for bedrock versus alluvial channels does not effectively coincide with any distinction in channel substrate or channel type in the Colorado Front Range dataset.

$H6_a$: Categories of stream type populations will not cluster together in discrete areas when plotted on an *S*-*A* diagram.

Not supported: stream types do cluster in discrete areas on an *S*-*A* diagram.

4 DISCUSSION

Classification of stream reaches in this study into Montgomery and Buffington (1997) stream types was based on visual approximation of predominant bedforms with the assumption that different streams types would be distinguished by specific gradients and channel geometry characteristics. The analysis associated with distinguishing between Montgomery and Buffington (1997) stream types indicates that no single variable or succinct combination of variables consistently discriminates among all stream types, but reach-scale gradient and substrate size appear to be the most successful channel geometry parameters in delineating stream types. Also, because stream types typically do not differ significantly between process domains or levels of confinement, both *S* and substrate size could be used to distinguish channel types across an entire region. However, because gradients associated with specific stream types in this study do not necessarily match the slopes predicted by Montgomery and Buffington (1997) for streams in the Pacific Northwest (Figure 13), predicting stream types in future studies would require regional calibration of *S* for stream types. DEMs, which can predict reach-scale *S* to some degree of accuracy, could then be used in conjunction with regional calibration of stream types to remotely approximate the spatial distribution of channel types throughout a catchment.

Although statistical results do not necessarily indicate that channel geometry characteristics of stream types are significantly different in all sites, between process domains, or within a process domain, reaches in glacial terrain display much more variability in channel geometry characteristics than reaches in fluvial terrain. This is evidenced by the range of values of channel geometry (Table 2, Appendix C), greater difficulty in classifying stream types in a classification tree, less pronounced downstream hydraulic geometry relationships in glacial sites in comparison to fluvial sites, and greater scatter of glacial sites on an *S*-*A* diagram. In addition, stream types are distinguished differently according to process domain – fluvial sites do not require measures of substrate to delineate between stream types, whereas glacial sites do.

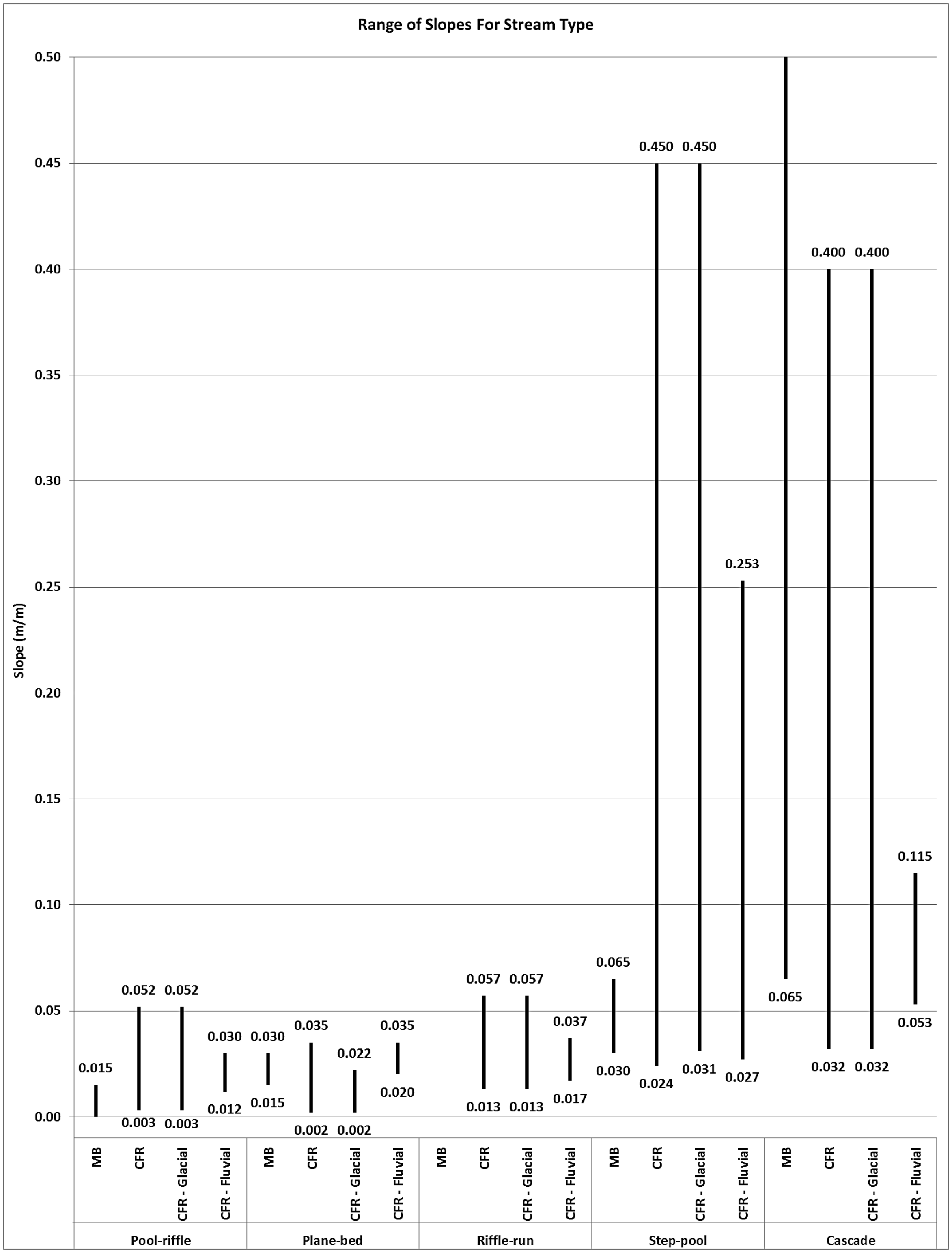

Figure 13: Comparison of Montgomery and Buffington (MB) (1997) stream type slope ranges versus slope ranges found in this study for the Colorado Front Range (CFR) and slope ranges by valley type.

The analysis of reach slopes derived from 10-meter DEMs in comparison to field-derived slopes indicated that DEMs of that scale are more reliable in glacial terrain than fluvial terrain. This is likely due to the fact that glacial valleys are more wide and flat, with stream channels being more discernible in an open environment as compared to the steeply-dipping hillslopes and narrow stream channels of fluvial valleys, which create uncertainty of depth and width on topographic maps. Furthermore, Figure 5 indicates that 10-meter DEMs tend to underestimate field slope, which is likely due to the scale of DEMs and could be more accurate with more precise DEMs. However, confinement can also be mapped from DEMs, and our understanding of how confinement affects stream morphology can assist in remote delineation of stream morphology and processes. Given the importance of headwater streams in the context of the entire river network (e.g., occupying the majority of stream length, supplying food and habitat for diverse and unique species, locations of sediment production), the uncertainty of DEM-derived slopes, and the discovery that slope alone does not dictate stream type, I suggest that those interested in management of mountain streams still be required to perform some degree of field calibration in order to formally understand stream morphology and processes at the reach scale, at least in the Colorado Front Range.

While the results of the downstream hydraulic geometry analysis indicate strong relationships of width and depth with discharge, indicating some degree of longitudinal progression, stream type does not appear to display any progressive pattern along longitudinal stream profiles (Figure 4, Appendix D). In both glacial terrain and fluvial terrain there is no clear progression of stream type; step-pools are located in many different drainage areas and are commonly preceded upstream by plane-bed or pool-riffle reaches. Also, despite the lack of significant differences in channel geometry between process domains, there does appear to be a difference in relative abundance of stream types according to process domains and confinement. For instance, confined valleys typically have cascade or step-pool morphology and cascades are more common in glacial valleys (Table 1).

In addition, stream types in the Colorado Front Range do not necessarily coincide with Montgomery and Buffington's (1997) classification of slope in that they exist with a very wide range of slopes that overlap significantly, particularly in glacial terrain (Figure 13). Low-gradient reaches in fluvial terrain match fairly well with slope values predicted by Montgomery and Buffington in the Pacific Northwest, but step-pools have much greater slopes, both in fluvial and glacial terrain, than the range published for the Pacific Northwest. The steepest mountain reaches were previously predicted to be cascades, and, although they are very steep in the Colorado Front Range, the steepest reach in this study is a step-pool, which has a gradient of 0.45; the steepest reach in fluvial terrain is also a step-pool. Step-pools are the most dominant stream morphology type in the study area in the Colorado Front Range and are found over very wide ranges of gradient. Because step-pool reaches are typically found in confined valleys (Table 1), confinement could be dictating the location, abundance, and higher slopes found in the Colorado Front Range.

Confined streams are typically significantly different from other confinement types in regards to slope, substrate, and depth, and confined streams are more typically cascade or step-pool morphology (Table 1). The locations of confined streams along the longitudinal profile, as well as the great variability among glacial reaches, indicate that both confinement and valley history, or local process domains, create local-scale variability that overrides clear patterns in the longitudinal stream profile. This suggests that streams located in glacial process domains continue to adjust to inherited glacial terrain (valley geometry, sediment supply), whereas streams located in fluvial terrain are better adjusted in their valleys relative to present water and sediment supply.

In regards to the *S-A* diagram, the data collected in this study appear to have a bedrock-coarse bed transition that has an intermediate intercept and gentler slope in comparison to the relations proposed by Sklar and Dietrich (1998) or Addy et al. (2011), which evaluated the transition in more humid environments than the Colorado Front Range. It intuitively makes sense that, for the semi-arid region of the Colorado Front Range, there is less discharge per drainage area, and steeper slopes per drainage area, than the other empirical data set (Addy et al., 2011), which comes from Scotland. Higher slopes are needed in the Front Range to create enough stream power to initiate bedrock incision. Lower discharge per unit drainage area in the Front Range than in many other mountainous regions may also help to explain the preponderance of very steep channel types (cascade and step-pool reaches) within the study area.

While the transitions between substrate types may have different locations on the Front Range and hypothetical *S*-*A* diagrams, the pattern of substrate fining is similar to Sklar and Dietrich's hypothetical diagram. Table 1 also illustrates substrate fining as *S* decreases, which corresponds to the Montgomery and Buffington (1997) classification. The boundaries separating streams of diverse substrate types are much less pronounced than the Sklar and Dietrich diagram implies, however, as illustrated by the coarse-bed channel reaches that plot well above the bedrock *S*-*A* threshold in Figure 10. At least some outliers occur in both directions: cobble-bed channels with small *S* and large *A* values, and pebble-bed channels with large *S* and small *A* values. The numerous outliers relative to predicted patterns suggest that local controls beyond *S* and *A* strongly influence stream substrate in the Front Range. An example of such a local control could be coarse sediment relict from glacial processes at higher elevations, or introduced by rockfall within the fluvial process domain.

Although previous studies found weak or limited downstream hydraulic geometry relationships in mountain rivers (Wohl et al., 2004; Wohl, 2004), the greater spatial variation and sample size associated with this study did find significant downstream hydraulic geometry relationships for the Colorado Front Range. Exponent values for both depth and width relationships are within the range proposed by Park (1977), but the average exponent for width (0.63) is higher and the average exponent for depth (0.28) is lower than those proposed by Leopold and Maddock (1953). In comparison to empirically derived hydraulic geometry equations for mountain streams in Colorado obtained in Eaton and Church (2007), this study has lower values for the width coefficient and higher exponent values; depth coefficients and exponents are both higher in this study than values expected by Eaton and Church (2007). These comparisons indicate that streams in the Colorado Front Range become wider more quickly downstream than many other streams, yet become deeper at a slower rate downstream than many other streams. The most revealing pattern in the analysis of downstream hydraulic geometry is that fluvial sites have more well-developed downstream hydraulic geometry relationships than glacial sites, likely due to the variability associated with glacial history; unconfined streams have well-developed width versus discharge relationships, likely due to the ability of a stream to adjust its width according to changing discharge; confined streams have well-developed depth versus discharge relationships, as stream depth can more readily rise in the event of increased streamflow; and downstream width relationships, but not depth relationships, are well-developed when reaches are divided into stream type, except for pool-riffles, indicating that width of a stream may be more a function of discharge, whereas depth is a function of confinement.

The question of the validity of progressive downstream trends versus the influence of local variability in predicting morphology of headwater mountain streams was thoroughly explored in this study. As end-member concepts, neither approach fully describes stream morphology in the Colorado Front Range. Although downstream hydraulic geometry relationships indicate progressive downstream trends in the study area, glacial history overrides the relationship of width and depth of streams in glaciated terrain. Previous studies on downstream progression of *S* (Montgomery and Buffington, 1997) and *S*-*A* relationships do not match the results in the Colorado Front Range, either. The strong variation in valley confinement dictates the locations of certain stream types as well. Because of the clear role that process domains play in local channel geometry characteristics and prediction, I believe that local variability more accurately describes channel morphology and must be evaluated in studies involving headwater mountain streams.

5 CONCLUSIONS

Delineation of Montgomery and Buffington (1997) stream types for the Colorado Front Range as visually categorized in the field indicated a lack of consistent differences in channel geometry characteristics among stream types. Although reach-scale *S* and substrate size effectively distinguish most stream types, the specific variable that most effectively distinguishes stream types varies between process domains and between different degrees of confinement. Process domains, which influence local sediment and water dynamics, play an integral role in reach-scale channel morphology and channel geometry of headwater mountain streams. Streams located in glacial valleys in the Colorado Front Range flow over inherited terrain, causing large variability in channel geometry characteristics and hence difficulty in prediction of morphology due to continued adjustment to sediment and water dynamics. This variability is expressed in larger ranges of channel geometry characteristics in glacial versus fluvial reaches, greater difficulty in classifying glacial stream types in a classification tree, less pronounced downstream hydraulic geometry relationships in glacial sites in comparison to fluvial sites, and greater scatter of glacial sites on an *S-A* diagram. Streams located in confined valleys typically have different slopes, substrate sizes, and depths than streams located in other levels of valley confinement.

This study supplements previous studies that investigated prediction of mountain stream morphology and channel geometry by providing regional data from the semi-arid, tectonically stable Colorado Front Range. Drier conditions in the study area lead to less discharge per drainage area, and stream types are associated with greater slopes per drainage area than previous studies in more humid regions. In the study area, local variability in valley type and sediment dynamics override longitudinal downstream progression in channel morphology and geometry characteristics. The disproportionately high importance of headwater mountain streams in regards to total stream length, biological productivity and habitat, and sediment production, combined with the difficulty of morphology prediction due to local variability in valley type and sediment dynamics, indicate the need for field-calibration and verification from managers and agencies in future research and restoration projects in the Colorado Front Range.

5.1 Future Work

Future work associated with this study could include supplementing the data set with additional reaches with fluvial sites in general, more fluvial unconfined sites, and more plane-bed reaches. Using these data, researchers could test the downstream hydraulic geometry relationships among other sites in the South Platte River watershed. DEM slopes and slope ranges from this study could be used to remotely map the entire South Platte River watershed by stream type or process domain and test the accuracy of predicting other reaches from conclusions in this study. Given the findings of continued adjustment of streams in glacial valleys, future work could also include looking at glacial terrain from a mechanistic perspective to determine and quantify how glacial valleys are adjusting over time and how one could use such information to predict stream types and channel geometry.

6 REFERENCES

Addy, S., C. Soulsby, A.J. Hartley and D. Tetzlaff. 2011. Characterisation of channel reach morphology and associated controls in deglaciated montane catchments in the Cairngorms, Scotland. Geomorphology 132, 176-186.

Amerson, B.E., D.R. Montgomery, and G. Meyer. 2008. Relative size of fluvial and glaciated valleys in central Idaho. Geomorphology 93, 537-547.

Anderson, R.S, C.A. Riihimaki, E.B. Safran, and K.R. MacGregor. 2006. Facing reality: Late Cenozoic evolution of smooth peaks, glacially ornamented valleys, and deep river gorges of Colorado’s Front Range, in S.D. Willet et al., eds., Tectonics, climate, and landscape evolution: Geological Society of America Special Paper 398, Penrose Conference series, 397-418, doi: 10.1130/2006.2398(25)

Braddock, W.A., and J.C. Cole. 1990. Geologic map of Rocky Mountain National Park and vicinity. U.S. Geological Survey Miscellaneous Investigation Series, Colorado. Map I-1973, scale 1:50,000, 1 sheet.

Brardinoni, F., and M.A. Hassan. 2007. Glacially induced organization of channel-reach morphology in mountain streams. J. Geophys. Res. 112, F03013, doi:10.1029/2006JF000741.

Buffington, J.M., and D. Tonina. 2009. Hyporheic exchange in mountain rivers II: effects of channel morphology on mechanics, scales, and rates of exchange. Geography Compass 3, doi:10.111/.1749-8198.2009.00225.x

Buffington, J.M., D.R. Montgomery, and H.M. Greenberg. 2004. Basin-scale availability of salmonid spawning gravel as influenced by channel type and hydraulic roughness in mountain catchments. Can. J. Fish. Aquat. Sci. 61, 2085-2096

Capesius, J.P., and V.C. Stephens. 2009. Regional regression equations for estimation of natural streamflow statistics in Colorado: U.S. Geological Survey Scientific Investigations Report 2009–5136, 46 p.

Eaton, C.E. and M. Church. 2007. Predicting downstream hydraulic geometry: A test of rational regime theory. J. Geophys. Res. 112, F03025, doi:10.1029/2006JF000734.

Ehlen, J. and E. Wohl. 2002. Joints and landform evolution in bedrock canyons. Transactions, Japanese Geomorphological Union 23-2, 237-255.

Flores, A. N., B.P. Bledsoe, C.O. Cuhaciyan, and E.E. Wohl. 2006. Channel-reach morphology dependence on energy, scale, and hydroclimatic processes with implications for prediction using geospatial data. Water Resources Research 42, W06412, doi: 10.1029/2005WR004226.

Freeman, M.C., C.M. Pringle, and C.R. Jackson. 2007. Hydrologic connectivity and the contribution of stream headwaters to ecological integrity at regional scales. Journal of the Am. Water Resources Association 43-1, 5-14.

Gomi, T., R.C. Sidle, and J. S. Richardson. 2002. Understanding processes and downstream linkages of headwater systems. BioScience 52-10, 905-916.

Leopold, L.B., and T.M. Maddock. 1953. The hydraulic geometry of stream channels and some physiographic implications. USGS Professional Paper 252, 57 p.

Meyer, J.L, D.L. Strayer, J.B. Wallace, S.L. Eggert, G.S. Helfman, and N.E. Leonard. 2007. The contribution of headwater streams to biodiversity in river networks. Journal of the Am. Water Resources Association 43-1, 86-103.

Milliman, J.D., and J.P.M. Syvitski. 1992. Geomorphic/tectonic control of sediment discharge to the ocean: the importance of small mountainous rivers. Journal of Geology 100, 525-544.

Montgomery, D.R. 1999. Process domains and the river continuum. Journal of the Am. Water Resources Association 35, 397-410.

Montgomery, D.R., and J.M. Buffington. 1997. Channel-reach morphology in mountain drainage basins. Geological Society of America Bulletin 109, 596-611.

Montgomery. D.R., T.B. Abbe, J.M. Buffington, N.P. Peterson, K.M. Schmidt, and J.D Stock. 1996. Distribution of bedrock and alluvial channels in forested mountain drainage basins. Letters to Nature 138, 587-589.

Ott, R. L., and M. Longnecker, 2010. An introduction to statistical methods and data analysis, Sixth edition. Belmont, CA: Brooks/Cole.

Park, C.C. 1977. World-wide variations in hydraulic geometry exponents of stream channels: an analysis and some observations. Journal of Hydrology 33, 133-146.

Polvi, L.E., E.E. Wohl and D.M. Merritt. 2011. Geomorphic and process domain controls on riparian zones in the Colorado Front Range. Geomorphology 125, 504-516.

Royston, P. 1982. An extension of Shapiro and Wilk's W test for normality to large samples. Applied Statistics 31, 115-124.

Sklar, L., and W.E. Dietrich. 1998. River longitudinal profiles and bedrock incision models: stream power and the influence of sediment supply. In, Rivers over rock: fluvial processes in bedrock channels, Tinkler and Wohl, eds., Am. Geophysical Union Press, pp. 237-260.

Thompson, C., J. Croke, and I. Takken. 2008. A catchment-scale model of mountain stream channel morphologies in southeast Australia. Geomorphology 95, 119-144.

USGS National Water Information System. 2013. USGS 402114105350101 Big Thompson bl Moraine Park nr Estes Park, CO. <http://waterdata.usgs.gov/co/nwis/nwisman/?site_no=402114105350101>. Accessed 19 April 2013.

Vannote, R.L., G.W. Minshall, K.W. Cummins, J.R. Sedell, and C.E. Cushing. 1980. The river continuum concept. Can. J. Fish. Aquat. Sci. 37, 130-137.

Wohl, E. 2004. Limits of downstream hydraulic geometry. Geology 32, 897-900.

Wohl, E. 2010a. A brief review of the process domain concept and its application to quantifying sediment dynamics in bedrock canyons. Terra Nova 22, 411-416.

Wohl, E. 2010b. Mountain rivers revisited. American Geophysical Union Press, Washington, D.C.

Wohl, E. 2011a. Threshold-induced complex behavior of wood in mountain streams. Geology 39, 587-590.

Wohl, E. 2011b. What should these rivers look like? Historical range of variability and human impacts in the Colorado Front Range, USA. Earth Surface Processes and Landforms 36, 1378-1390.

Wohl, E., N.D. Beckman. 2013. Leaky rivers: implications of the loss of longitudinal fluvial disconnectivity in headwater streams, Geomorphology, doi:10.1016/j.geomorph.2011.10.022

Wohl, E., D. Cooper, L.R. Poff, F. Rahel, D. Staley, and D. Winters. 2007. Assessment of stream ecosystem function and sensitivity in the Bighorn National Forest, Wyoming. Environmental Management 40, 284-302.

Wohl, E., J.N. Kuzma and N.E. Brown. 2004. Reach-scale channel geometry of a mountain river. Earth Surface Processes and Landforms 29, 969-981.

Wohl, E. and D.M. Merritt. 2005. Prediction of mountain stream morphology. Water Resources Research 41, doi:10.1029/2004WR003779.

Wohl, E., and D.M. Merritt. 2008. Reach-scale channel geometry of mountain streams. Geomorphology 93, 168-185.

Wohl, E., K. Dwire, N. Sutfin, L. Polvi, and R. Bazan. 2012. Mechanisms of carbon storage in mountainous headwater rivers. Nature Communications 3:1263, doi:10.1028/ncomms2274.
Wolman, M.G. 1954. A method of sampling coarse river-bed material. Eos Trans. AGU 35, 951-956.

7 APPENDICES

7.1 Appendix A: Valley geometry comparisons

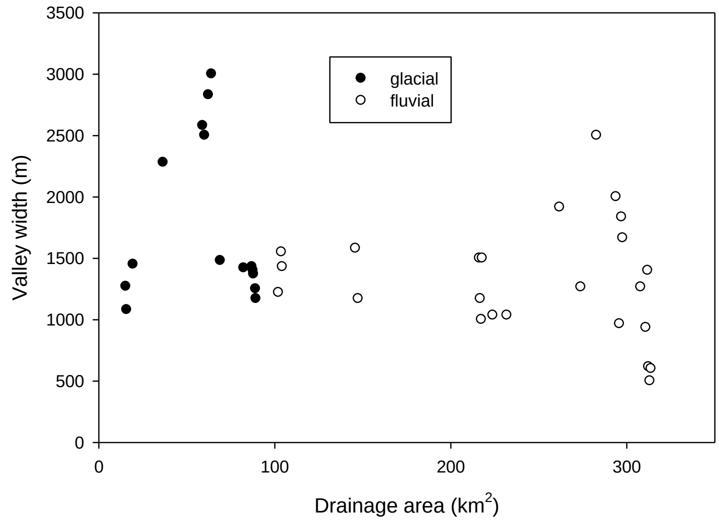

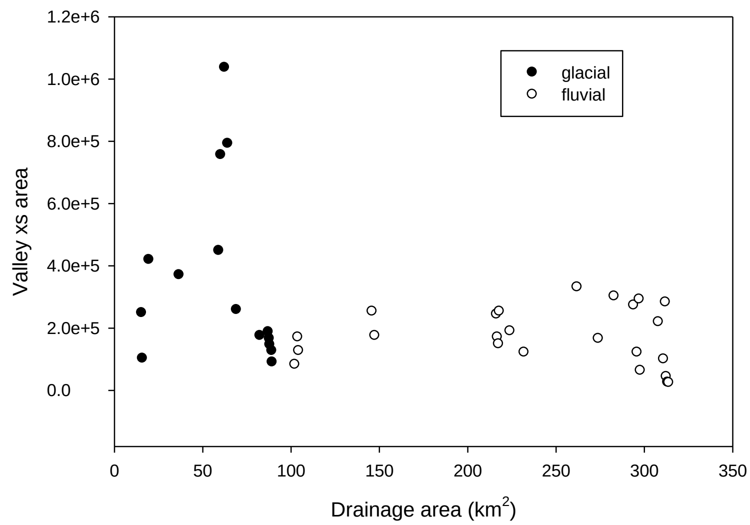

Figure 14: Plots of valley width versus drainage area and valley cross-sectional area versus drainage area do not show any clear trends, in contrast to studies from the Pacific Northwest and Idaho. Data: 15 glacial valley cross sections and 24 fluvial valley cross sections.

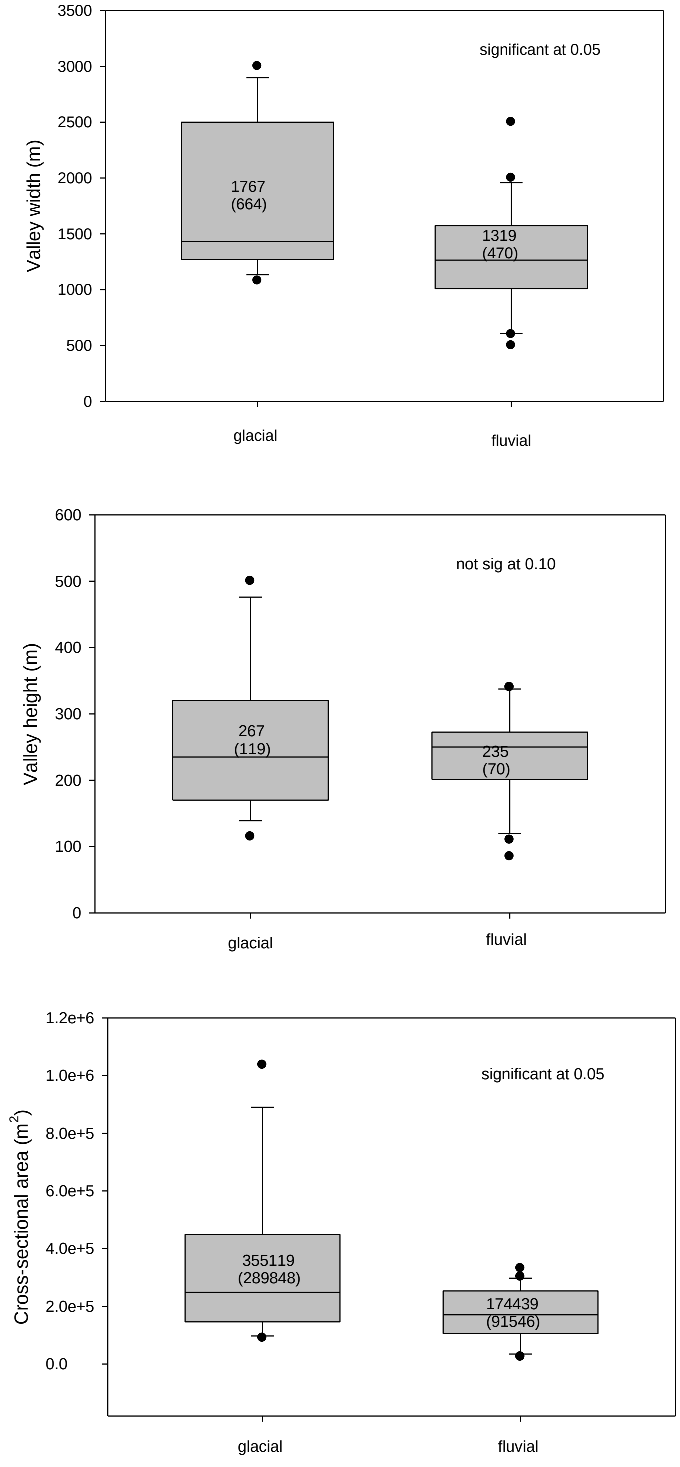

Figure 15: Box plots of valley width, valley height, and valley cross-sectional area for glacial versus fluvial valley segments indicate significant differences in valley width and valley cross-sectional area, with glacial valleys wider and larger. Data: 15 glacial valley cross sections and 24 fluvial valley cross sections.

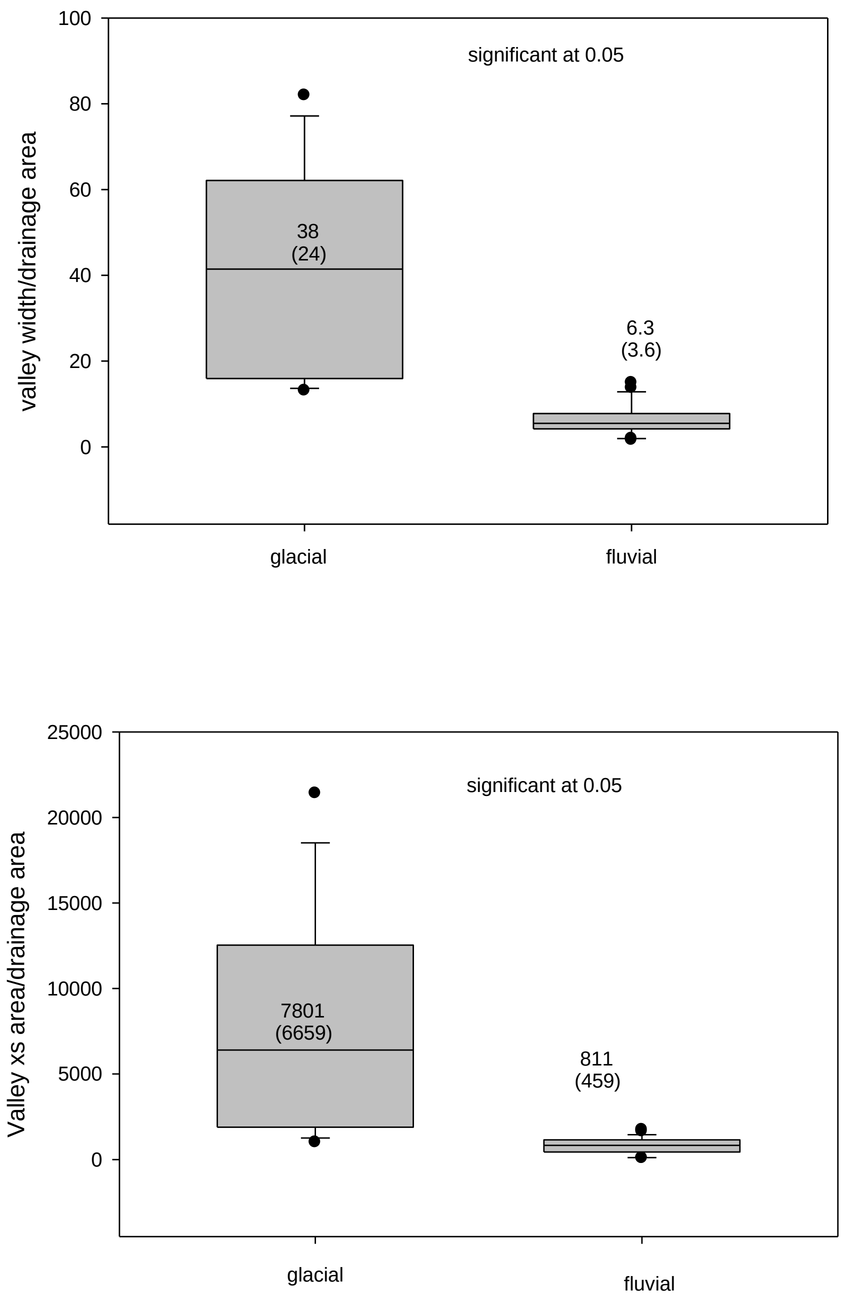

Figure 16: Plots of normalized valley width and cross-sectional area (valley width/drainage area and cross-sectional area/drainage area) show even larger differences between glacial and fluvial valley segments.

7.2 Appendix B: Raw data

Name	MB	Substrate	Valley	Confinement	S_{field}	S_{DEM}	QPK2 (m^3)	DA (km^2)	Width (m)	Depth (m)	D_{50} (mm)	D_{84} (mm)
CC1PB	PB	pebble	glacial	part. confined	0.019	0.034	3.82	13.21	9	0.6967	35	75
CC2SP	SP	cobble	glacial	confined	0.059	0.053	3.85	13.47	6.5	0.79	80	190
CC3Cas	Cas	boulder	glacial	confined	0.124	0.095	3.88	13.49	8.1	0.77	390	750
OC1SP	SP	cobble	glacial	part. confined	0.031	0.019	3.97	10.08	6	0.51	150	265
OC2PB	PB	cobble	glacial	part. confined	0.022	0.015	3.97	10.08	8.7	0.7067	75	165
OC3SP	SP	pebble	glacial	confined	0.035	0.018	3.97	10.10	10.4	0.57	55	120
OC4Cas	Cas	cobble	glacial	part. confined	0.056	0.091	3.97	10.15	11.2	0.71	190	450
OC6Cas	Cas	cobble	glacial	confined	0.130	0.091	3.99	10.26	5.7	0.82	210	445
OC7SP	SP	pebble	glacial	unconfined	0.050	0.057	3.99	10.39	3.1	0.35	35	70
OC8PB	PB	pebble	glacial	unconfined	0.015	0.047	4.08	10.85	6.5	0.4967	60	120
OC9SP	SP	cobble	glacial	part. confined	0.045	0.033	4.11	11.09	5.4	0.7467	120	280
OC10Cas	Cas	boulder	glacial	part. confined	0.123	0.067	4.11	11.27	6.6	0.94	270	440
OC11Cas	Cas	boulder	glacial	confined	0.116	0.058	4.11	11.27	6.9	0.71	430	660
OC12SP	SP	cobble	glacial	confined	0.080	0.048	4.25	12.30	11.6	0.6567	80	150
OC13Cas	RR	cobble	glacial	confined	0.036	0.078	4.25	12.30	5	0.9267	220	390

OC14Cas	RR	cobble	glacial	part. confined	0.057	0.055	4.28	12.54	5.65	0.7	220	400
OC15SP	SP	pebble	glacial	part. confined	0.042	0.053	4.31	12.87	6	0.7667	50	90
OC16Cas	RR	cobble	glacial	part. confined	0.036	0.045	4.31	12.90	4.8	0.6767	130	210
OC17SP	SP	cobble	glacial	confined	0.050	0.094	4.31	12.95	5.7	0.58	100	170
OC18Cas	Cas	bedrock	glacial	confined	0.236	0.257	4.31	12.98	7.3	0.7367	390	940
CCT1Cas	Cas	cobble	glacial	confined	0.100	0.088	1.18	3.76	2	0.45	230	420
CCT2Cas	Cas	boulder	glacial	unconfined	0.210	0.203	1.18	3.78	1.7	0.47	280	470
CCT3Cas	Cas	boulder	glacial	unconfined	0.400	0.321	1.19	3.83	2	0.7133	360	470
CCT4Cas	Cas	cobble	glacial	confined	0.200	0.196	1.19	3.86	1.7	0.7233	250	410
CCT5SP	SP	cobble	glacial	confined	0.130	0.133	1.21	3.91	1.5	0.42	100	190
CCT6SP	SP	cobble	glacial	confined	0.217	0.200	1.24	4.09	2.35	0.4633	180	380
CCT7SP	SP	cobble	glacial	part. confined	0.065	0.133	1.24	4.12	1.7	0.3767	100	150
CCT8SP	SP	cobble	glacial	part. confined	0.192	0.173	1.25	4.14	1.5	0.5267	150	410
NSVT1SP	SP	pebble	glacial	unconfined	0.385	0.277	0.42	1.24	0.4	0.11	40	95
CMC1SP	SP	pebble	glacial	confined	0.373	0.287	0.49	1.24	1	0.1933	60	210
CMC2SP	SP	pebble	glacial	confined	0.069	0.077	0.49	1.27	2.05	0.32	35	90
CMC3SP	SP	cobble	glacial	confined	0.250	0.120	0.72	2.28	1.2	0.4033	85	190
CMC4SP	SP	pebble	glacial	confined	0.121	0.154	0.73	2.31	1.05	0.2633	45	160

CMC5PR	PR	pebble	glacial	part. confined	0.006	0.037	0.92	3.50	3	0.3267	35	85
CMC6SP	SP	pebble	glacial	unconfined	0.050	0.077	0.92	3.50	1	0.3	45	95
CMC7SP	SP	pebble	glacial	confined	0.090	0.100	0.94	3.52	1.7	0.32	55	105
CMC8SP	SP	cobble	glacial	confined	0.450	0.368	0.95	3.73	2.1	0.3567	130	310
CMC9PR	PR	pebble	glacial	unconfined	0.050	0.090	0.96	3.86	1.5	0.3867	40	85
CMC10SP	SP	cobble	glacial	confined	0.260	0.250	0.97	3.89	1.75	0.31	95	190
NSV1PB	PB	cobble	glacial	unconfined	0.019	0.028	15.24	81.33	8	0.9433	115	200
NSV2PR	PR	pebble	glacial	unconfined	0.017	0.015	15.27	82.10	9.1	0.4433	50	85
NSV3PB	PB	pebble	glacial	part. confined	0.011	0.007	15.24	83.40	22.2	0.3967	60	85
GC1PR	PR	cobble	glacial	part. confined	0.033	0.035	3.63	5.72	3.9	0.5233	80	130
GC2Cas	Cas	bedrock	glacial	confined	0.071	0.064	3.63	5.78	14.7	0.5567	250	430
GC3PR	PR	cobble	glacial	part. confined	0.003	0.086	3.63	5.80	10.3	0.4567	75	110
GC4Cas	Cas	bedrock	glacial	confined	0.080	0.110	3.65	5.85	7.25	0.5167	200	390
NSV4PR	PR	cobble	glacial	part. confined	0.007	0.006	15.18	83.66	22.8	0.4767	70	100
NSV5Cas	Cas	cobble	glacial	part. confined	0.032	0.013	15.21	83.92	10.6	0.83	160	530
NSV6PB	PB	cobble	glacial	unconfined	0.002	0.011	15.18	83.92	13.1	0.7367	75	110
GC5RR	RR	pebble	glacial	unconfined	0.013	0.023	4.93	8.70	5.6	0.46	50	90
GC6PR	PR	pebble	glacial	unconfined	0.004	0.027	4.96	8.73	4.5	0.5933	40	60

GC7SP	SP	bedrock	glacial	confined	0.118	0.100	4.96	8.81	7	0.8267	110	210
GC8RR	RR	bedrock	glacial	part. confined	0.033	0.040	5.27	9.69	5.5	0.4033	100	150
GC9PR	PR	pebble	glacial	part. confined	0.008	0.008	5.35	9.92	4.85	0.5367	35	55
NSV15SP	SP	cobble	glacial	confined	0.079	0.124	6.03	19.45	9	0.6533	120	220
NSV16SP	SP	cobble	glacial	confined	0.055	0.067	6.06	19.63	8.8	0.7333	100	280
NSV17SP	SP	cobble	glacial	part. confined	0.039	0.063	6.09	20.05	8.8	0.7267	100	190
NSV18SP	SP	bedrock	glacial	confined	0.077	0.089	9.01	33.93	7.6	0.89	240	540
NSV19RR	RR	cobble	glacial	confined	0.032	0.060	9.26	36.52	8.6	0.7	100	190
NSV20Cas	Cas	bedrock	glacial	confined	0.080	0.098	12.07	55.17	8.6	1.2333	300	600
FnC1SP	SP	cobble	glacial	confined	0.089	0.123	3.00	7.23	2.8	0.6167	140	230
BT1SP	SP	bedrock	glacial	confined	0.035	0.084	17.08	84.17	8.9	0.8033	220	440
BT2SP	SP	cobble	glacial	confined	0.068	0.030	17.11	84.17	10.7	0.6833	230	510
BT3SP	SP	cobble	glacial	confined	0.033	0.041	17.20	85.21	12.2	0.6833	150	260
BT4RR	RR	cobble	glacial	confined	0.020	0.015	17.25	86.51	9.4	0.6067	130	240
PR1PR	PR	cobble	glacial	confined	0.015	0.039	4.25	17.69	4	0.6	110	220
PR2PR	PR	pebble	glacial	confined	0.012	0.009	4.08	16.60	4	0.6733	55	150
PR3PR	PR	pebble	glacial	part. confined	0.013	0.007	3.99	16.08	10	0.55	60	135
PR4PR	PR	pebble	glacial	part. confined	0.021	0.017	2.82	9.95	13.9	0.3433	50	105

PR5PR	PR	cobble	glacial	part. confined	0.011	0.023	1.86	5.80	5.4	0.5667	70	120
PR6PR	PR	cobble	glacial	confined	0.052	0.028	0.87	2.28	2.7	0.42	65	165
PR7PR	PR	pebble	glacial	confined	0.011	0.018	0.74	1.84	11.8	0.26	30	60
HC1PB	PB	pebble	fluvial	part. confined	0.035	0.053	1.07	7.41	1.65	0.41	40	70
HC2SP	SP	pebble	fluvial	part. confined	0.080	0.053	1.08	7.46	1.6	0.38	50	130
HC3PR	PR	pebble	fluvial	part. confined	0.030	0.060	1.09	7.80	1.55	0.2333	20	45
HC4SP	SP	pebble	fluvial	part. confined	0.050	0.055	1.09	7.80	2.2	0.3367	55	90
HC5SP	SP	sand	fluvial	part. confined	0.070	0.055	1.11	8.03	3.3	0.42	1	1
HC6SP	SP	cobble	fluvial	confined	0.060	0.057	1.12	8.24	2.4	0.3667	90	280
HC7SP	SP	cobble	fluvial	part. confined	0.040	0.076	1.14	8.47	3	0.3333	80	140
NSV7Cas	Cas	boulder	fluvial	confined	0.115	0.106	15.18	84.43	25.75	1.6667	310	580
NSV8Cas	Cas	cobble	fluvial	confined	0.066	0.076	15.18	84.43	16.8	1.19	200	560
NSV9SP	SP	bedrock	fluvial	confined	0.039	0.107	15.18	84.95	9.8	0.9467	130	250
NSV10Cas	Cas	cobble	fluvial	confined	0.071	0.049	15.18	84.95	16.2	0.9833	210	480
HC8SP	SP	cobble	fluvial	confined	0.048	0.065	1.16	8.86	2.7	0.5167	130	320
NSV11RR	RR	cobble	fluvial	confined	0.028	0.037	15.33	95.31	12	0.97	230	430
NSV12Cas	Cas	bedrock	fluvial	confined	0.053	0.057	15.33	95.57	15.2	0.6667	180	440
NSV13RR	RR	bedrock	fluvial	confined	0.037	0.037	15.33	101.53	11.5	0.8367	90	270

FC1SP	SP	pebble	fluvial	part. confined	0.057	0.054	1.12	8.34	2.1	0.3633	45	85
FC2SP	SP	bedrock	fluvial	confined	0.086	0.082	1.19	9.71	4.8	0.75	80	170
FC3SP	SP	cobble	fluvial	part. confined	0.034	0.078	1.20	9.71	2.5	0.3633	95	160
RC1SP	SP	cobble	fluvial	part. confined	0.048	0.070	3.82	35.74	5.9	0.6433	120	270
RC2RR	RR	cobble	fluvial	part. confined	0.027	0.035	3.82	36.00	5.25	0.4033	80	120
RC3SP	SP	cobble	fluvial	confined	0.042	0.045	3.82	36.00	6.2	0.5567	80	220
BC1PB	PB	pebble	fluvial	part. confined	0.022	0.071	0.57	4.74	1.6	0.4533	20	40
BC2SP	SP	pebble	fluvial	confined	0.035	0.109	0.58	4.97	1.5	0.28	45	180
RC4RR	RR	cobble	fluvial	part. confined	0.029	0.028	3.14	25.90	4.5	0.4567	75	100
RC5SP	SP	cobble	fluvial	part. confined	0.065	0.037	3.14	25.90	5	0.5633	100	210
RC6PR	PR	pebble	fluvial	unconfined	0.022	0.040	2.89	20.56	6	0.42	55	90
RC7SP	SP	cobble	fluvial	part. confined	0.045	0.046	2.89	20.62	3.4	0.56	75	130
NSV14SP	SP	bedrock	fluvial	confined	0.050	0.062	21.22	208.49	17	1.4467	220	490
NSV14.5SP	SP	bedrock	fluvial	confined	0.047	0.062	21.22	208.49	13	0.7267	210	470
CG1SP	SP	bedrock	fluvial	confined	0.253	0.111	0.72	6.58	2	0.4667	110	210
CG2SP	SP	cobble	fluvial	confined	0.069	0.041	0.62	5.91	3	0.3167	80	200
CG3PB	PB	pebble	fluvial	part. confined	0.020	0.016	0.57	5.34	4	0.3767	40	120
CG4SP	SP	cobble	fluvial	part. confined	0.042	0.055	0.39	3.63	1.7	0.2933	70	150

BG1SP	SP	pebble	fluvial	confined	0.071	0.084	0.22	2.05	2.6	0.2433	60	150
NSV21RR	RR	cobble	fluvial	part. confined	0.017	0.010	21.30	198.13	18.3	0.7533	130	230
NSV22RR	RR	bedrock	fluvial	confined	0.026	0.050	21.36	207.98	16	0.8267	170	270
NSV23SP	SP	bedrock	fluvial	confined	0.027	0.035	21.36	208.24	16	0.8133	240	380
NFP1PR	PR	cobble	fluvial	confined	0.012	0.012	19.18	981.00	14.4	0.8	193	367
NFP2PR	PR	cobble	fluvial	confined	0.012	0.012	19.24	986.00	12.4	0.6	143	246

7.3 Appendix C: Boxplots of raw data

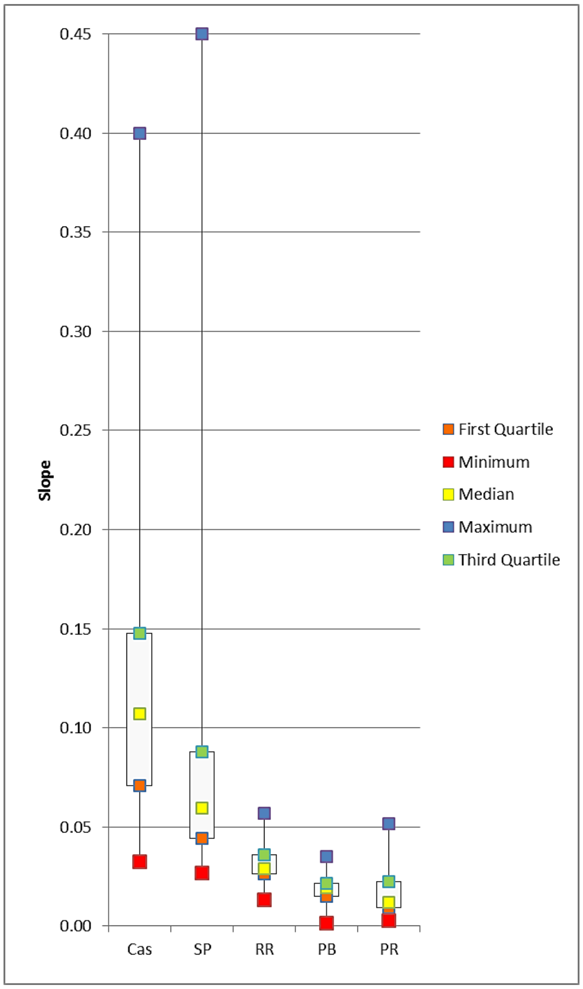

Figure 17: Boxplot of slope by MB stream type.

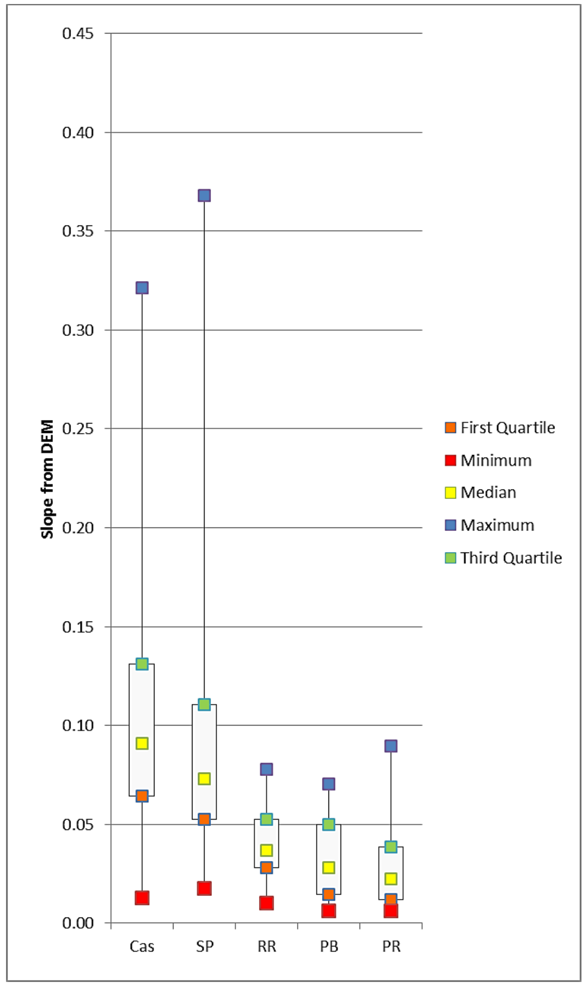

Figure 18: Boxplot of slope from DEM by MB stream type.

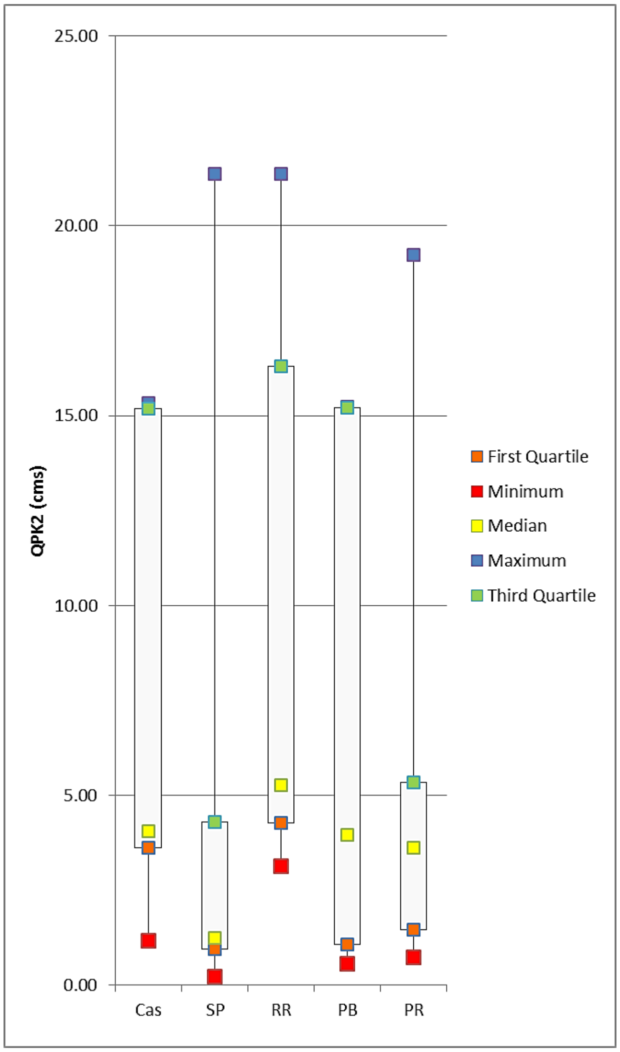

Figure 19: Boxplot of 2-year peak discharge by MB stream type.

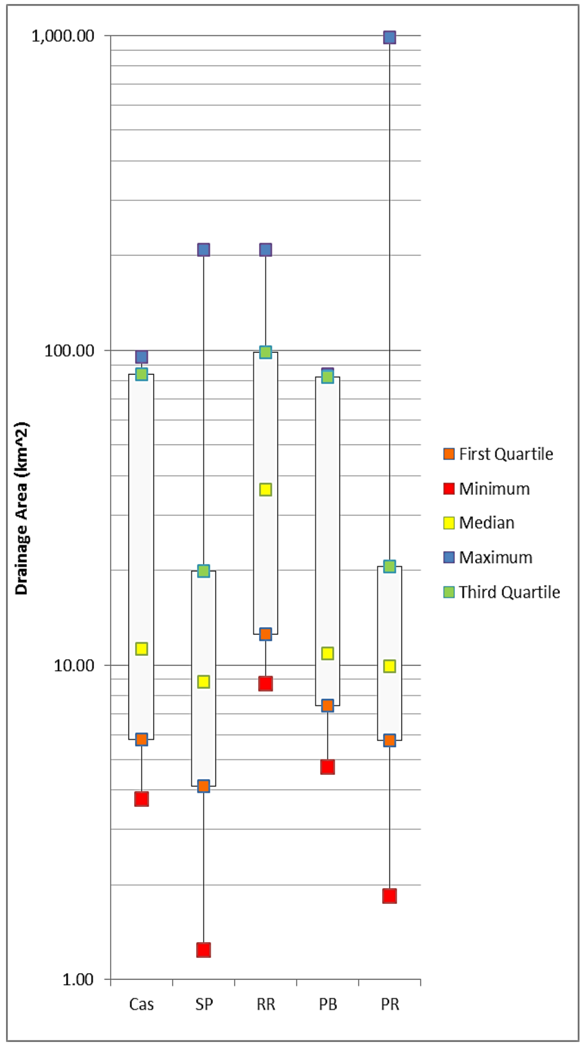

Figure 20: Boxplot of drainage area by MB stream type.

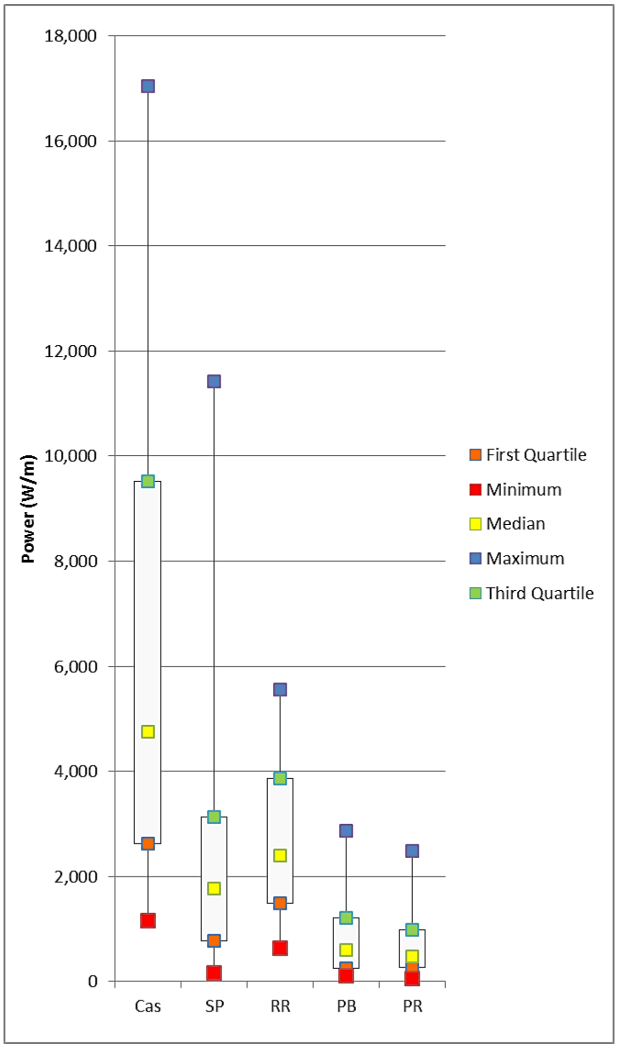

Figure 21: Boxplot of stream power by MB stream type.

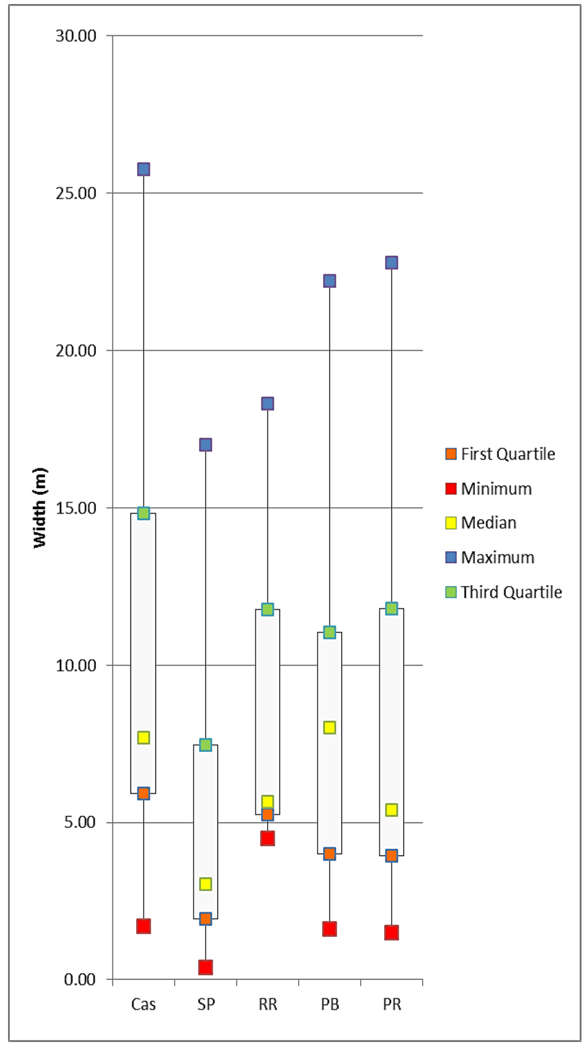

Figure 22: Boxplot of bankfull width by MB stream type.

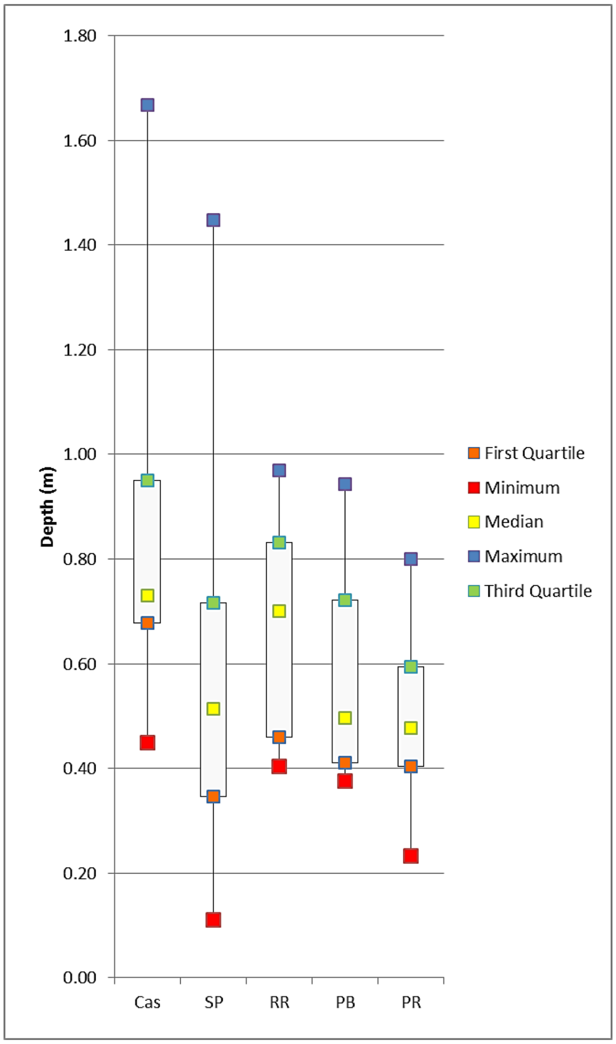

Figure 23: Boxplot of bankfull depth by MB stream type.

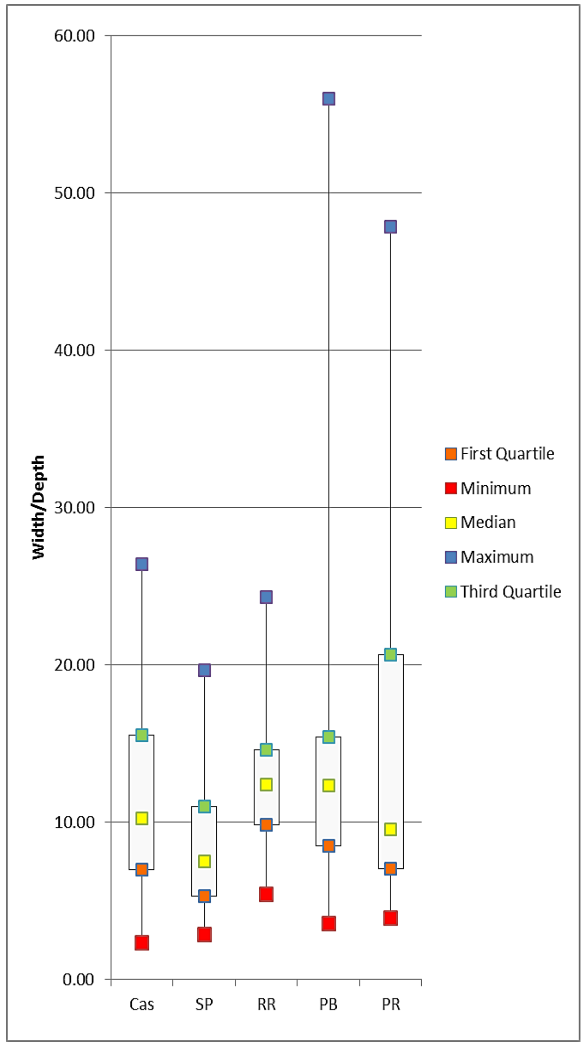

Figure 24: Boxplot of width to depth ratio by MB stream type.

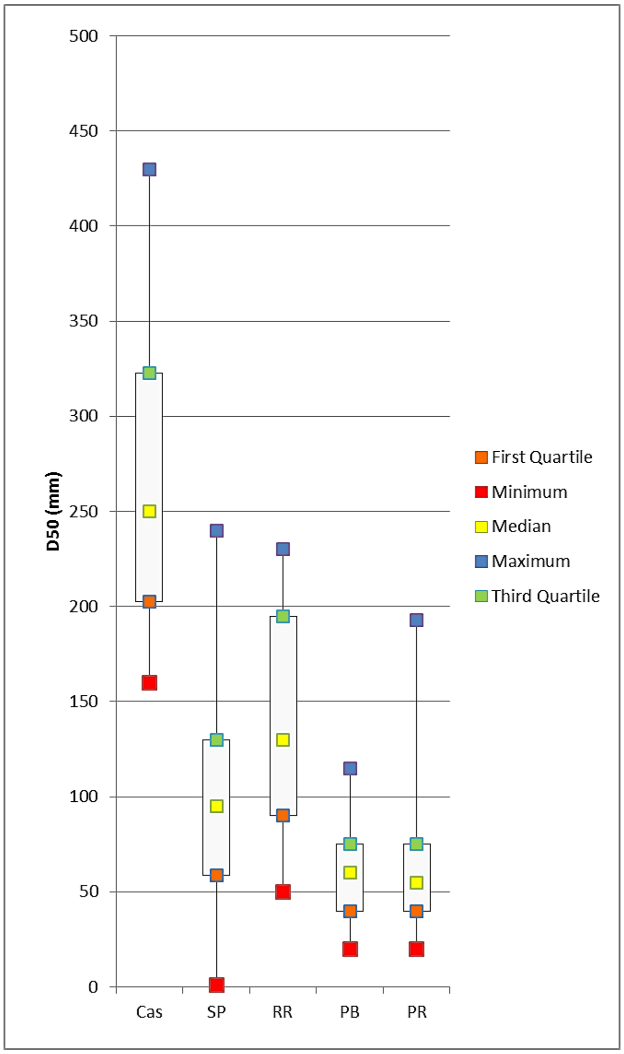

Figure 25: Boxplot of D_{50} by MB stream type.

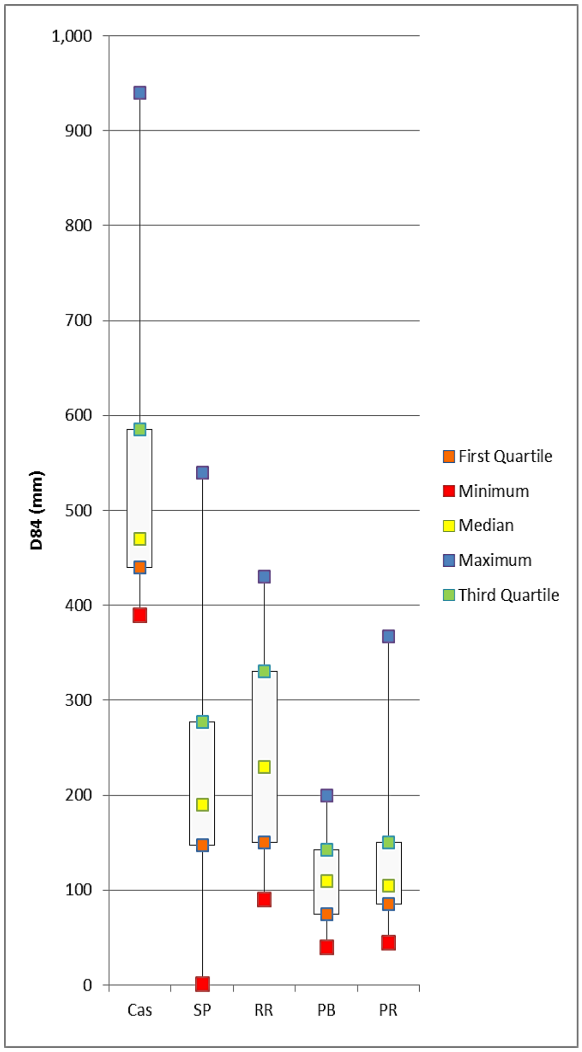

Figure 26: Boxplot of D_{84} by MB stream type.

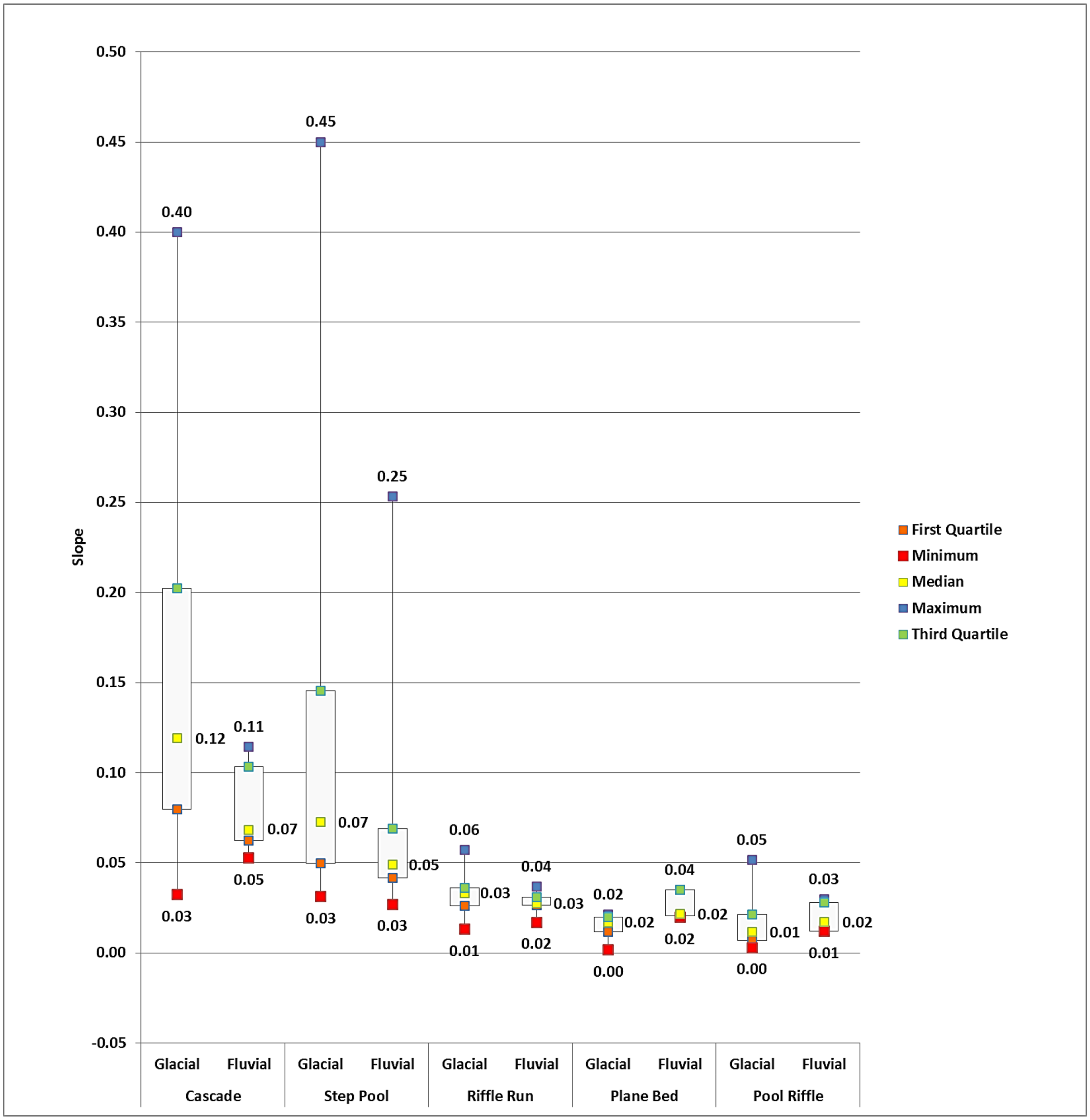

Figure 27: Boxplot of surface-water slope by MB stream type and valley history.

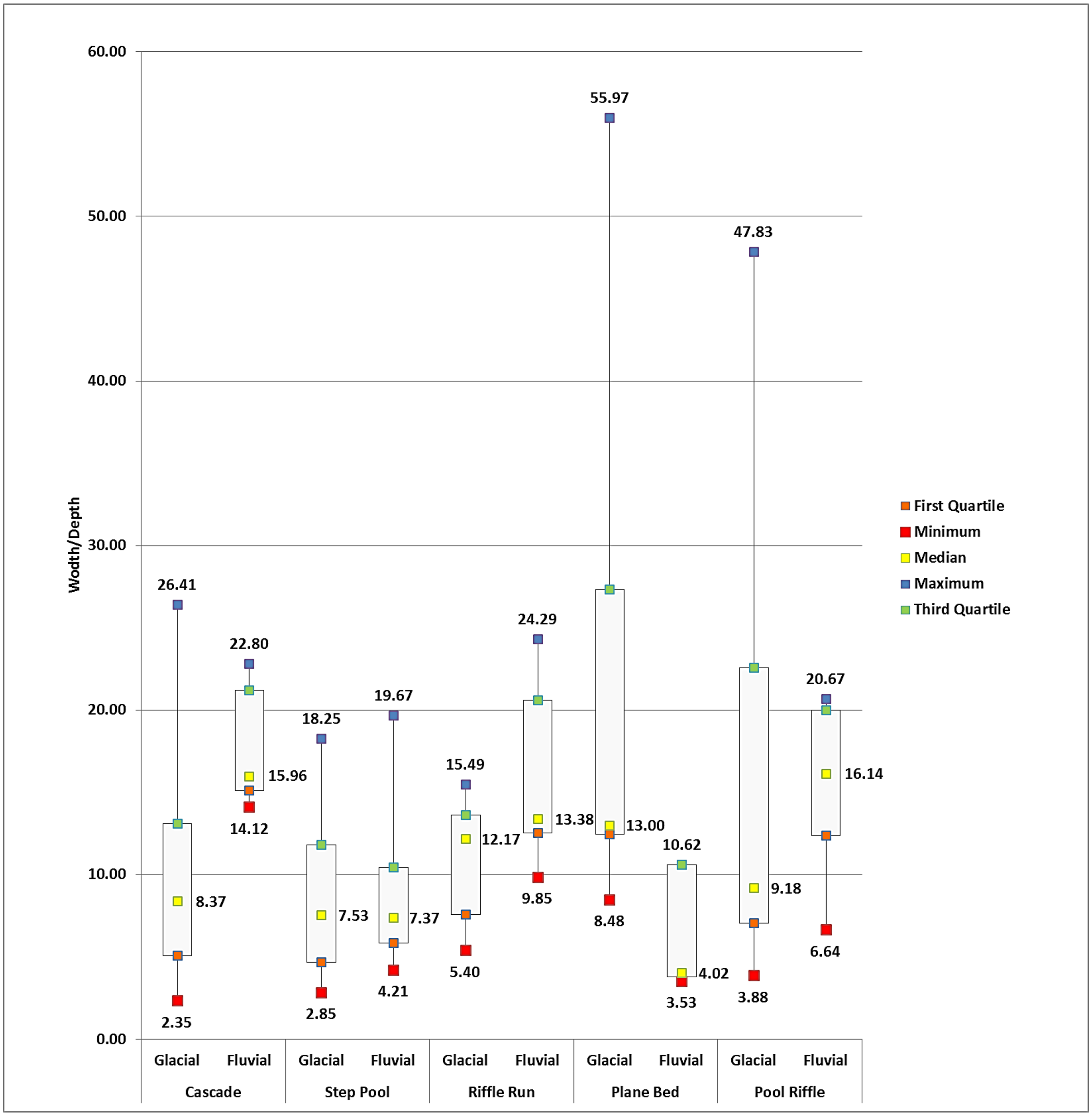

Figure 28: Boxplot of width to depth ratio by MB stream type and valley history.

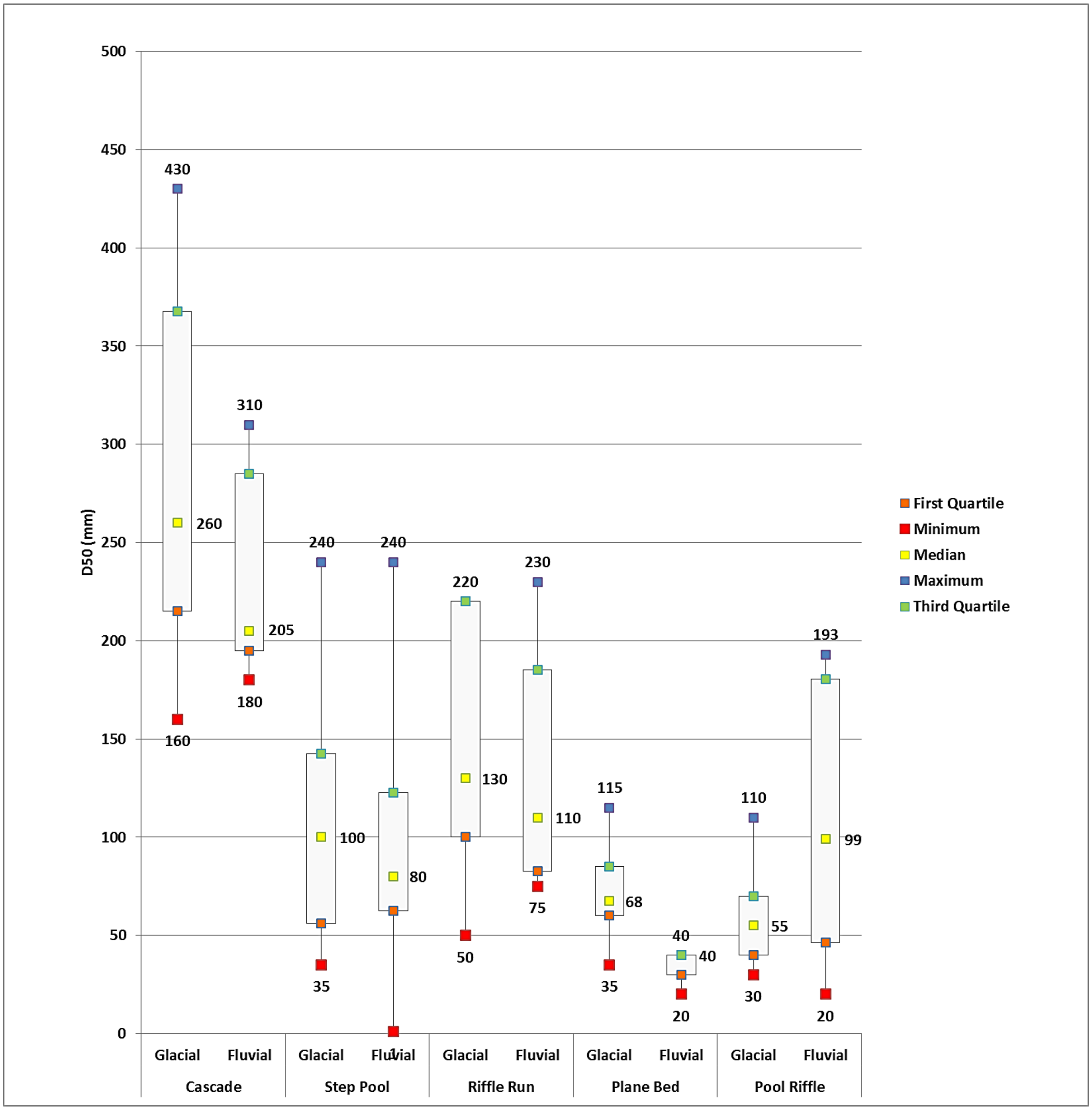

Figure 29: Boxplot of D_{50} by MB stream type and valley history.

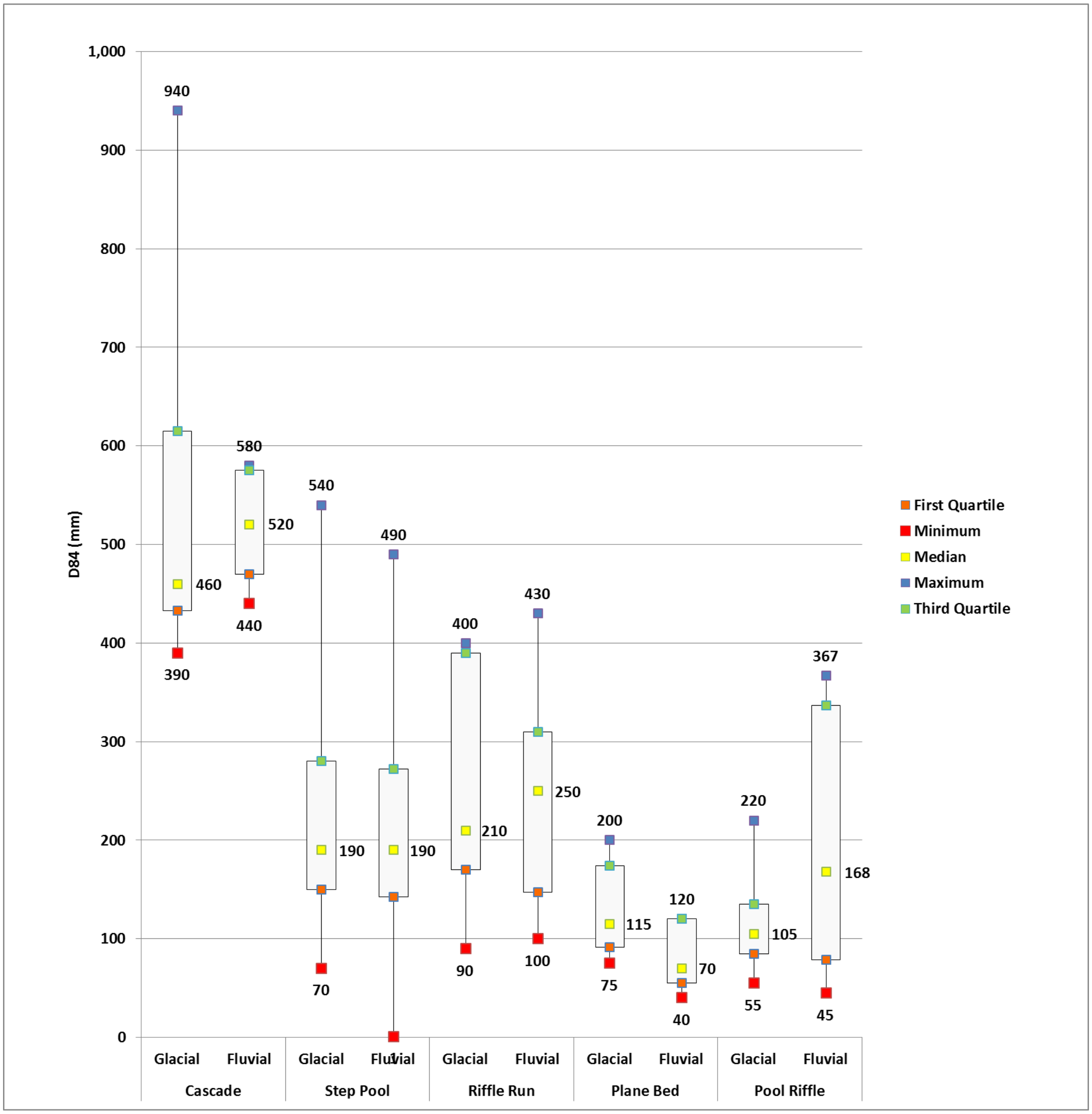

Figure 30: Boxplot of D_{84} by MB stream type and valley history.

7.4 Appendix D: Reach location maps

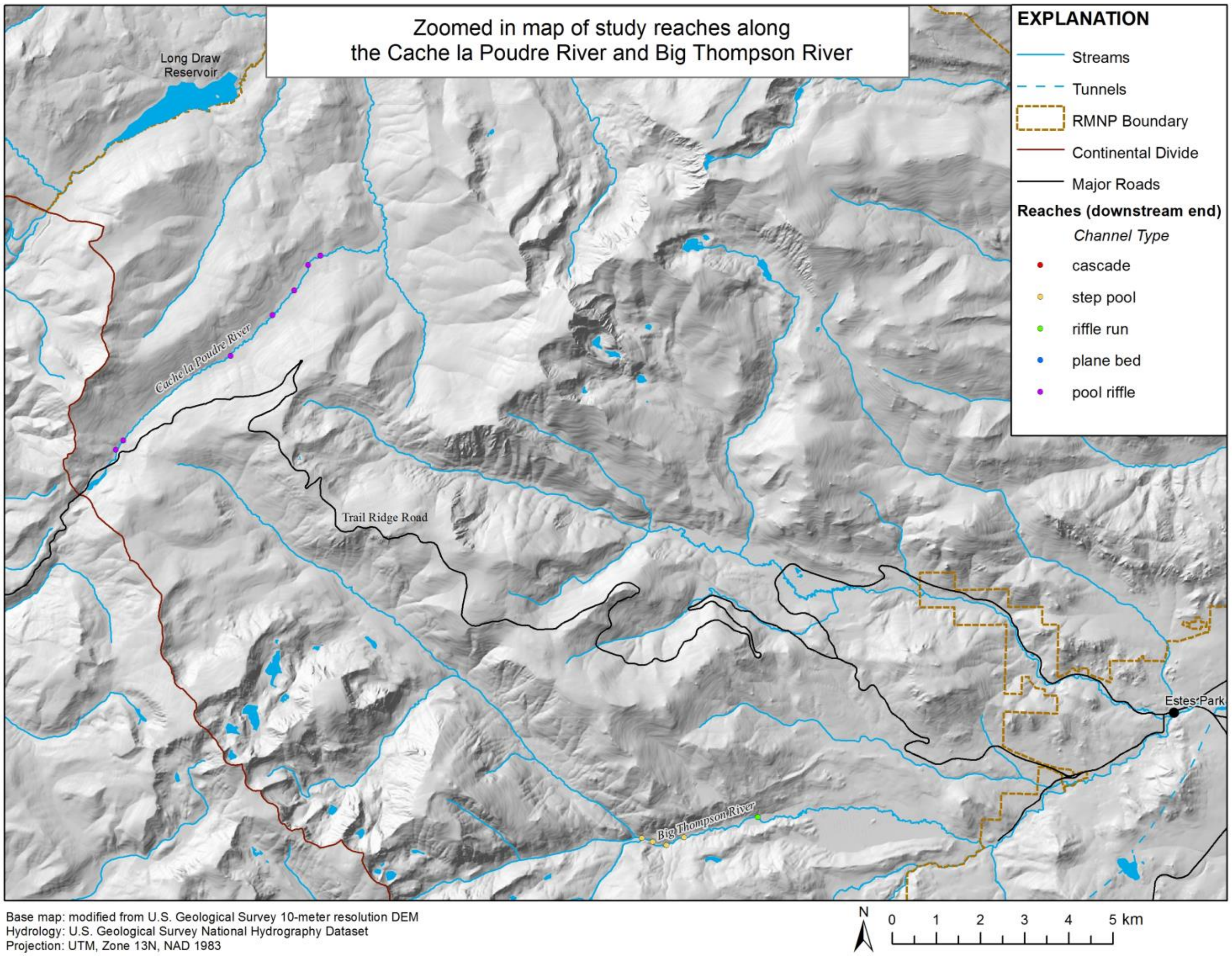

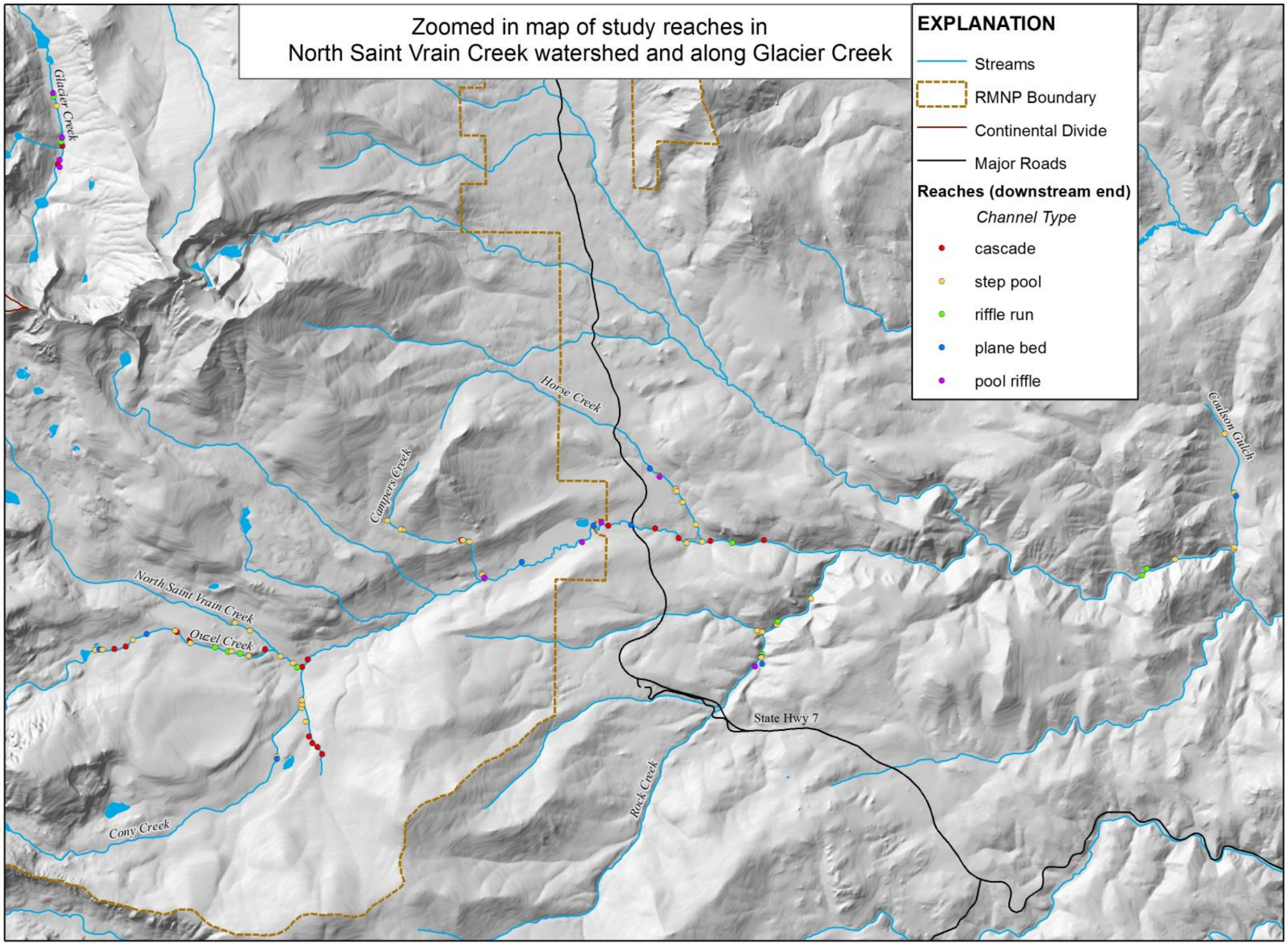

Base map: modified from U.S. Geological Survey 10-meter resolution DEM
Hydrology: U.S. Geological Survey National Hydrography Dataset
Projection: UTM, Zone 13N, NAD 1983

7.5 Appendix E: Field photographs


BC1PB


BC2SP


BG1SP

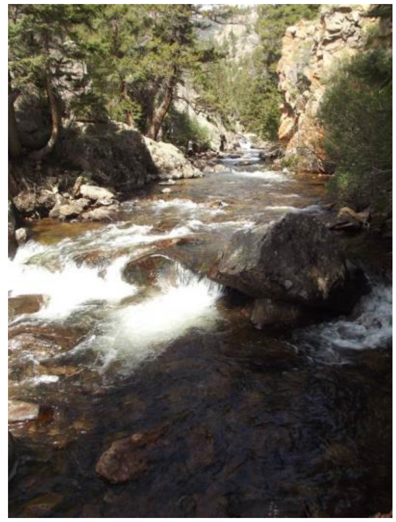
BT1SP


BT2SP

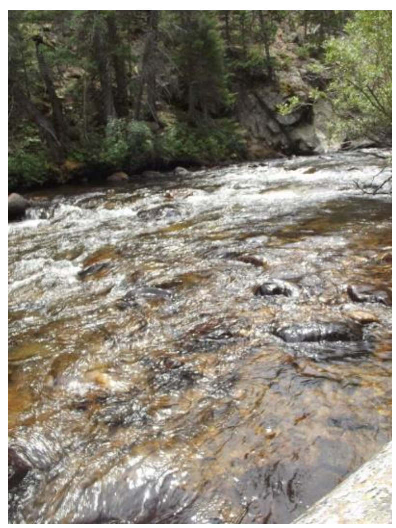
BT3SP


BT4RR


CC3CAS

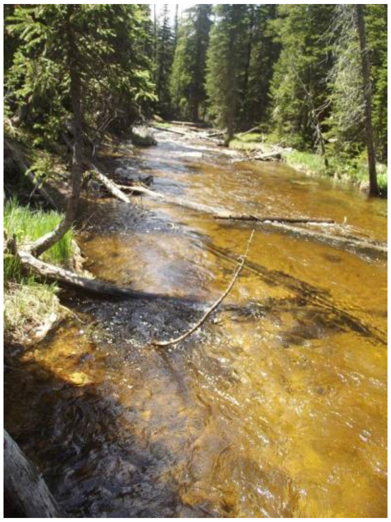
CC1PB


CCT1CAS

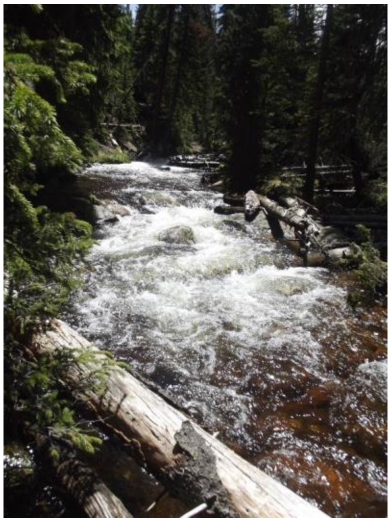
CC2SP


CCT2CAS


CCT3CAS

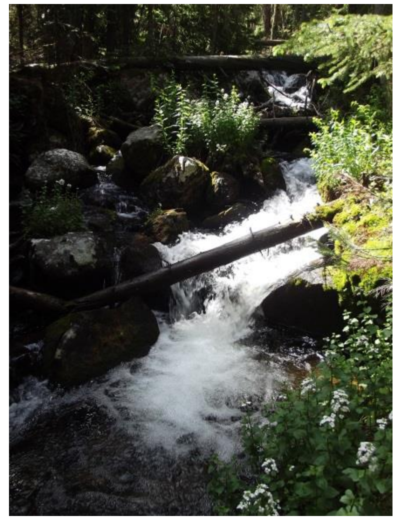
CCT6SP


CCT4CAS


CCT6SP

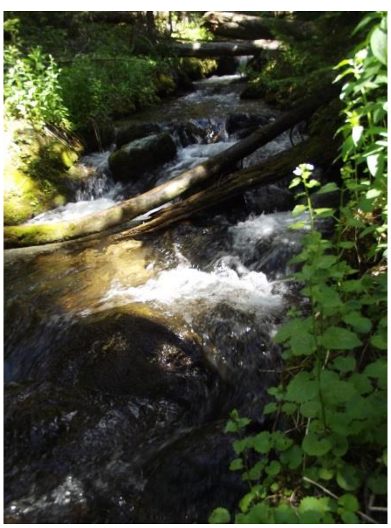
CCT5SP

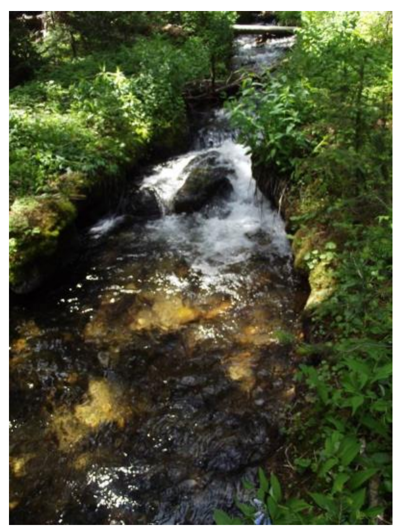
CCT7SP


CCT8SP


CG3PB


CG1SP


CG4SP


CG2SP

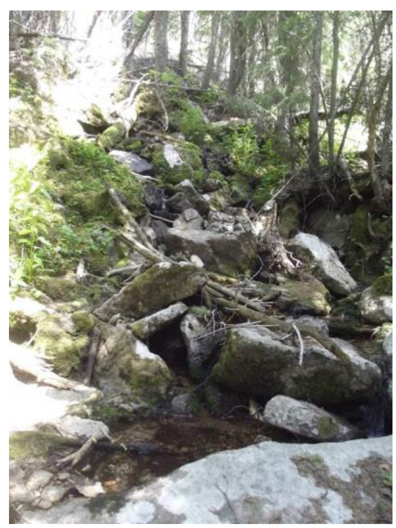
CMC1SP


CMC2SP

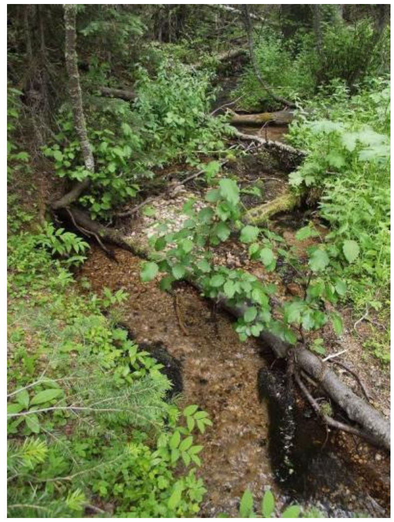
CMC5PR


CMC3SP


CMC6SP

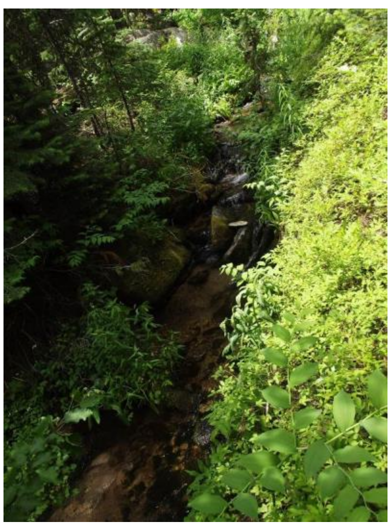
CMC4SP

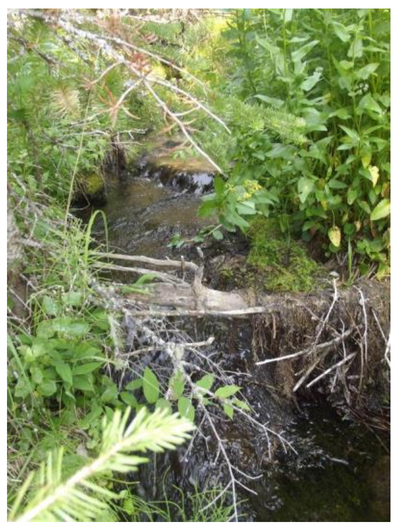
CMC7SP


CMC8SP


FC1SP


CMC9PR


FC2SP


CMC10SP


FNC1SP


GC1PR

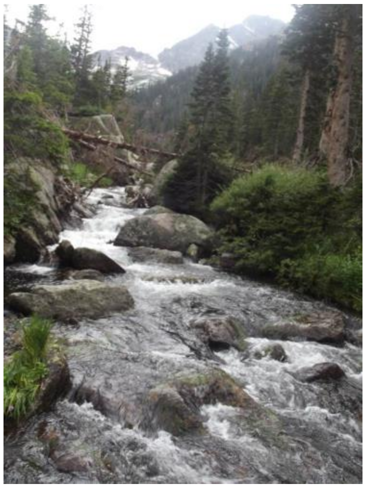
GC4CAS


GC2CAS


GC5RR


GC3PR


GC6PR


GC7SP


GC8RR

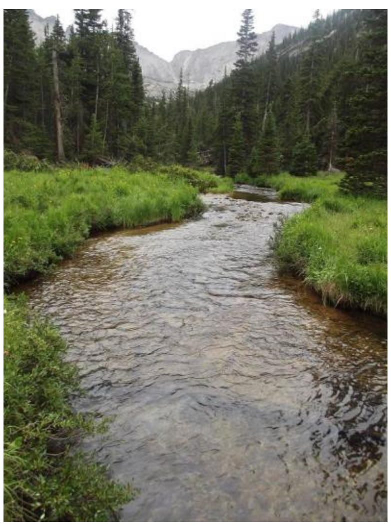
GC9PR


HC1PB

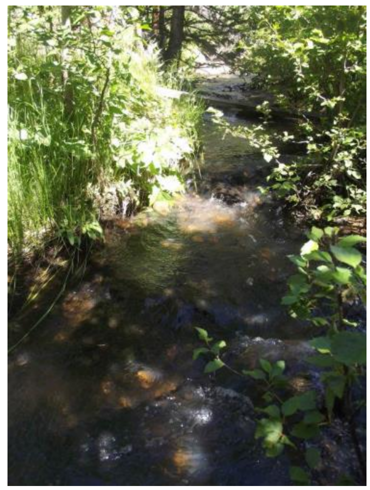
HC2SP

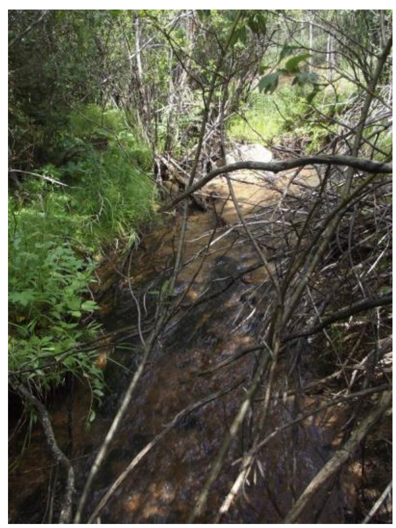
HC3PR


HC4SP

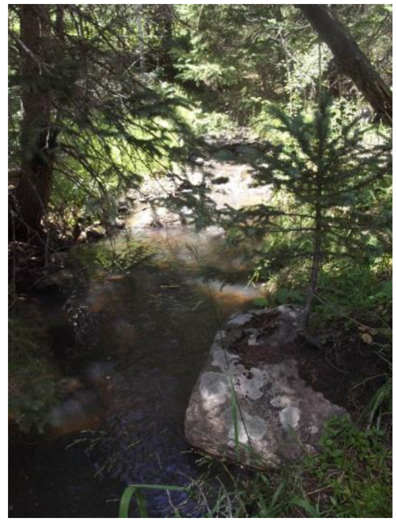
HC7SP


HC5SP


HC8SP


HC6SP


NSV1PB

NSV2PR

NSV5RR

NSV3PB

NSV6PB

NSV4PR

NSV7CAS

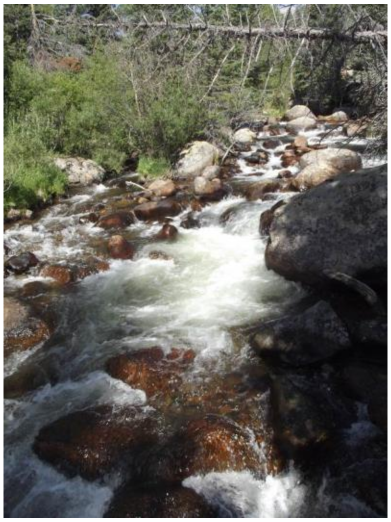

NSV8CAS

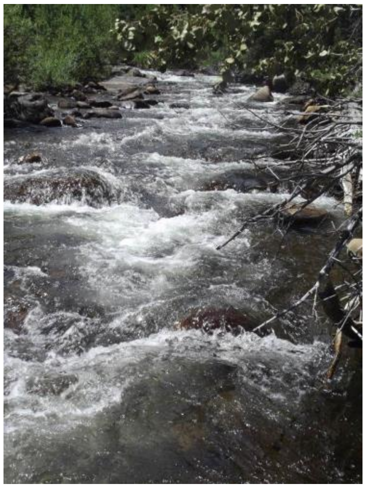

NSV11RR

NSV9SP

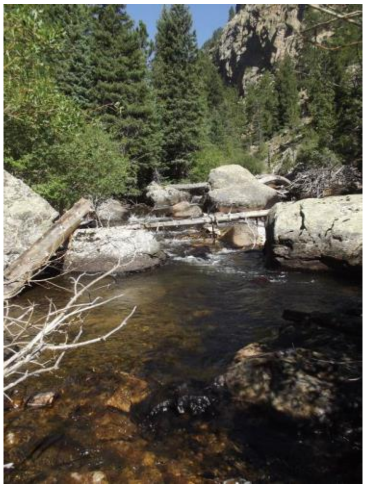

NSV12CASU

NSV10CAS

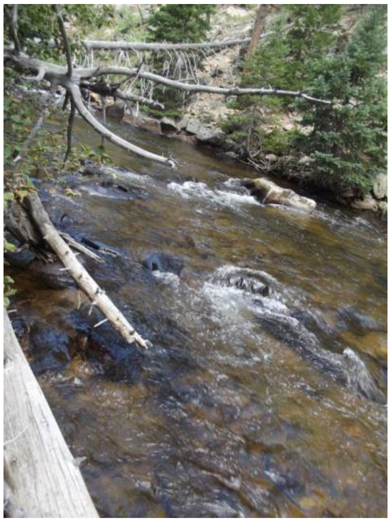

NSV13RR


NSV14.5SP

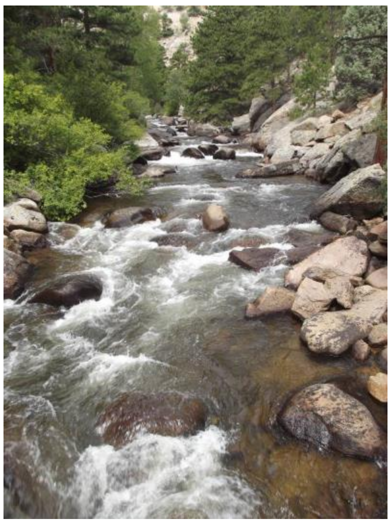
NSV14SP


NSV15SP

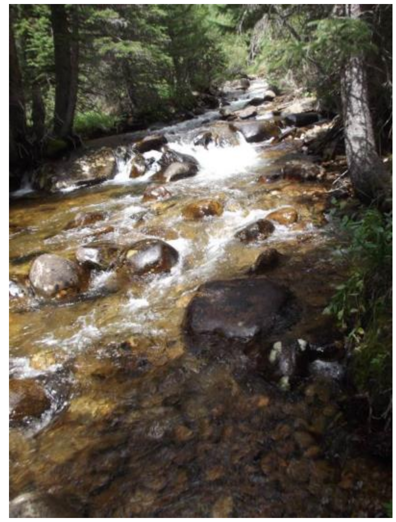
NSV16SP


NSV17SP

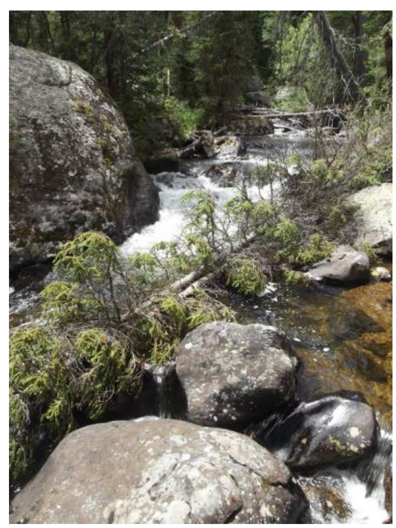
NSV18SP


NSV19RR


NSV22RR


NSV20CAS


NSV23SP

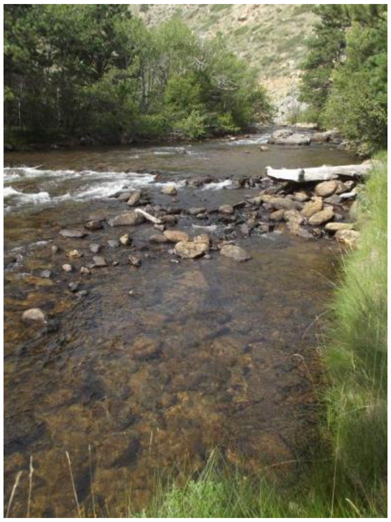
NSV21RR


NSVT1SP

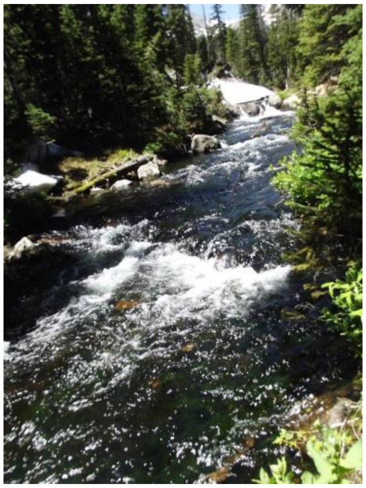
OC1SP

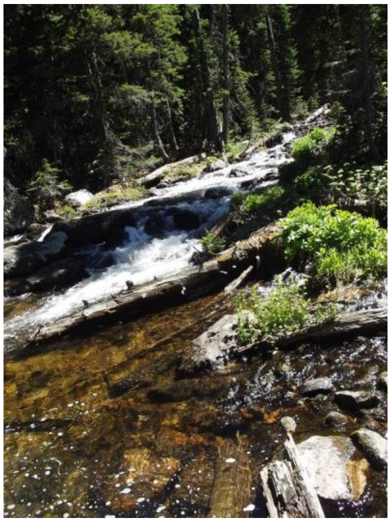
OC4CAS

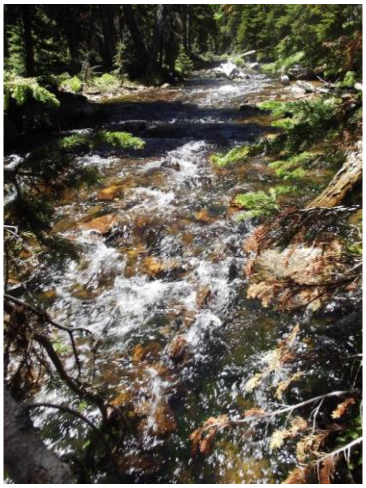
OC2PB


OC6CAS

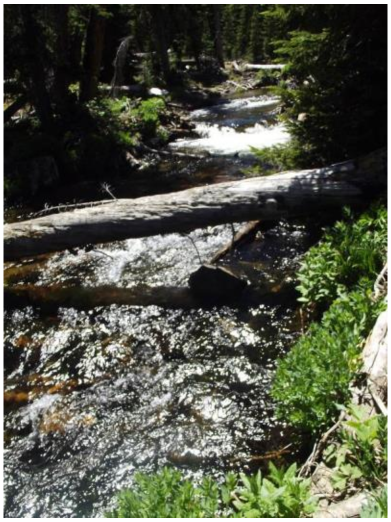
OC3SP


OC7SP1

OC7SP2

OC10CAS

OC8PB

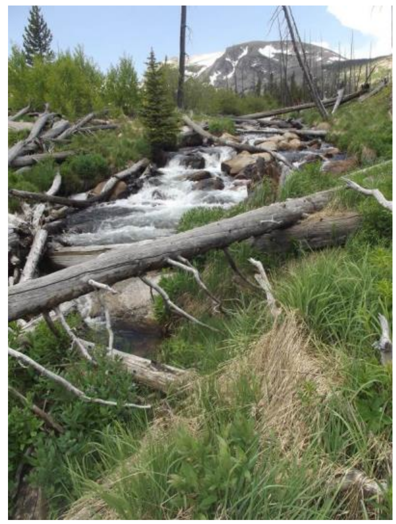

OC11CAS

OC9SP

OC12SP


OC13RR


OC14RR

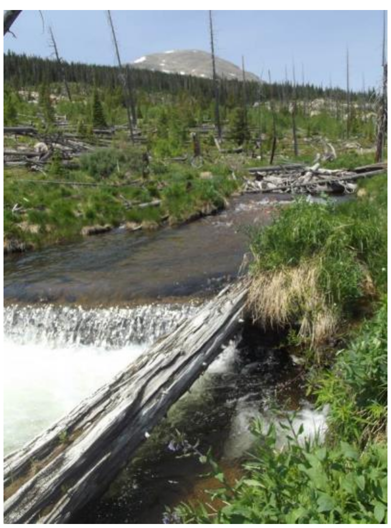
OC15SP


OC16RR

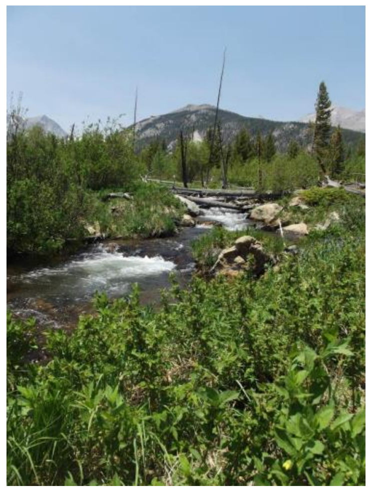
OC17SP

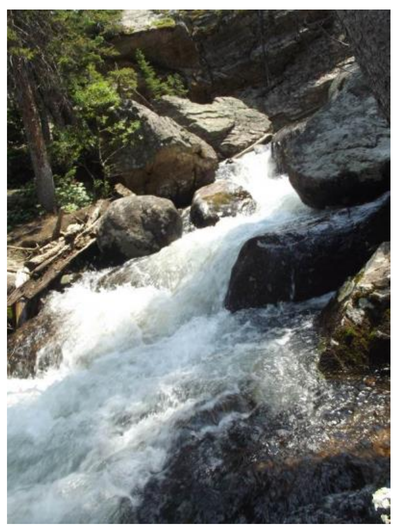
OC18CAS

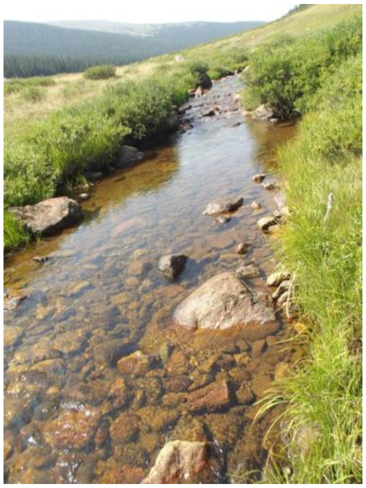
PR1PR


PR2PR

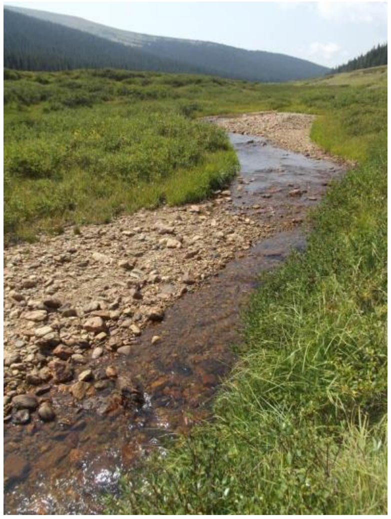
PR3PR


PR4PR


PR5PR

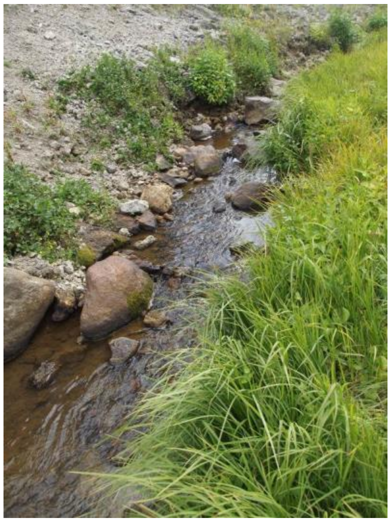
PR6PR


PR7PR


RC3SP

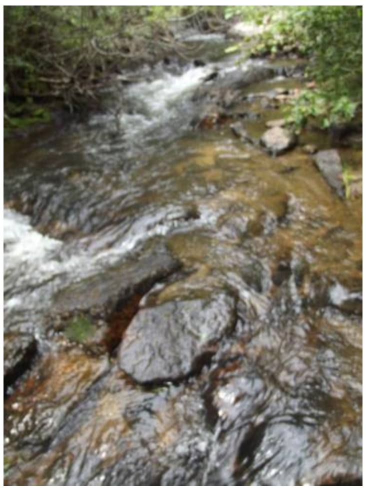
RC1SP

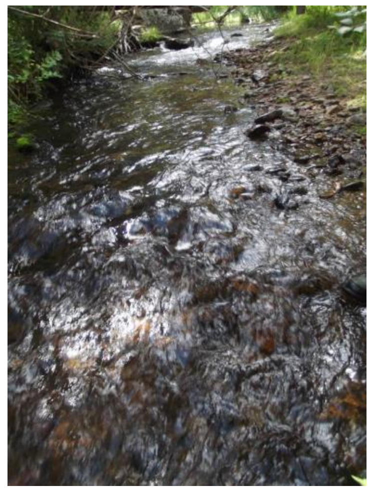
RC4RR


RC2RR

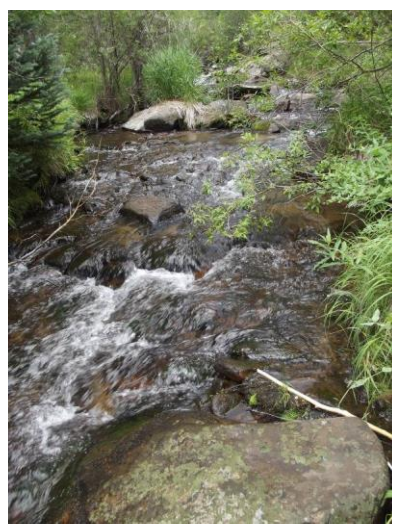
RC5SP

RC6PR

RC7SP

7.6 Appendix F: Classification trees by confinement

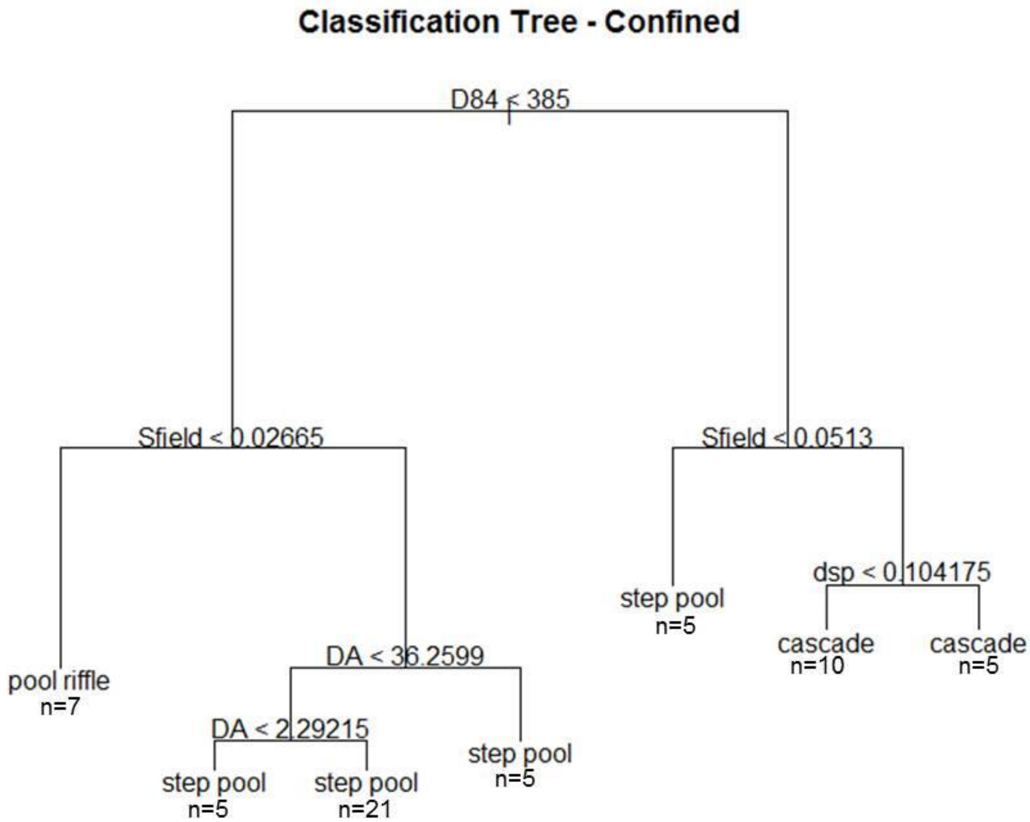

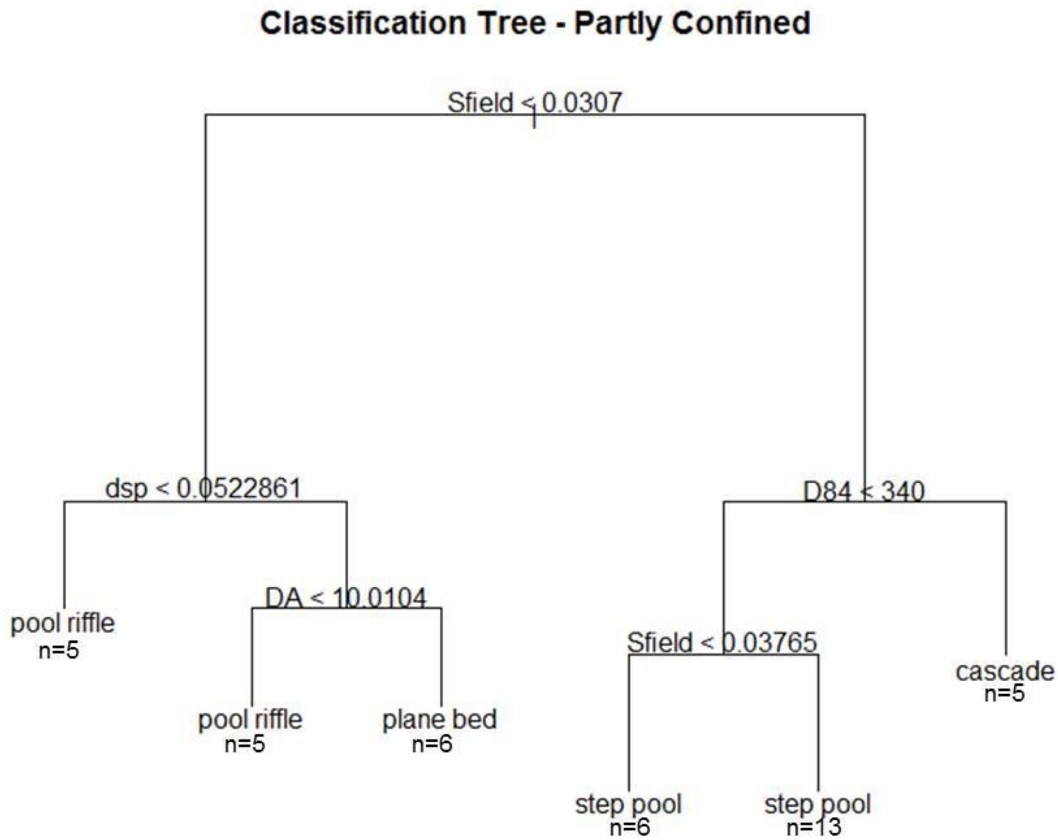

Classification Tree - Partly Confined
Sfield < 0.0307
dsp < 0.0522861
D84 < 340
pool riffle
n=5
DA < 10.0104
pool riffle
n=5
plane bed
n=6
Sfield < 0.03765
step pool
n=6
step pool
n=13
cascade
n=5

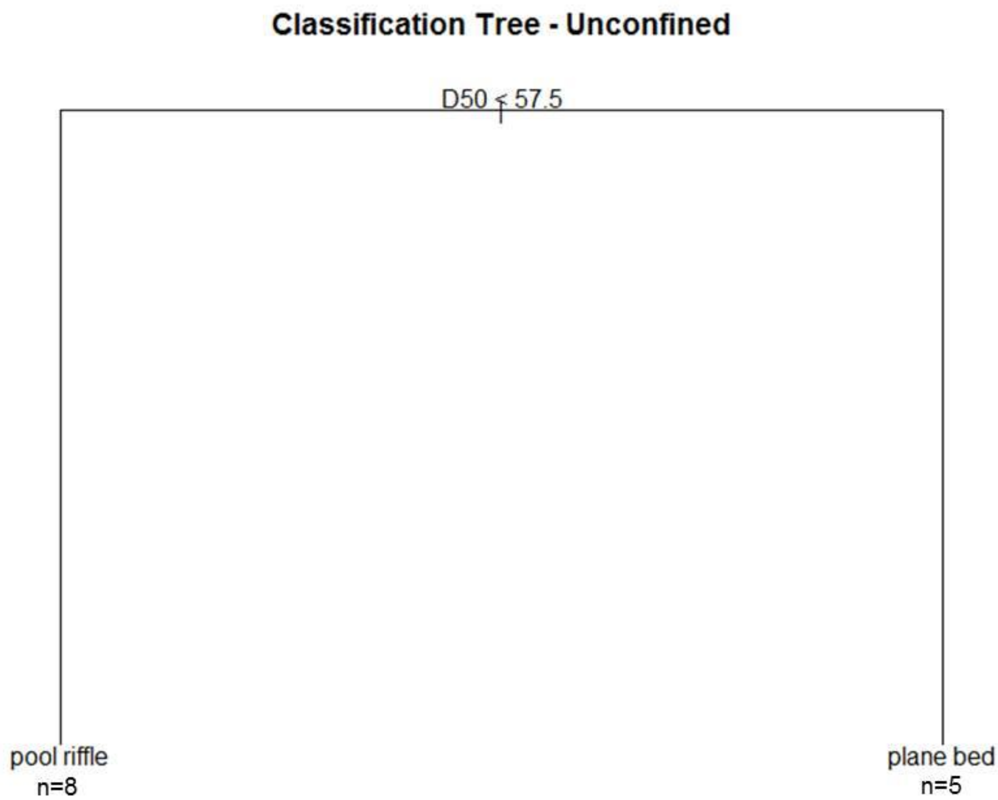
Classification Tree - Unconfined
D50 < 57.5
pool riffle
n=8
plane bed
n=5

7.7 Appendix G: Downstream hydraulic geometry plots

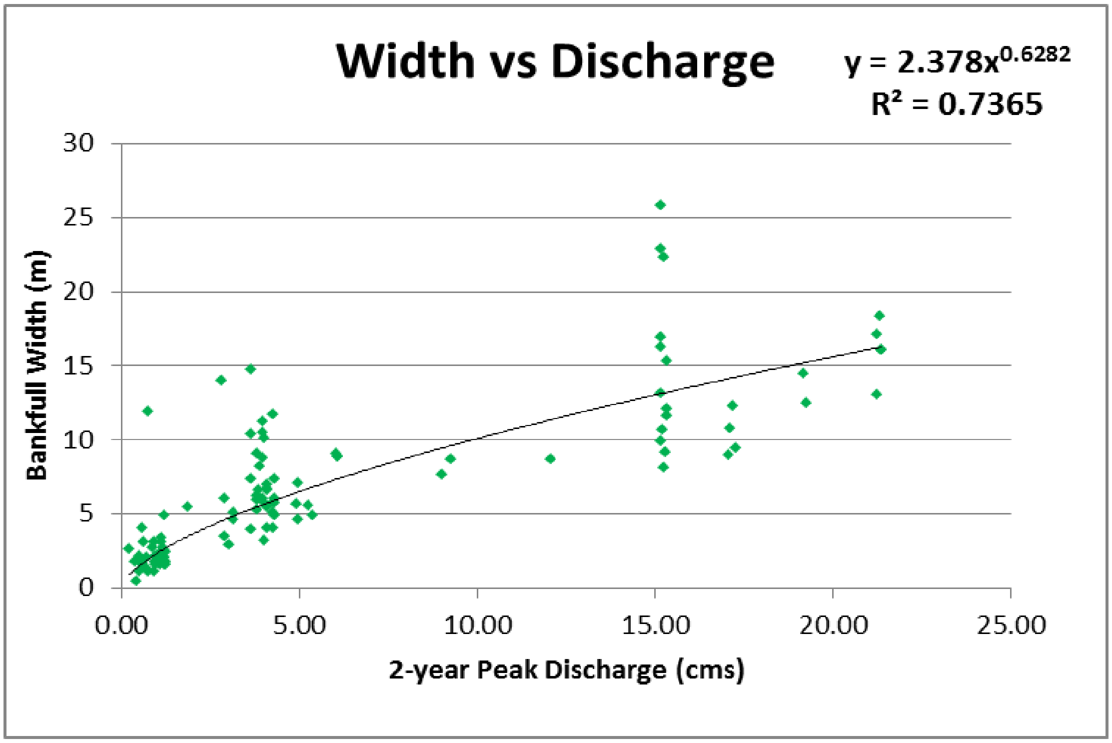

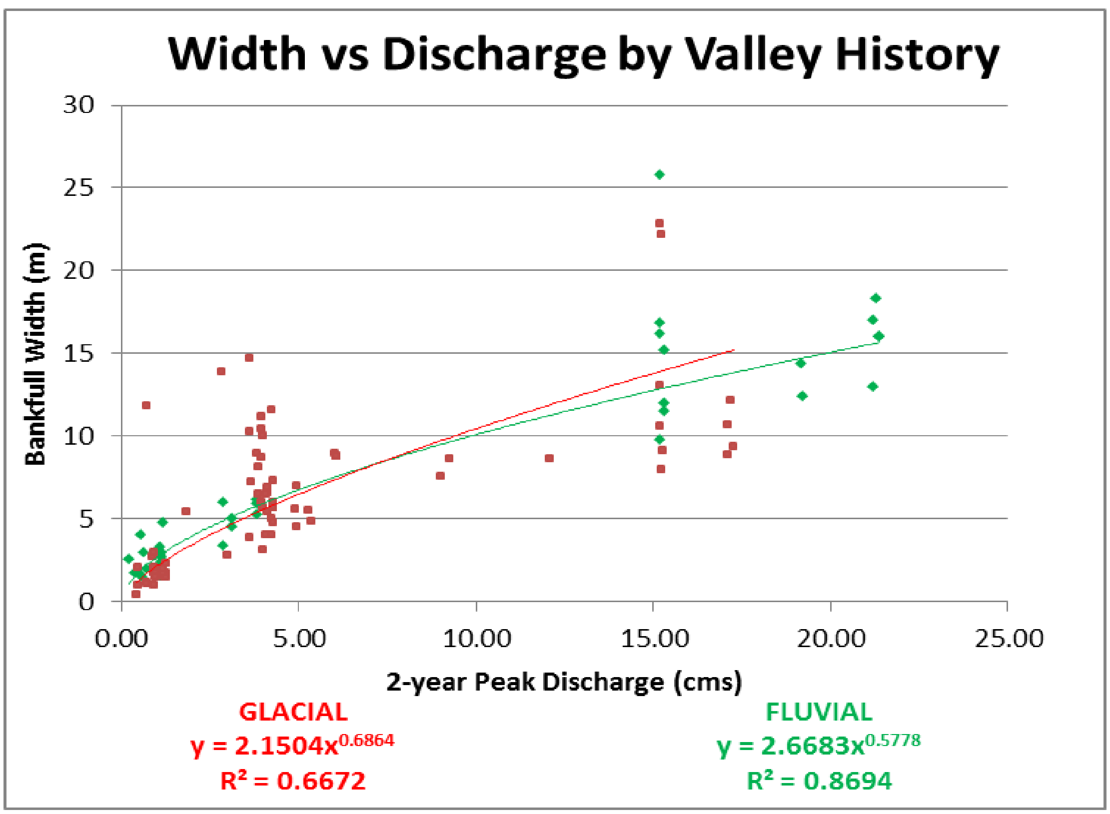

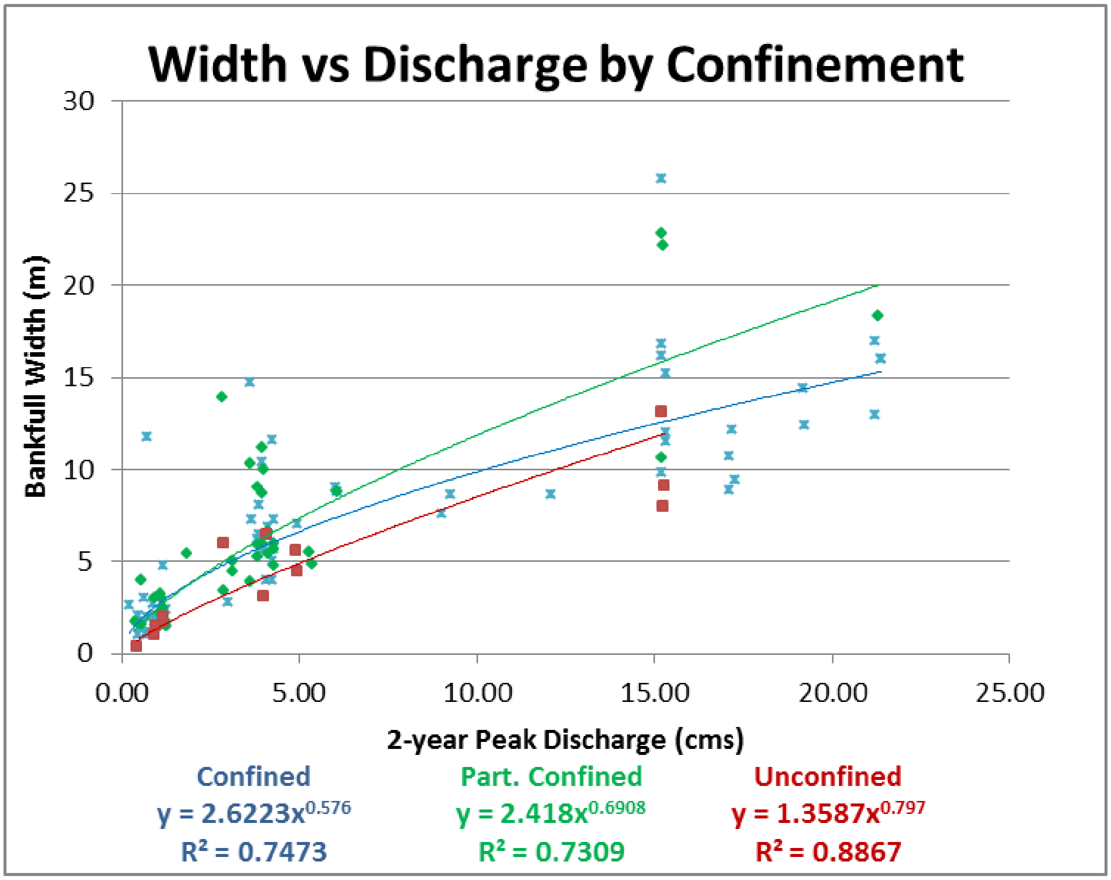

Width vs Discharge by Confinement
Bankfull Width (m)
2-year Peak Discharge (cms)
0
5
10
15
20
25
30
0.00
5.00
10.00
15.00
20.00
25.00
Confined
y = 2.6223x^0.576
R² = 0.7473
Part. Confined
y = 2.418x^0.6908
R² = 0.7309
Unconfined
y = 1.3587x^0.797
R² = 0.8867

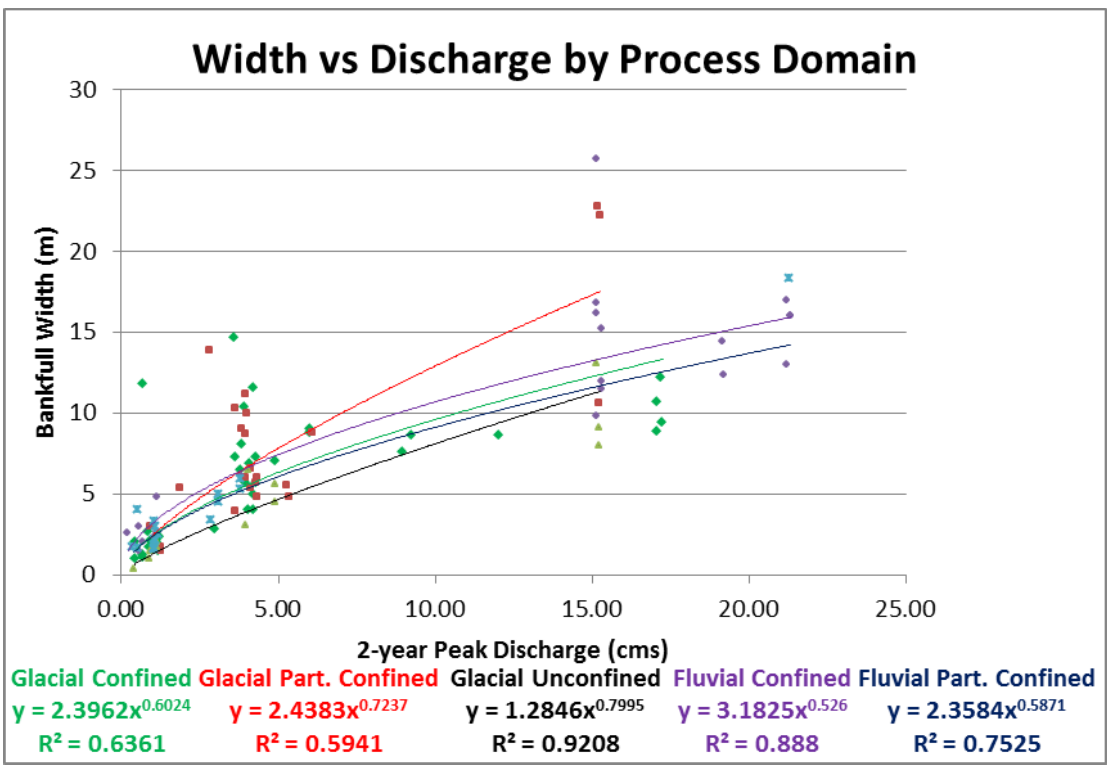

Width vs Discharge by Process Domain
Bankfull Width (m)
2-year Peak Discharge (cms)
0
5
10
15
20
25
30
0.00
5.00
10.00
15.00
20.00
25.00
Glacial Confined
y = 2.3962x^0.6024
R² = 0.6361
Glacial Part. Confined
y = 2.4383x^0.7237
R² = 0.5941
Glacial Unconfined
y = 1.2846x^0.7995
R² = 0.9208
Fluvial Confined
y = 3.1825x^0.526
R² = 0.888
Fluvial Part. Confined
y = 2.3584x^0.5871
R² = 0.7525

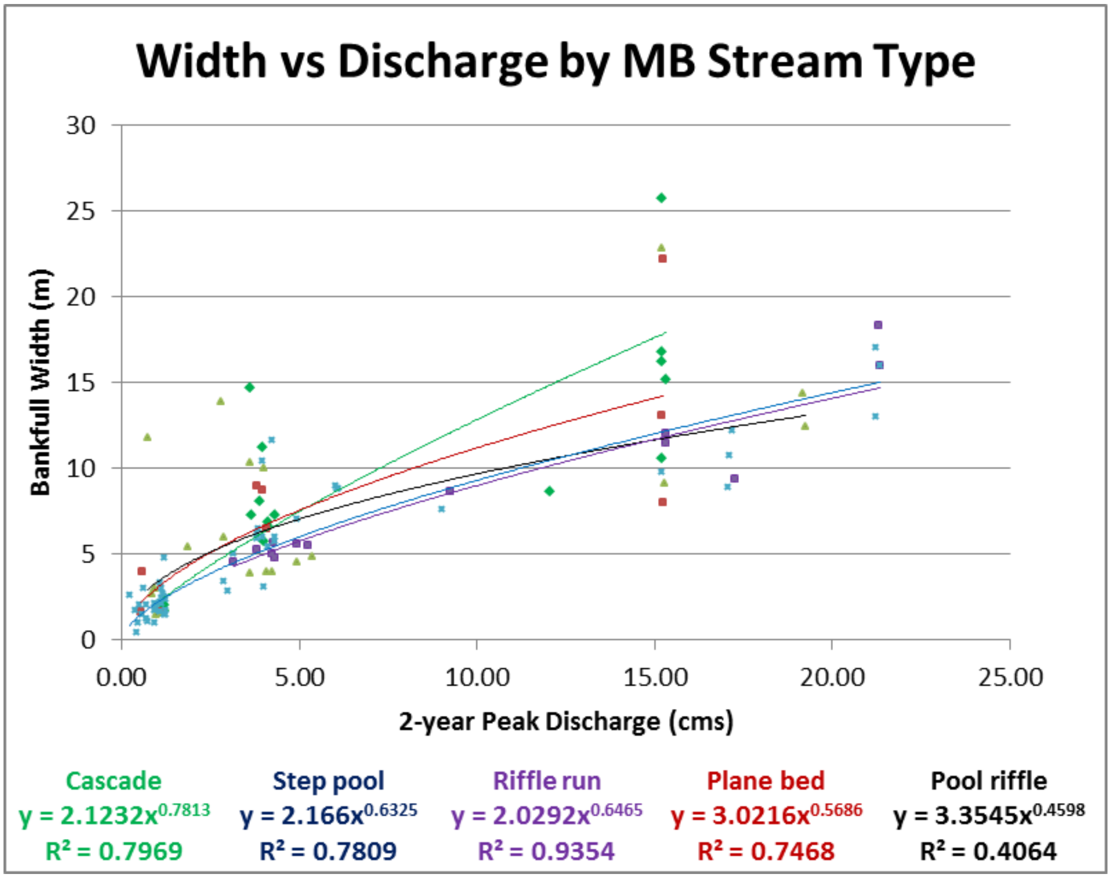

Width vs Discharge by MB Stream Type
Bankfull Width (m)
2-year Peak Discharge (cms)
0
5
10
15
20
25
30
0.00
5.00
10.00
15.00
20.00
25.00
Cascade
y = 2.1232x0.7813
R² = 0.7969
Step pool
y = 2.166x0.6325
R² = 0.7809
Riffle run
y = 2.0292x0.6465
R² = 0.9354
Plane bed
y = 3.0216x0.5686
R² = 0.7468
Pool riffle
y = 3.3545x0.4598
R² = 0.4064

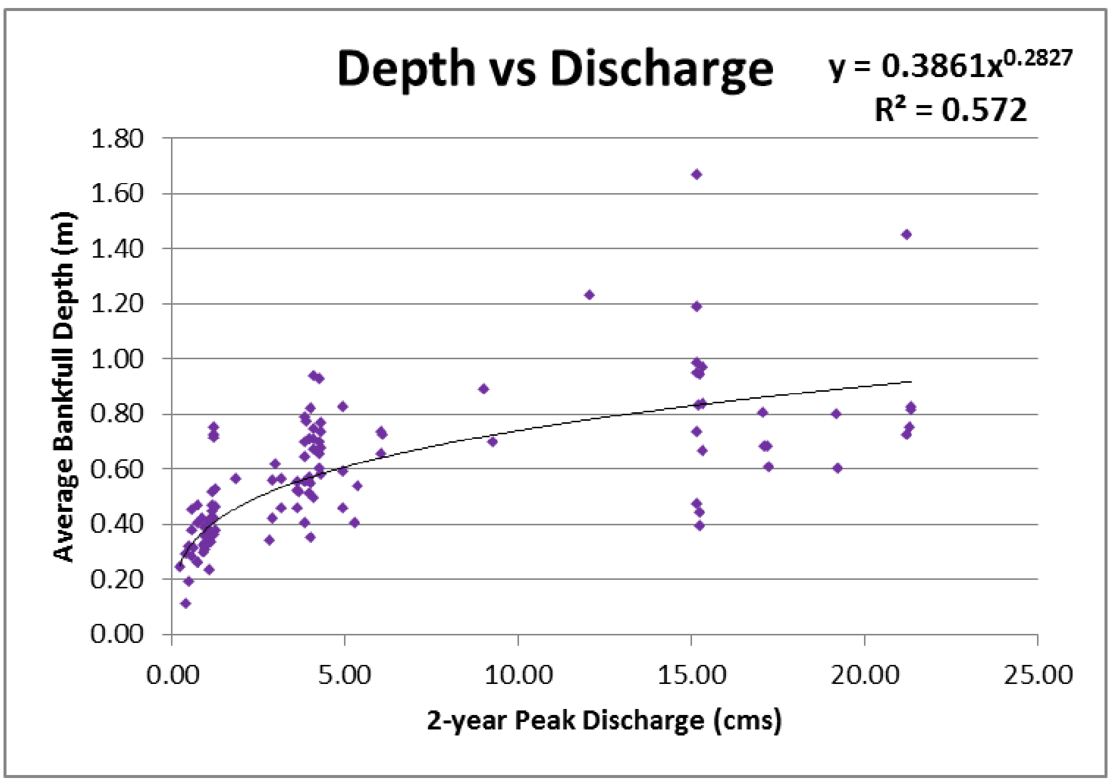

Depth vs Discharge
y = 0.3861x0.2827
R² = 0.572
Average Bankfull Depth (m)
2-year Peak Discharge (cms)
0.00
0.20
0.40
0.60
0.80
1.00
1.20
1.40
1.60
1.80
0.00
5.00
10.00
15.00
20.00
25.00

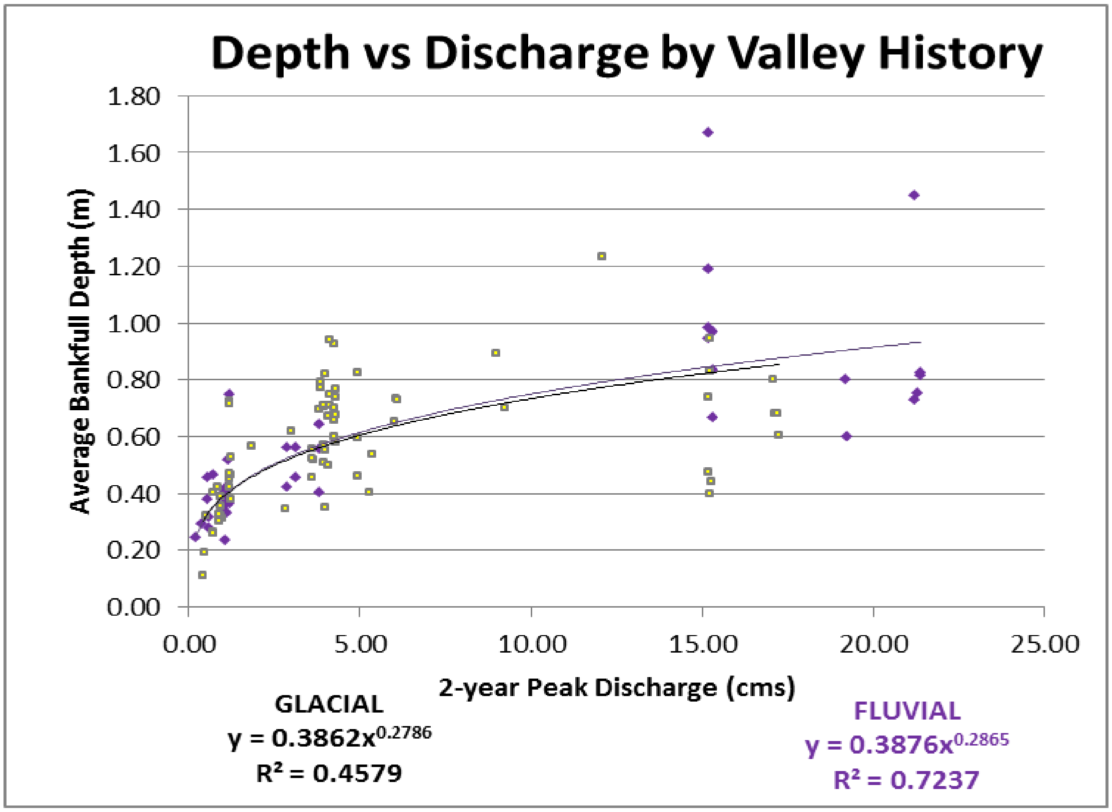
Depth vs Discharge by Valley History
Average Bankfull Depth (m)
1.80
1.60
1.40
1.20
1.00
0.80
0.60
0.40
0.20
0.00
0.00
5.00
10.00
15.00
20.00
25.00
2-year Peak Discharge (cms)
GLACIAL
y = 0.3862x^0.2786
R² = 0.4579
FLUVIAL
y = 0.3876x^0.2865
R² = 0.7237

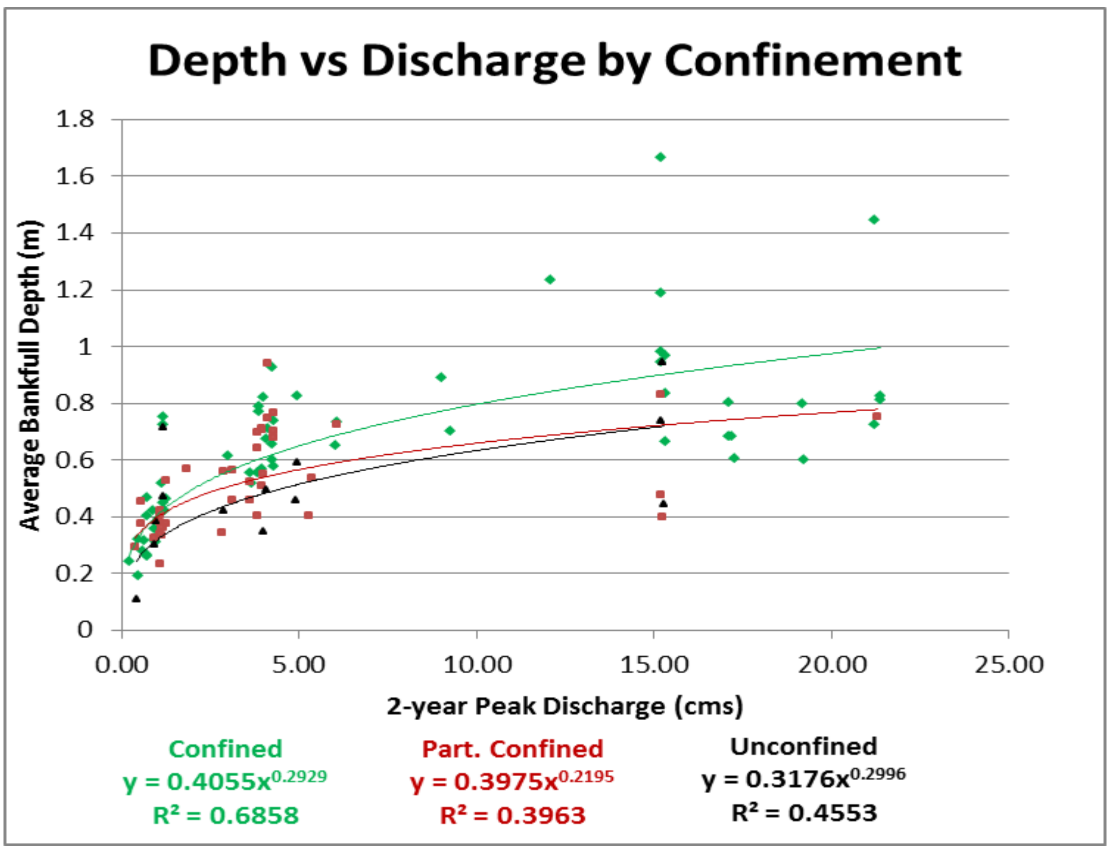
Depth vs Discharge by Confinement
Average Bankfull Depth (m)
1.8
1.6
1.4
1.2
1
0.8
0.6
0.4
0.2
0
0.00
5.00
10.00
15.00
20.00
25.00
2-year Peak Discharge (cms)
Confined
y = 0.4055x^0.2929
R² = 0.6858
Part. Confined
y = 0.3975x^0.2195
R² = 0.3963
Unconfined
y = 0.3176x^0.2996
R² = 0.4553

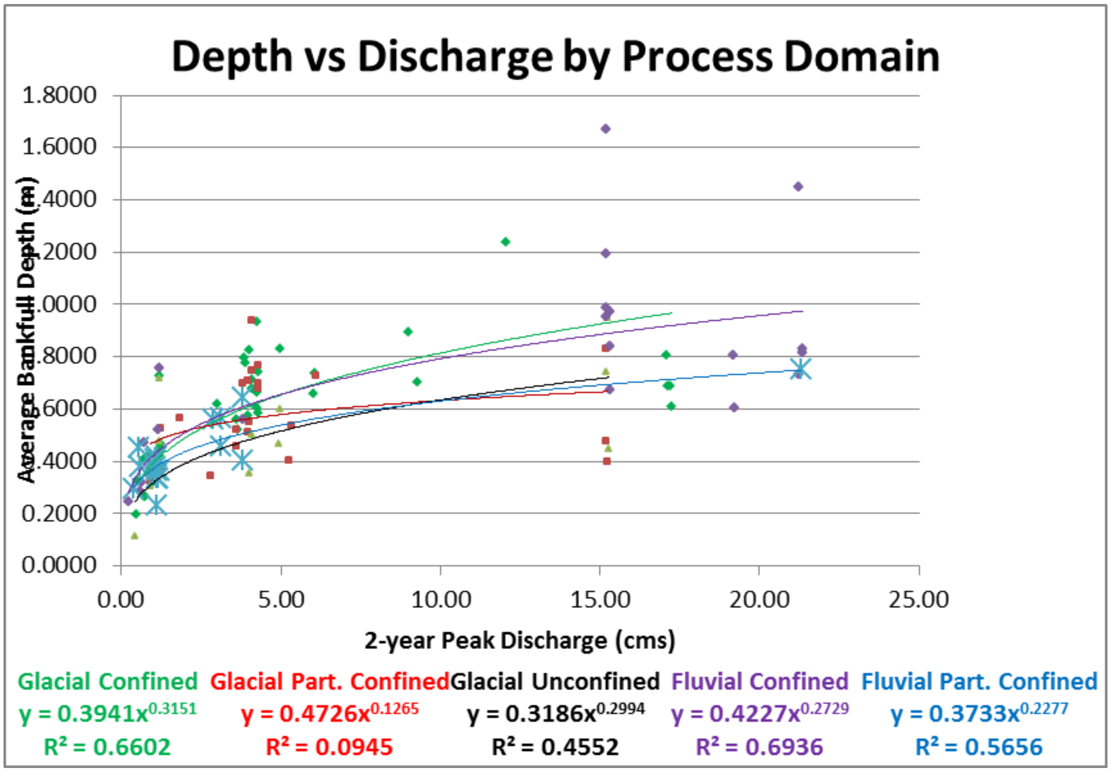
Depth vs Discharge by Process Domain
Average Bankfull Depth (m)
1.8000
1.6000
1.4000
1.2000
1.0000
0.8000
0.6000
0.4000
0.2000
0.0000
0.00
5.00
10.00
15.00
20.00
25.00
2-year Peak Discharge (cms)
Glacial Confined
y = 0.3941x^0.3151
R² = 0.6602
Glacial Part. Confined
y = 0.4726x^0.1265
R² = 0.0945
Glacial Unconfined
y = 0.3186x^0.2994
R² = 0.4552
Fluvial Confined
y = 0.4227x^0.2729
R² = 0.6936
Fluvial Part. Confined
y = 0.3733x^0.2277
R² = 0.5656

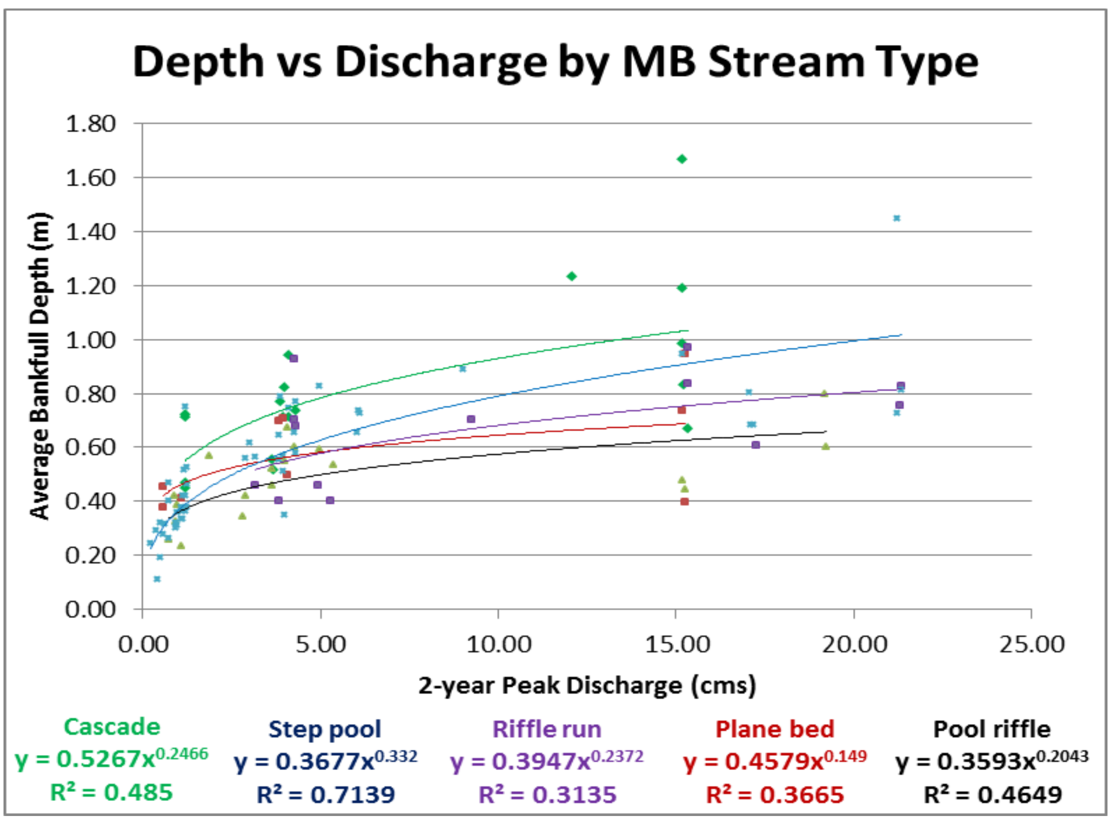
Depth vs Discharge by MB Stream Type
Average Bankfull Depth (m)
1.80
1.60
1.40
1.20
1.00
0.80
0.60
0.40
0.20
0.00
0.00
5.00
10.00
15.00
20.00
25.00
2-year Peak Discharge (cms)
Cascade
y = 0.5267x^0.2466
R² = 0.485
Step pool
y = 0.3677x^0.332
R² = 0.7139
Riffle run
y = 0.3947x^0.2372
R² = 0.3135
Plane bed
y = 0.4579x^0.149
R² = 0.3665
Pool riffle
y = 0.3593x^0.2043
R² = 0.4649